7. REFERENCES

[1] PBMR website; http://www.pbmr.co.za/download/Operation.pdf; (2006/08/18).

[2] Minato K, Fukuda K, Ishikawa A, Mita N; Advanced coatings for HTGR fuel particles against corrosion of SiC layer; Journal of Nuclear Materials **246;** (1997); pp 215-217.

[3] PBMR website; http://www.pbmr.co.za/download/FuelSystem.pdf); (2006/08/18).

[4] Fissel A; Artificially layered heteropolytypic structures based on SiC polytypes: molecular beam epitaxy, characterization and properties; Physics reports **379**; (2003); pp 152-154, 162-166, 180-181, 187.

[5] Nakashima S, Higashihira M, Maeda K; Raman scattering characterization of polytype in silicon carbide ceramics: comparison with x-ray diffraction, Journal of the American ceramic society **86**; (2003), pp 823-824.

[6] Ortiz A.L, Sanchez-Bajo F, Padture N.P, Cumbrera F.L, Guiberteau F, Quantitative polytype-composition analyses of SiC using X-ray diffraction: a critical comparison between the polymorphic and Rietveld method; Journal of the European ceramic society **21**, (2001), pp 1237-1246.

[7] Peters R; Personal communication; PBMR (Pty) Ltd.; (2006/06/29).

[8] Minato K, Ogawa T, Fukuda K, Tayama Y, Shimizu M, Tayama Y, Takahashi I; Fission product behavior in Triso-coated UO_2 fuel particles; Journal of Nuclear Materials **208** (1994); pp 266,270, 273-281.

[9] Helary D, Bourrat X, Dugne O, Maveyraud G, Perez M, Guillermier P; Microstructure of silicon carbide and pyrocarbons coatings for fuel particles for high temperature

reactors, in: Proceedings of the 2nd international topic meeting on high temperature reactor technology, Beijing, September (2004); #Paper B 07 pp 1-3, 5-7.

[10] PBMR, http://www.pbmr.co.za/contenthtml/pictureFX/imgcache/20051117 FuelElemDesCom.jpg, (2006/08/18).

[11] Snead L, Nozawa T, Katoh Y, Byun T, Kondo S, Petti D; Handbook of SiC properties for fuel performance modeling; Journal of Nuclear Materials **371**; (2007); pp 329-377.

[12] Minato K, Kikuchi H, Fukuda K, Suzuki N, Tomimoto H, Kitamura N; Failure mechanisms of fuel particle coating for High-Temperature Gas-Cooled reactors during the coating processes; Nuclear technology **111**; (1995) pp 260-261.

[13] Hofmann D.H, Müller M.H; Prospects of the use of liquid phase techniques for the growth of bulk silicon carbide crystals; Materials Science and Engineering B61–62; 1999; pp 30.

[14] Knippenberg W.F; Growth phenomena in silicon carbide; Philips Research Report **18**; 1963; pp 161-274.

[15] Scace R.I, Slack G.A; Solubility of carbon in silicon and germanium; Journal of Chemical Physics **30**; 1959; pp 1551-1556.

[16] Dolloff R.T; Research study to determine the phase equilibrium relations of selected metal carbides at high temperatures; WADD Technical Report **60**; (1960); pp 143

[17] Verma A.R, Krishna P; Polymorphism and polytypism in crystals; John Wiley & sons Inc; New York; (1966).

[18] Minato K, Fukuda K; SiC coating of small particles in a fluidized bed reactor; Advanced Materials & Manufacturing Processes; 3(4); (1988) pp 617, 637.

[19] Einspruch N.G, Claiborne L.T; Elastic constants of SiC; Journal of the Acoustical Society of America **35**; (1963); pp 925-926.

[20] Hongchao L, Changlin K; Quantitative analysis of SiC polytype distributions by the Rietveld method; Journal of Nuclear Materials **32**; (1997); pp 2661-2664.

[21] Bechstedt F, Käckell P, Zywietz A, Karch K, Adolph B, Tenelsen K, Furthmüller; Polytypism and properties of silicon carbide; Physica Status Solidi B **202**; (1997); pp 35-42.

[22] Thibault N. W; Morphological and structural crystallography and optical properties of silicon carbide; American Mineralogist **29;** (1944); pp 249–278.

[23] Daulton T.L, Bernatowicz T. J, Lewis R.S, Messenger S, Stadermann F.J, Amari S; Polytype distribution of circumstellar silicon carbide: Microstructural characterization by transmission electron microscopy; Geochimica et Cosmochimica Acta, vol. 67; no. 24; (2003); pp 4746-4748.

[24] Tairov Y.M, Tsvetkov V.F.; Process in controlling the growth of polytypic crystals; Progress in crystal growth and characterization (ed. P. Krishna); Oxford, New York, Pergamon Press; (1982); pp 111-162.

[25] Ramsdell L. S; Studies on silicon carbide; American Mineralogist **32**; (1947); pp 64–82.

[26] Zhdanov G. S; The numerical symbol of close packing of spheres and its application in the theory of close packings; Comptes. Rendus de l'Académir des Sciences. USSR. **48**; (1945); pp 39–42.

[27] Harris D.C, Bertolucci, M.D; Symmetry and Spectroscopy: An Introduction to Vibrational and Electronic Spectroscopy; Dover Publications; New York; (1989)

[28]Grasselli J.G, Bulkin B. J, Snavely M. K, Chemical applications of Raman spectroscopy, New York, John Wiley & sons, inc., (1981), pp 2-6.

[29] Smith E, Dent G; Modern Raman spectroscopy; John Wiley & sons Ltd, Chichester; (2005) pp 2-5

[30] McCreery R L; Raman spectroscopy for chemical analysis, Volume 157 in Chemical analysis (series editor: Wineforder J D); (2000); pp 15-24, 103-106, 295-300

[31] Schrader B; General survey of vibrational spectroscopy in infrared and Raman spectroscopy - methods and applications; ed. Schrader B; VCH; Wieinheim; (1995); pp 7-61

[32] Everall N.J; Raman Spectroscopy of the Condensed phase, in 'Handbook of Vibrational Spectroscopy'; eds. Chalmers J. M. and Griffiths P. R; Wiley, Chichester; (2002); pp 141 -149.

[33] Stander B; Tools for Infrared and Raman Spectroscopy in 'Infrared and Raman spectroscopy: Methods and Applications', ed. Stander B; VCH, Weinheim; (1995); pp 138-143

[34] Turrel G; Raman sampling, in 'Practical Raman Spectroscopy', eds. Gardiner D.J and Graves P.R; Springer-Verlag; Berlin; (1989); pp 31-37

[35] Everall N, Lumsdon J; Journal of Materials Science **26**; (1991); pp 5269

[36] McCreery R.L; Raman Spectroscopy for chemical analysis; Wiley Chemical Analysis Series, ed. Winefordner J; Wiley & Sons; New York; (2000)

[37] Fryling M, Frank C.J, McCreery R.L; Applied Spectroscopy **47**; (1993); pp 1965

[38] Feldman D.W, Parker J.H, Jr., Choyke W.J, Patrick L; Phonon dispersion curves by Raman scattering in SiC polytypes 3C, 4H, 6H, 15R and 21R; Physics Review **173** [3]]; (1968); pp 787-793

[39] Nakashima S, Katahama H, Nakakura Y, Mitsuishi A; Physics Review B **33**(8); (1986); pp 5721.

[40] Loudon R; Advances in Physics **13**; (1964); pp 423

[41] Chollon G; Structural and textural analyses of SiC-based and carbon CVD coatings by Raman Microspectroscopy; Thin Solid Films **516**; (2007); pp 388-396

[42] Khanna, R.K. (1957). Evidence of ion-pairing in the polarized Raman spectra of a Ba^{2+}CrO doped KI single crystal. John Wiley & Sons, Ltd.

[43] Ward Y, Young R.J, Shatwell R.A; A microstructural study of silicon carbide fibres through the use of Raman microscopy; Journal of materials science **36**; 2001; pp 55, 57-58.

[44] Nakashima S, Ohta H, Hangyo M, Palosz B; Detection of defects in SiC crystalline films by Raman scattering; Philosophical Magazine **B70**; (1994); pp 971.

[45] Gouadec G, Comlomban P; Non-destructive mechanical characterization of SiC fibres by is Raman spectroscopy; Journal of the European ceramic society **21**; (2001); pp 1251, 1255, 1257.

[46] Nakashima S, Kisoda K, Niizuma H, Harima H; Raman scattering of disordered SiC; Physica **B219&220** (1996) pp 371-373.

[47] Fisher G.R, Barnes P; Towards a unified view of polytypism in silicon carbide; Philosophical Magazine **B61**; (1990); pp 217

[48] Barnes P, Kelly J.F, Fisher G.R; Observation of fine one-dimensionally disordered layers in silicon carbide; Philosophical Magazine Letters **64** (1991); pp 21.

[49] Lu Y.M, Leu I.C; Quantitative study of beta silicon carbide residual stress by Raman spectroscopy; Thin solid films **377-378**; (2000); pp 389-393.

[50] Olega D, Cardona M; Pressure dependence of Raman phonons of Ge and 3*C*-SiC; Physical Review **B25**; (1982); pp 1151.

[51] Krautwasser P, Begun G.M, Angelini P; Raman spectral characterization of silicon carbide nuclear fuel coatings; Journal of the American Ceramic Society **66** [6]; (1983); pp 425.

[52] Veprek S, Iqbal Z, Oswald H.R, Webb; Properties of polycrystalline silicon prepared by chemical transport in hydrogen plasma at temperatures temperatures between 80 and 400^{o}C; Journal of Physics C **14** [3]; (1981); pp 295-308.

[53] Smith J.W Jr, Brodsky M.H, Crowder B.L, Nathan M.I; Raman scattering in amorphous Si, Ge and III-IV semiconductors; Journal of Non-Crystalline Solids **8-10**; (1972); pp 179-184.

[54] Tuinstra F, Koenig J.L; Raman spectra of graphite; Journal of Chemical Physics **53** [3]; (1970); pp 1126-30.

[55] Elman B.S, Dresselhaus M.S, Dresselhaus G, Maby E.W, Mazurek H; Raman scattering from ion-implanted graphite; Physics Review B **24** [2]; (1981); pp 1027-1034.

[56] Nathan M.I, Smith J.E, Tu K.N; Raman spectra of glassy carbon; Journal of Applied Physics **45** [5]; (1974); pp 2370.

[57] Perez-Rodriguez A, Cornet A, Morante J.R, Physical techniques for silicon layer analysis, Microelectronic engineering **80**, 1998; pp 228-232.

[58] Hongchao L, Changlin K; Quantitative analysis of SiC polytype distributions by the Rietveld method; Journal of Materials Science **32**, 1997; pp 2661-2664.

[59] Young R.A; The Rietveld method; International Union of Crystallography Monographs on Crystallography; Oxford science publications; (1996).

[60] Werner P.E, Salomé S, Malmros G, Thomas O.J; Quantitative analysis of multicomponent powders by full-profile refinement of Guinier-Hägg X-ray film data; Journal of Applied Crystallography **12**; (1979); pp 107-109.

[61] Hill R.J, Howard C.J; Quantitative phase analysis from neutron powder diffraction data using the Rietveld method; Journal of Applied Crystallography **20**; (1987); pp 467-474.

[62] Bish D.L, Howard S.A; Quantitative phase analysis using the Rietveld method; Journal of Applied Crystallography **21**; (1988); pp 86-91.

[63] O'Connor B.H, Raven M.D; Applications of the Rietveld refinement procedure in assaying powdered mixtures; Powder Diffraction **3**; (1988); pp 2-6.

[64] Hill R.J; Expanded use of the Rietveld method in studies of phase abundance in multiphase mixtures; Powder Diffraction **6**; (1991); pp 74 -77.

[65] Klug H.P, Alexander L.E; X-ray diffraction procedures for polycrystalline and amorphous materials; Wiley-Interscience. New York; (1974).

[66] Bridley G.W; The effect of grain or particle size on X-ray reflexions from mixed powders and alloy considered in relation to the quantitative determination of crystalline substances by X-ray methods; Philosophical Magazine. **36**; (1945); pp 347-369.

[67] Hermann H, Ermrich M; Microabsorption correction of x-ray intensities diffracted by multiphase powder specimens; Powder Diffraction **4**; (1989); pp 189-195.

[68] Will G, Parrish W, Huang T.C; Crystal-structure refinement by profile fitting and least-squares analysis of powder diffractometer data; Journal of Applied Crystallography **16**; (1983); pp 611-622

[69] Hill R.J, Howard C.J; Quantitative phase analysis from neutron powder diffraction data using the Rietveld method; Journal of Applied Crystallography. **20**; (1987); pp 467-74

[70] Ortiz A.L, Sanchez-Bajo F, Padture N.P, Cumbrera F.L, Guiberteau F, Quantitative polytype-composition analyses of SiC using X-ray diffraction: a critical comparison between the polymorphic and Rietveld methods, Journal of the European ceramic society **21**, 2001, pp 1237-1238,1241, 1246

[71] Beck M, Mittemeijer E.J; Simultaneous determination of specimen temperature and specimen displacement in high-temperature X-ray diffractometry applying Bragg-Brentano geometry; Journal of Applied Crystallography **35**; (2002); pp 103-107.

[72] Pecharsky V, Zavilij P; Fundamentals of Powder Diffraction and Structural Characterization of Materials; Dordrecht: Kluwer; (2003).

[73] Touloukian Y.S, Kirby R.K, Taylor R.E, Lee T.Y.R; Thermal Expansion of Nonmetallic Solids; Thermophysical Properties of Matter **13**; (1977); pp 176-185.

[74] Taylor D; Thermal expansion data: 1 Binary oxides with the sodium chloride and wurtzite structures, MO; British Ceramic Transactions Journal **83**; (1984); pp 92-98.

[75] Stinton G.W, Evans J.S.O; Parametric Rietveld refinement; Journal of Applied Crystallography **40**; (2007); pp 88-92.

[76] Li Z, Bradt R.C; Thermal expansion of the Cubic (3C) Polytype of SiC; Journal of Materials Science **21** [12]; (1986); pp 4366-4368

[77] Li Z, Bradt R.C; Thermal expansion of the Hexagonal (4H) Polytype of SiC; Journal of Applied Physics **60** [2]; (1986); pp 612-614

[78] Li Z, Bradt R.C; Thermal expansion of the Hexagonal (6H) Polytype of SiC; Journal of the American Ceramic Society **69** [12]; (1986); pp 863-866

[79] Li Z, Bradt R.C; Thermal expansion and thermal expansion anisotropy of SiC polytypes; Journal of the American Ceramic Society **70** [7]; (1987); pp 445-448

[80] Megaw H.D; Crystal Structures and Thermal Expansion; Materials Research Bulletin **8**; (1971); pp 1007-1018

[81] Hazen R.M, Finger L.M; Comparative Crystal Chemistry; Wiley-Interscience, New York; (1984); pp 115

[82] Pojur A.F, Yates B, Kelly B.T; Thermal expansion at elevated temperatures III, A hemispherical laminar composite of pyrolytic graphite, silicon carbide and its constituents between 300 and 800K; Journal of Physics D: Applied Physics Vol. **5**; (1972) pp 1321-1329

[83] Kern E.L, Hamill D.W, Deem H.W, Sheets H.D; Thermal properties of β-Silicon Carbide from 20 to 2000^{o}C; Thermal Properties **4** [SiC issue]; (1968); pp 25-32

[84] Riley D.P; The thermal expansion of graphite part II: Theoretical; Proceedings of the Physical Society, London **57**; (1945); pp 486-495

[85] Morgan W.C; Thermal expansion coefficients of graphite crystal; BNWL-SA-3838; (1971)

[86] Kellet E.A, Richards B.P; The thermal expansion of graphite within the layer planes; Journal of Nuclear Materials **12**; (1964); pp 184-192

[87] Steward E.G, Look B.P, Kellet E.A; Dependence on temperature of the interlayer spacing in carbons of different graphite perfection; Nature **187**; (1960); pp 1015-1016

[88] Tsang D.K.L, Marsden B.J, Fok S.L, Hall G; Graphite thermal expansion relationship for different temperature ranges; Carbon **43**; (2005); pp 2902-2906

[89] Nelson J.B, Riley D.P; Thermal expansion of graphite from 15^{o}C to 800^{o}C, Part I. Experimental; Proceedings of the Physical Society, London **57**; (1945); pp 477-486

[90] Yates B, Pirgon Q, Kelly B.T; Proceedings of the 4th international carbon and graphite conference, London: Society of Chemical Industry; (1974)

[91] Harrison J.W; Absolute measurements of the coefficients of thermal expansion of pyrolytic graphite from room temperature to 1200 K and a comparison with current theory. High Temp-High Pressure **9**; (1977); pp 211-229

[92] Reimer L; Transmission electron microscopy, physics of image formation and microanalysis, 3rd edition; Springer-Verlag, Berlin Heidelberg; (1993); pp 6-10, 115, 272

[93] Williams D.B, Carter B.C; Transmission Electron Microscopy: A Textbook for Materials Science; Springer; (1996); pp 9-11

[94] Edington J.W; Practical electron microscopy in materials science, Monograph two, Electron Diffraction in the electron microscope; Phillips publishing, Eindhoven; (1975); pp 4-7

[95] Labspec version 404; Jobin Yvon Horiba, Labspec spectral software

[96] AUTOQUAN Version 2.70; GE Inspection Technologies GmbH; (2005)

[97] TOPAS Version 3.0; GmbH; Karlsruhe, West Germany; (2003-2005)

[98] Stadelmann P; JEMS software for MS Windows; (2005)

[99] O'Grady A, Dennis A.C, Denvir D, McGarvey J.J, Bell S.E.J; Quantitative Raman Spectroscopy of Highly Fluorescent Samples Using Pseudosecond Derivatives and Multivariate Analysis; Analytical Chemistry **73** (9); (2001); pp 2058-2065

[100] Kim B, Hahn J, Han K; Quantitative phase analysis in tetragonal-rich tetragonal/ monolithic two phase zirconia by Raman spectroscopy; Journal of Materials Science letters **16**; (1997); pp 669-671

[101] Pecharsky V.K, Zavalij P.Y; Fundamentals of powder diffraction and structural characterization of materials; Springer; (2005); p 713

APPENDIX A1
Qualitative Raman Spectra

Sample PO1

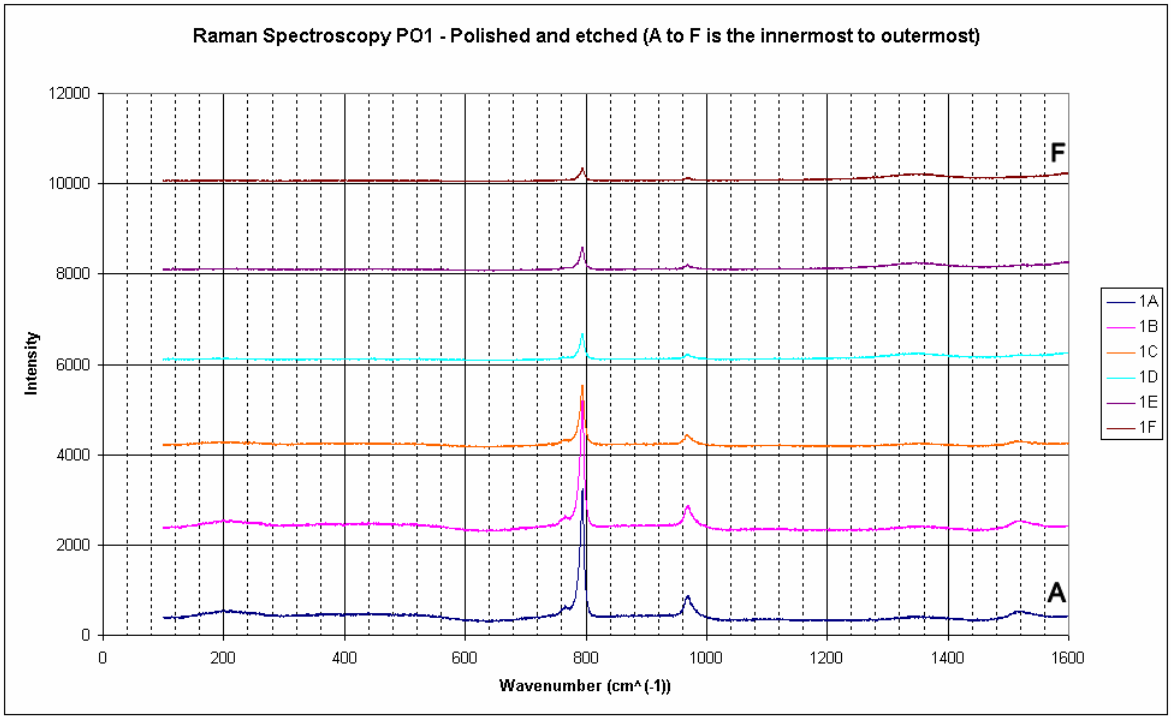

Raman spectra of the SiC coating of PO1 polished and etched coated particle. A is the innermost and F is the outermost spot along the SiC cross-section. There is no polycrystalline silicon. There is peak splitting evident across the inner part of the SiC and therefore 6H SiC. The SiC peaks progressively get smaller from analysis A to F. This is thought to be as a result of a variation of crystallinity and absorption, with point A having the most crystalline SiC crystals.

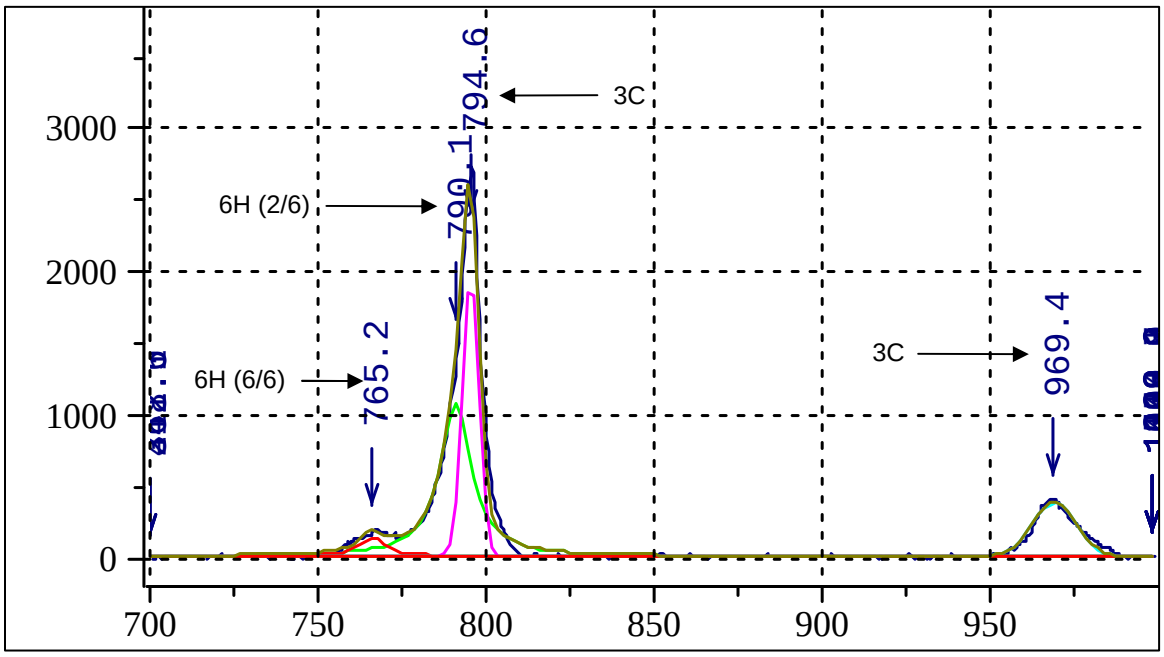

Raman spectra of the TO SiC peaks after deconvolution for analysis 1A (etched). It was assumed that there were two components making up the main peak. The peaks indicate the presence of the 3C and 6H polytypes.

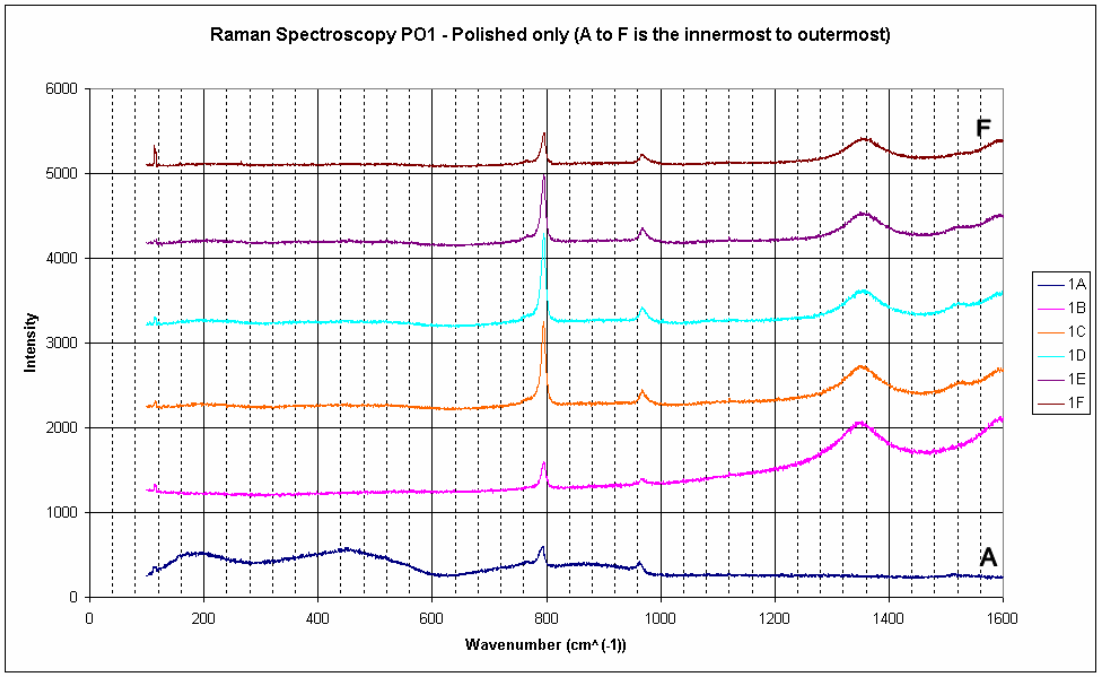

Raman spectra of the SiC coating of PO1 polished coated particle. A is the innermost and F is the outermost spot along the SiC cross-section. There is no polycrystalline silicon. There is peak splitting evident for some of the SiC profiles, confirming the presence of 6H SiC. There is evidence of free carbon from analysis B to F. The most intense SiC peaks are towards the outer part of the SiC layer. This is thought to be as a result of a variation of crystallinity and absorption of the crystals.

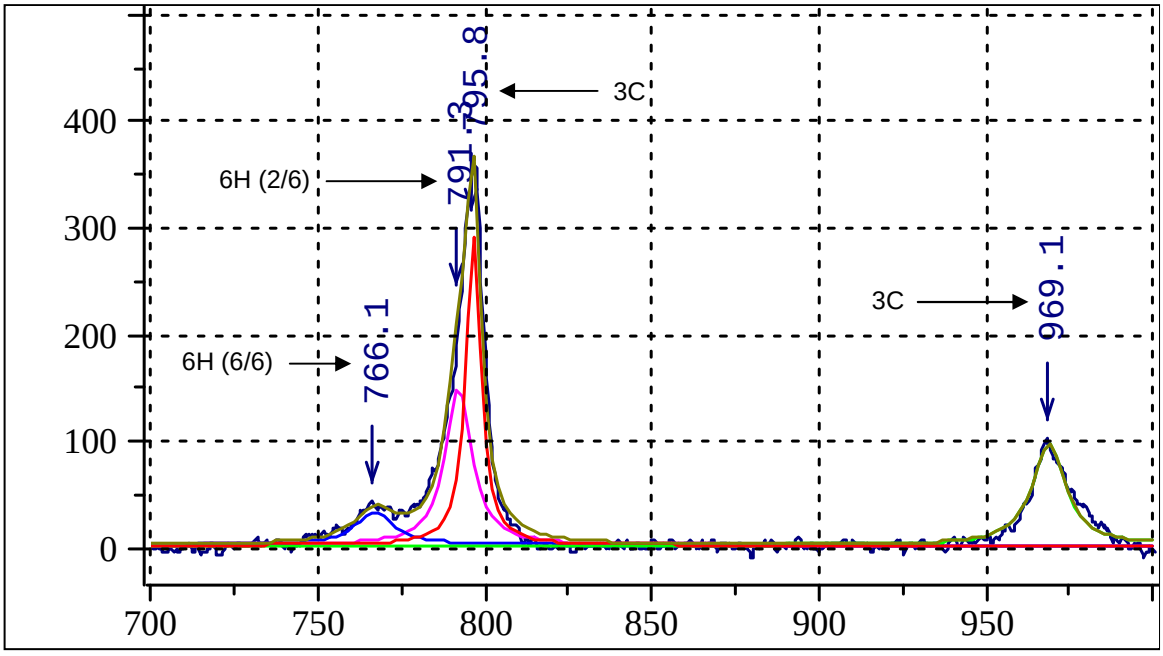

Raman spectra of the TO SiC peaks after deconvolution for analysis 1A (polished). It was assumed that there were two components making up the main peak. The peaks indicate the presence of the 3C and 6H polytypes.

Sample PO2

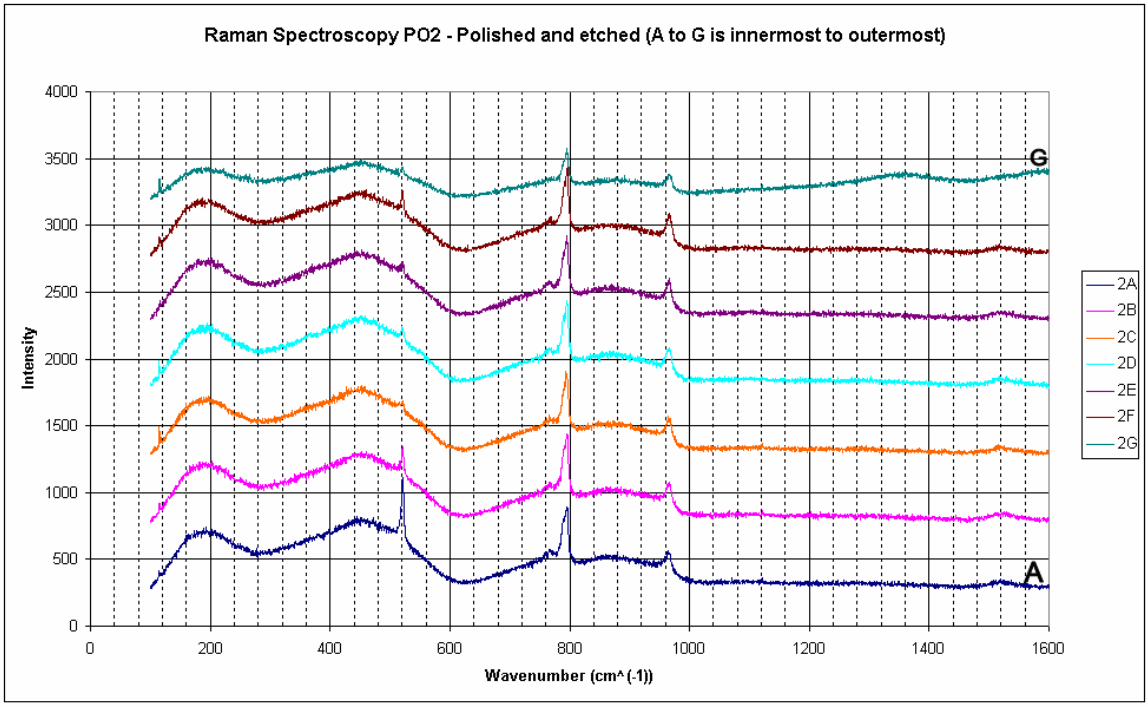

Raman spectra of the SiC layer of PO2 polished and etched coated particle. A is the innermost and G is the outermost spot along the SiC cross-section. The polycrystalline silicon peak is evident throughout the analyses, with the most intense peaks found across the inner parts of the SiC layer (analysis A and B). There is evidence of amorphous silicon throughout the analyses. There is peak splitting evident across the inner part of the SiC and therefore 6H SiC across the profile. The presence of graphite is only seen at analysis G.

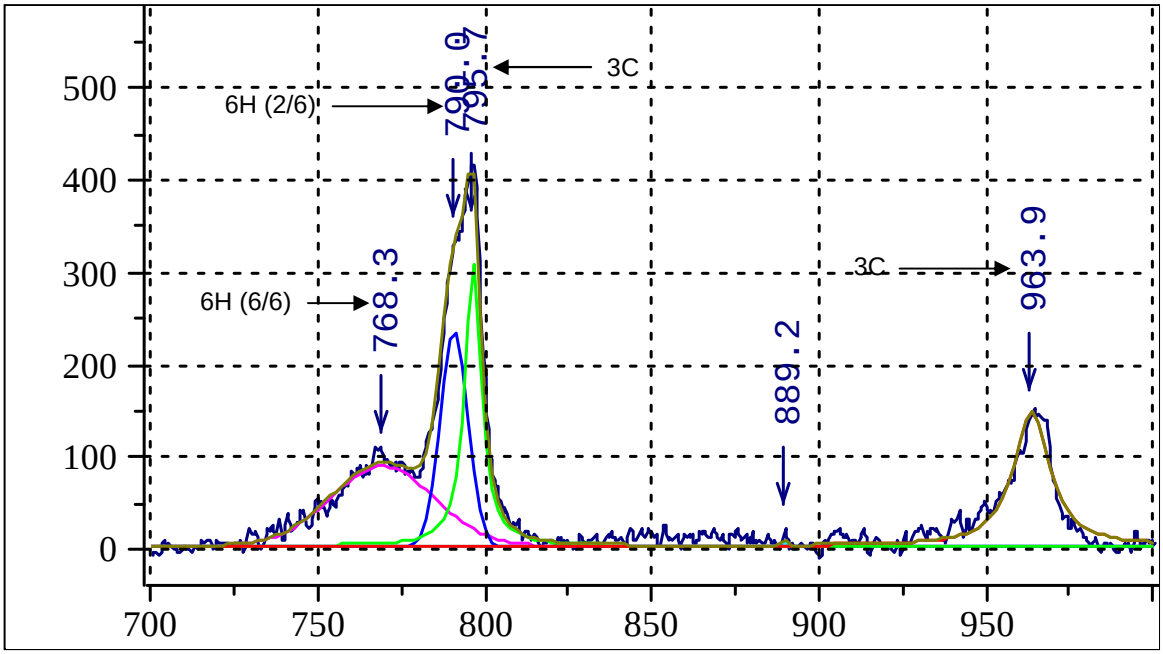

Raman spectra of the TO SiC peaks after deconvolution for analysis 2A (etched). It was assumed that there were two components making up the main peak. The peaks indicate the presence of the 3C and 6H polytypes.

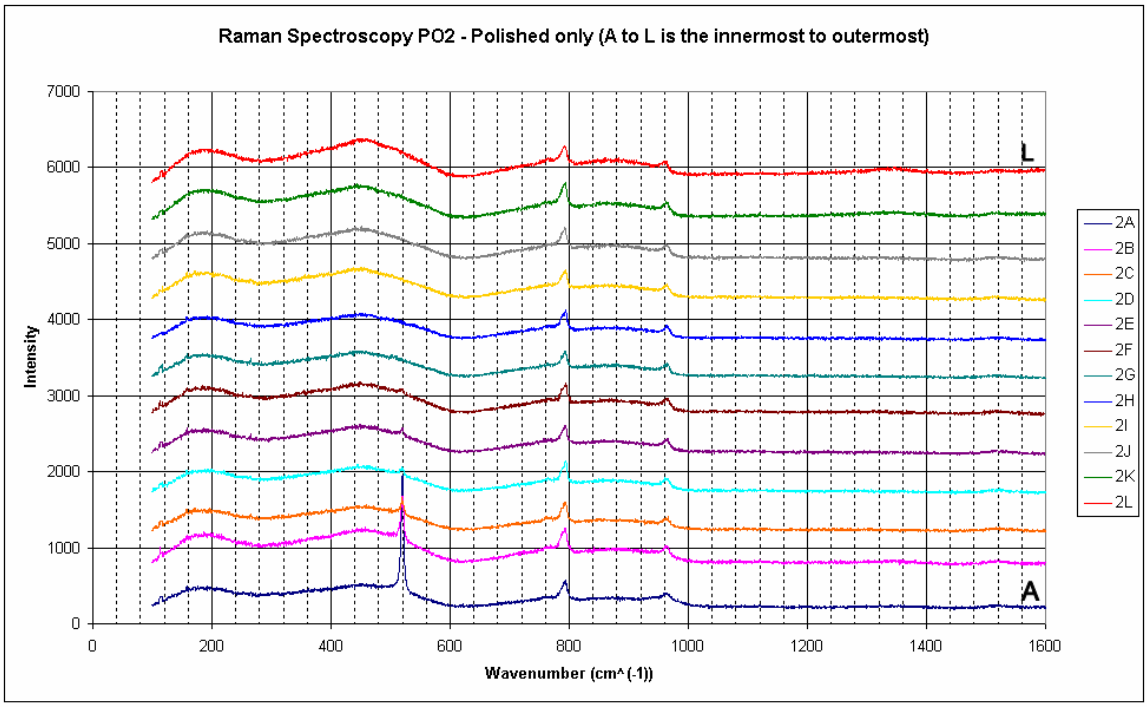

Raman spectra of the SiC coating of PO2 polished coated particle. A is the innermost and L is the outermost spot along the SiC cross-section. The polycrystalline silicon peak is evident throughout analyses A to F, with the most intense peaks found across the inner part of the SiC layer (analysis A). Amorphous silicon seems more evident closer to the OPyC layer. There is peak splitting evident across the inner part of the SiC and therefore 6H SiC across the profile. This is clearly evident from peak deconvolution. There is no evidence of graphite.

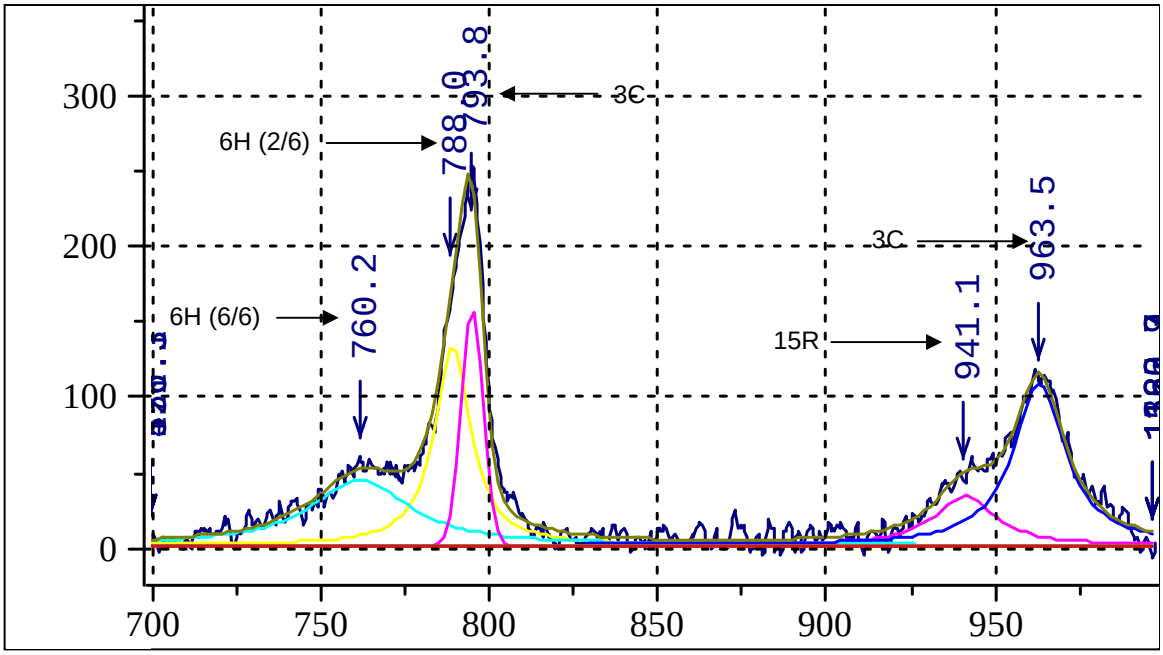

Raman spectra of the TO SiC peaks after deconvolution for analysis 2A (polished). It was assumed that there were two components making up the main peak. The peaks indicate the presence of the 3C and 6H polytypes.

Sample PO3

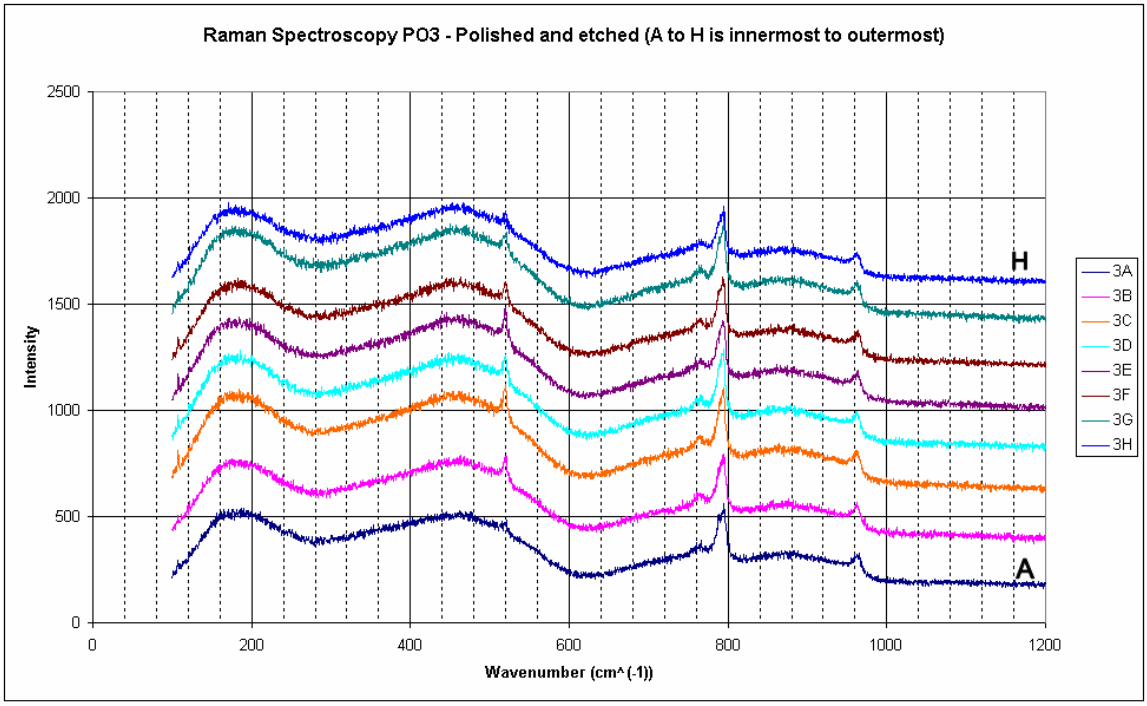

Raman spectra of the SiC layer of PO3 etched and polished coated particle. A is the innermost and H is the outermost spot along the SiC cross-section. There seems to be a mixture of amorphous and crystalline silicon throughout the analyses. The most intense crystalline silicon peaks occur in the middle of the SiC layer (analysis C to E) Peak splitting is clearly evident, indicating that the 3C polytype is not the only one that is stable.

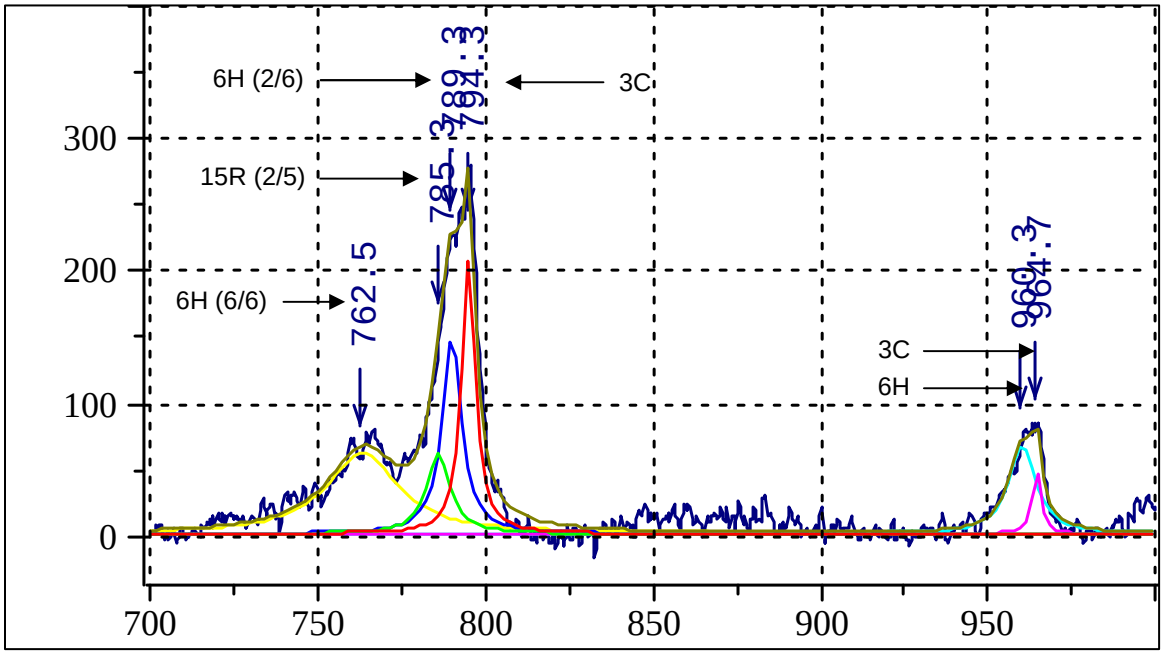

Raman spectra of the TO SiC peaks after deconvolution for analysis 3A (etched). It was assumed that there were three components making up the main peak. The peaks indicate the presence of the 3C, 6H and 15R polytypes.

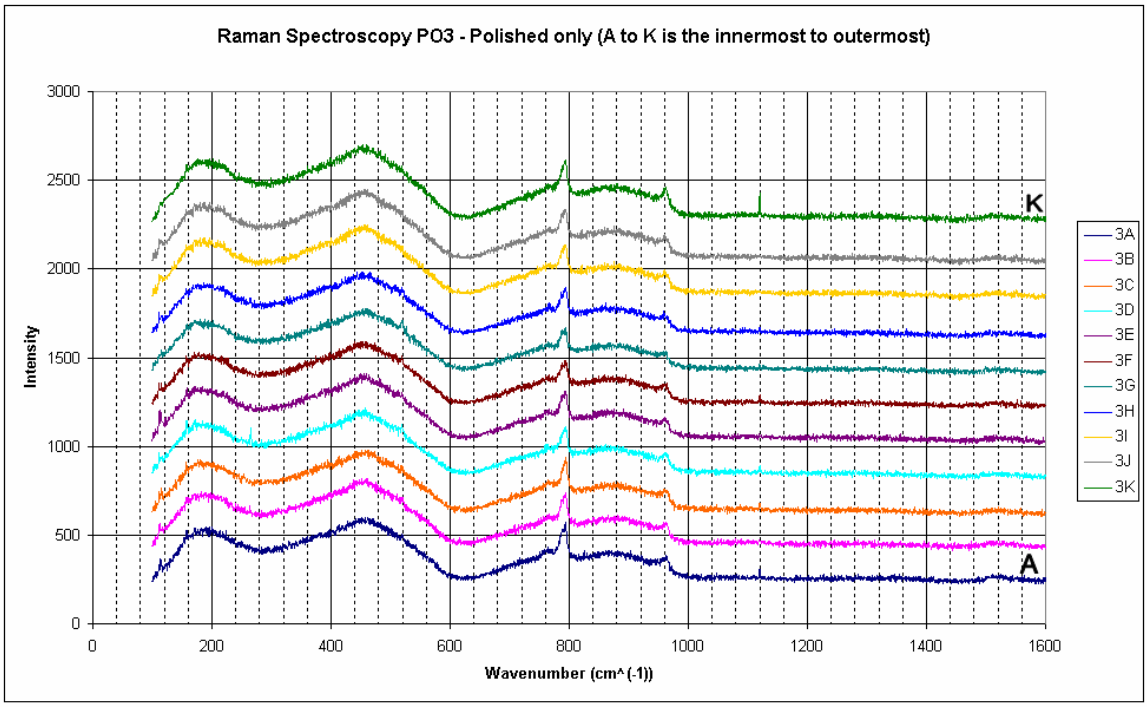

Raman spectra of the SiC coating of PO3 polished coated particle. A is the innermost and K is the outermost spot along the SiC cross-section. There seems to be predominantly amorphous, with small silicon peaks evident for some analyses. Peak splitting is clearly evident, indicating that the 3C polytype is not the only one that is stable. There is no evidence of graphite.

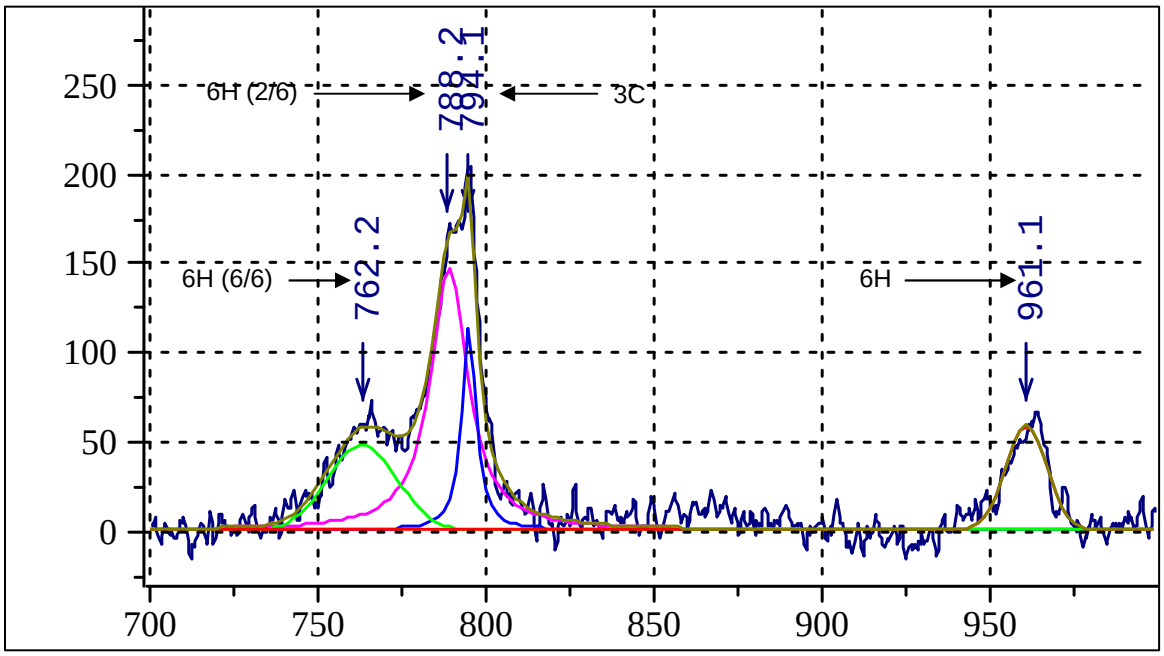

Raman spectra of the TO SiC peaks after deconvolution for analysis 3A (polished). It was assumed that there were three components making up the main peak. The peaks indicate the presence of the 3C, 6H and 15R polytypes.

Sample PO4

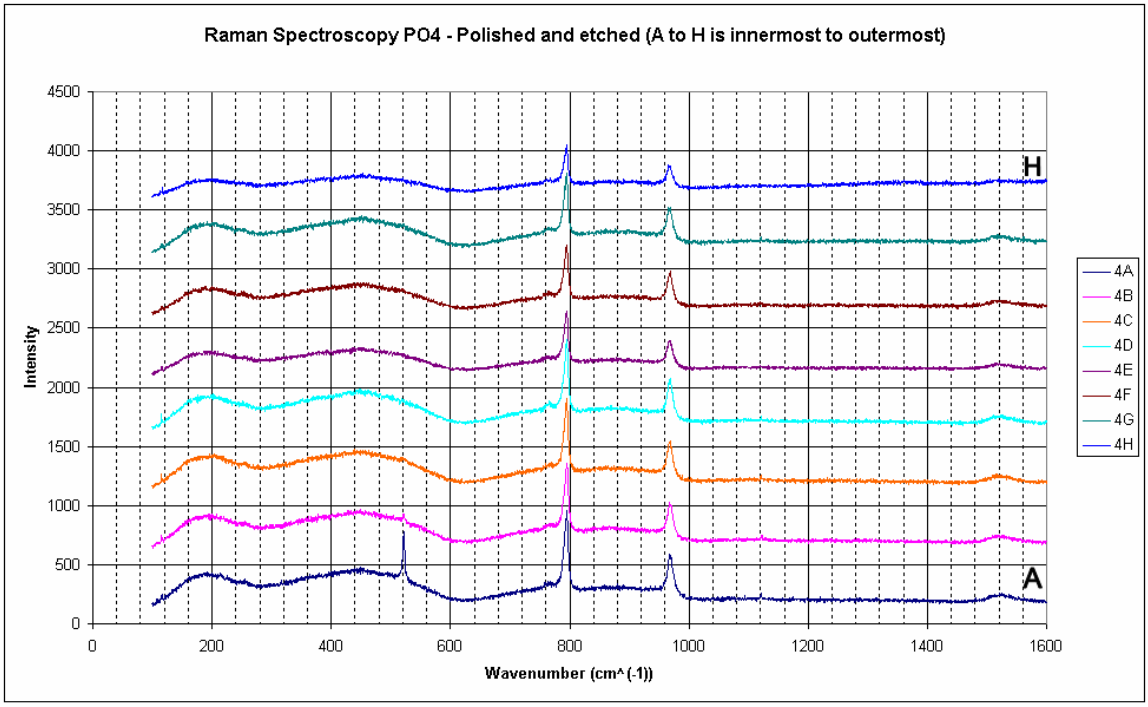

Raman spectra of the SiC coating of PO4 etched and polished coated particle. A is the innermost and K is the outermost spot along the SiC cross-section. There seems to be a mixture of amorphous and crystalline silicon towards the inner part of the SiC layer (analysis A-C). Analysis A has by far the most intense silicon peak. Peak splitting is clearly evident and is confirmed by the peak deconvolution. There is no evidence of graphite.

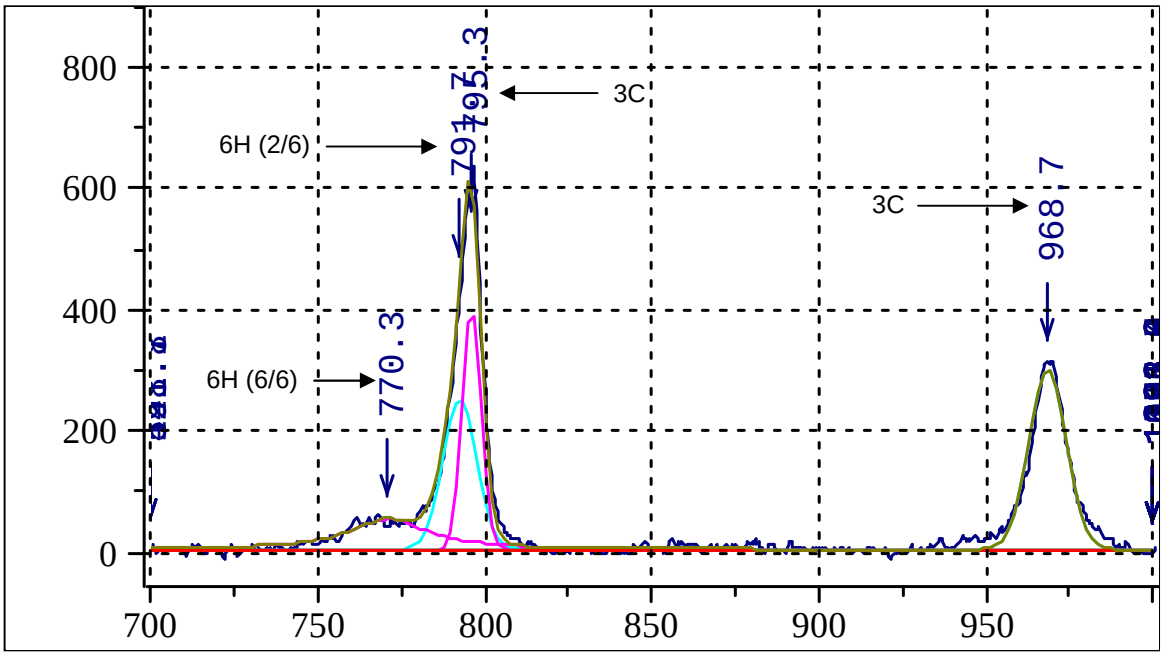

Raman spectra of the TO SiC peaks after deconvolution for analysis 4A (etched). It was assumed that there were two components making up the main peak. The peaks indicate the presence of the 3C and 6H polytypes.

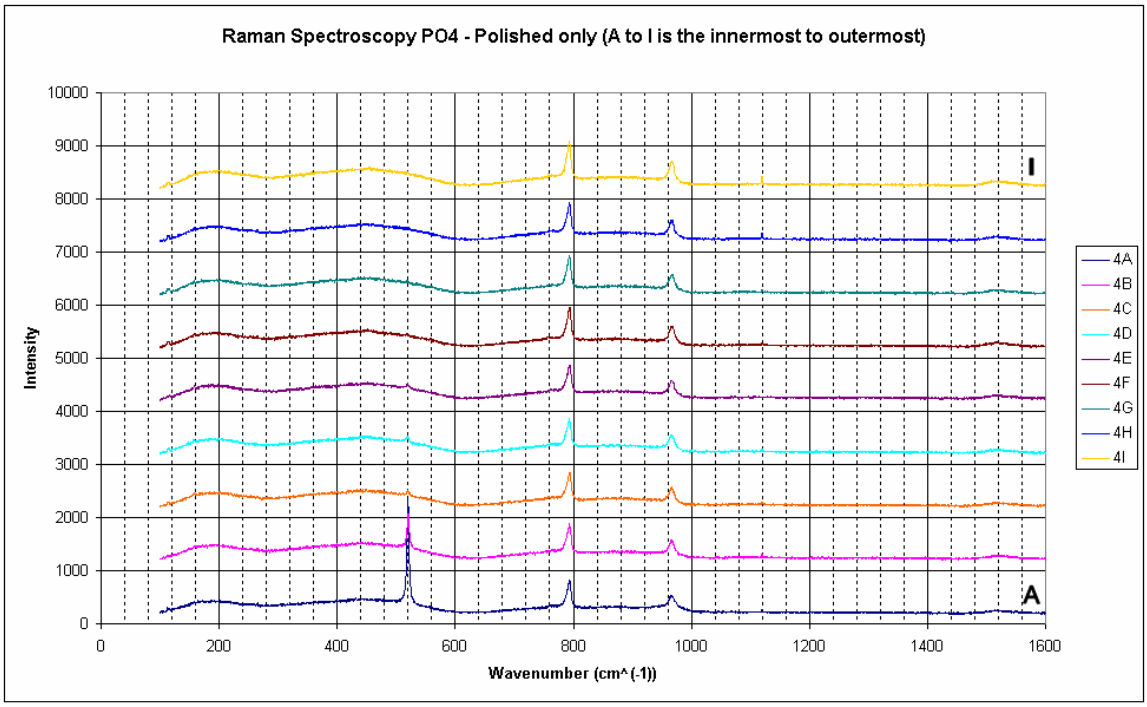

Raman spectra of the SiC coating of PO4 polished coated particle. A is the innermost and I is the outermost spot along the SiC cross-section. There seems to be a mixture of amorphous and crystalline silicon towards the inner part of the SiC layer (analysis B-E). Analysis A has by far the most intense silicon peak. Peak splitting is not clearly evident but is confirmed by the peak deconvolution. There is no evidence of graphite.

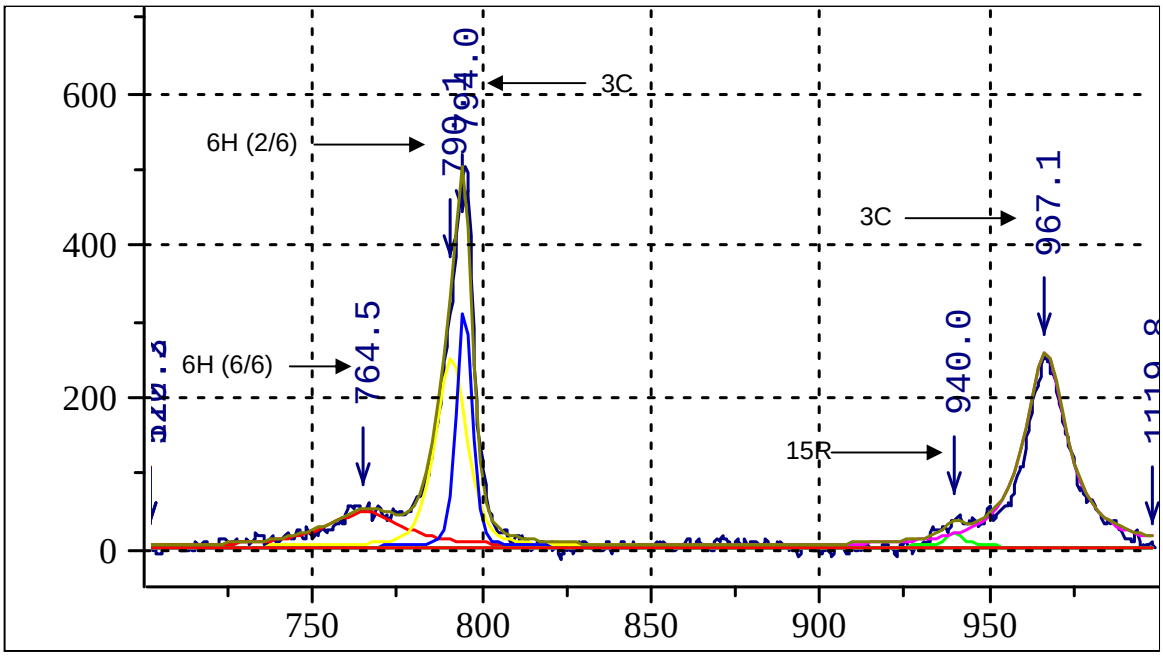

Raman spectra of the TO SiC peaks after deconvolution for analysis 4A (polished). It was assumed that there were two components making up the main peak. The peaks indicate the presence of the 3C and 6H polytypes.

Sample PO5

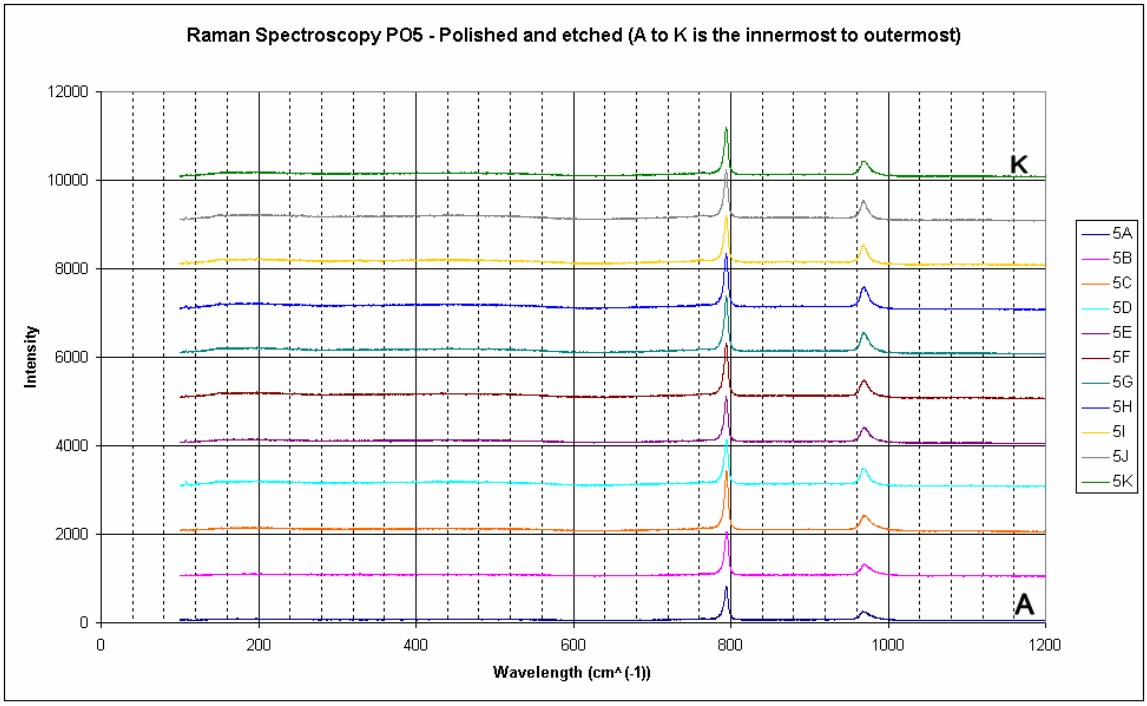

Raman spectra of the SiC coating of PO5 etched and polished coated particle. A is the innermost and K is the outermost spot along the SiC cross-section. Neither the amorphous nor crystalline silicon is seen throughout the SiC layer. The SiC peaks do not split, however peak deconvolution indicates the presence of a relatively small 6H peak.

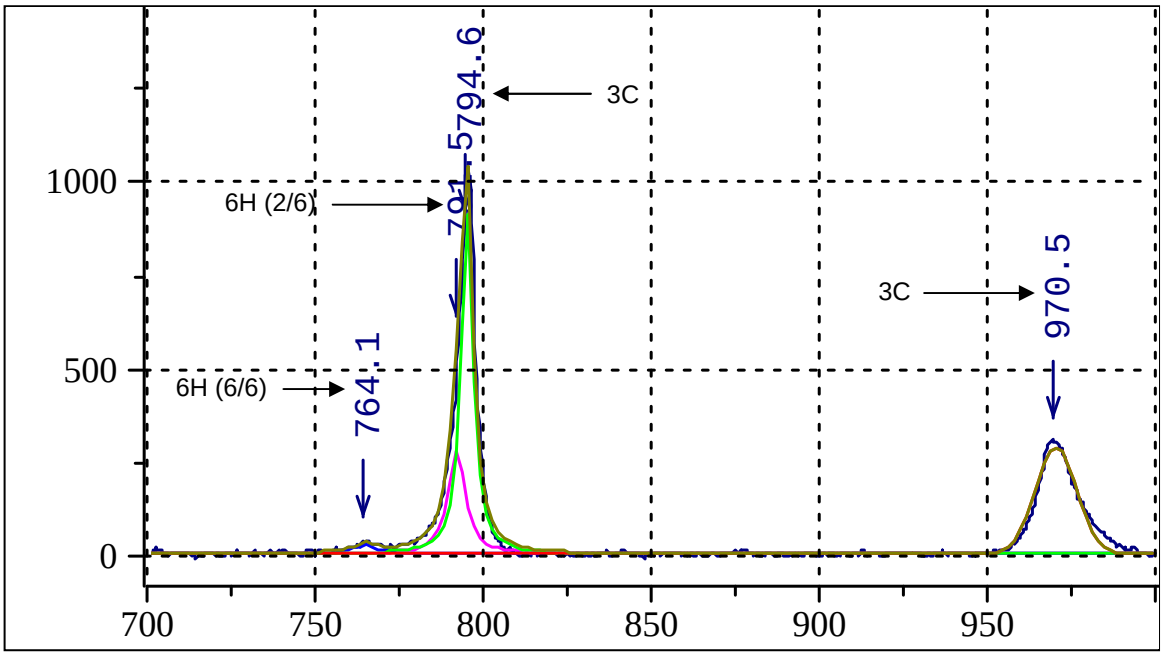

Raman spectra of the TO SiC peaks after deconvolution for analysis 5A (etched). It was assumed that there were two components making up the main peak. The peaks indicate the presence of the 3C and 6H polytypes.

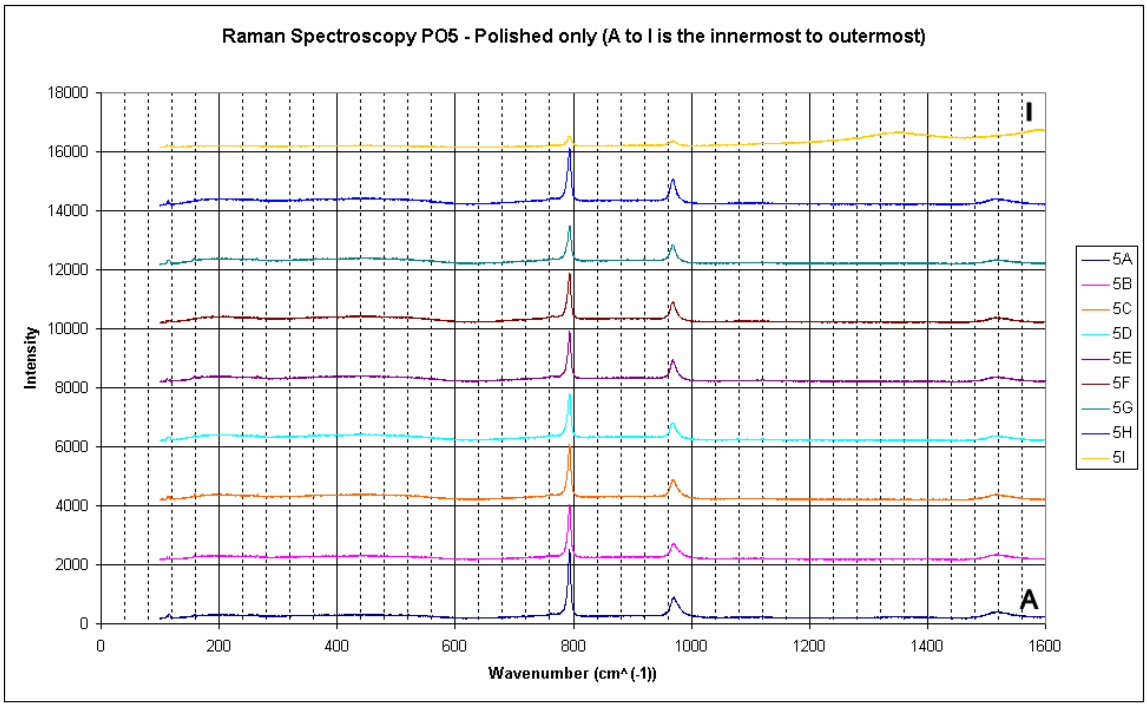

Raman spectra of the SiC coating of PO5 polished coated particle. A is the innermost and I is the outermost spot along the SiC cross-section. Neither the amorphous nor crystalline silicon is seen throughout the SiC layer. The SiC peaks do not split, however peak deconvolution indicates the presence of a relatively small 6H peak. Graphite is only seen at analysis I.

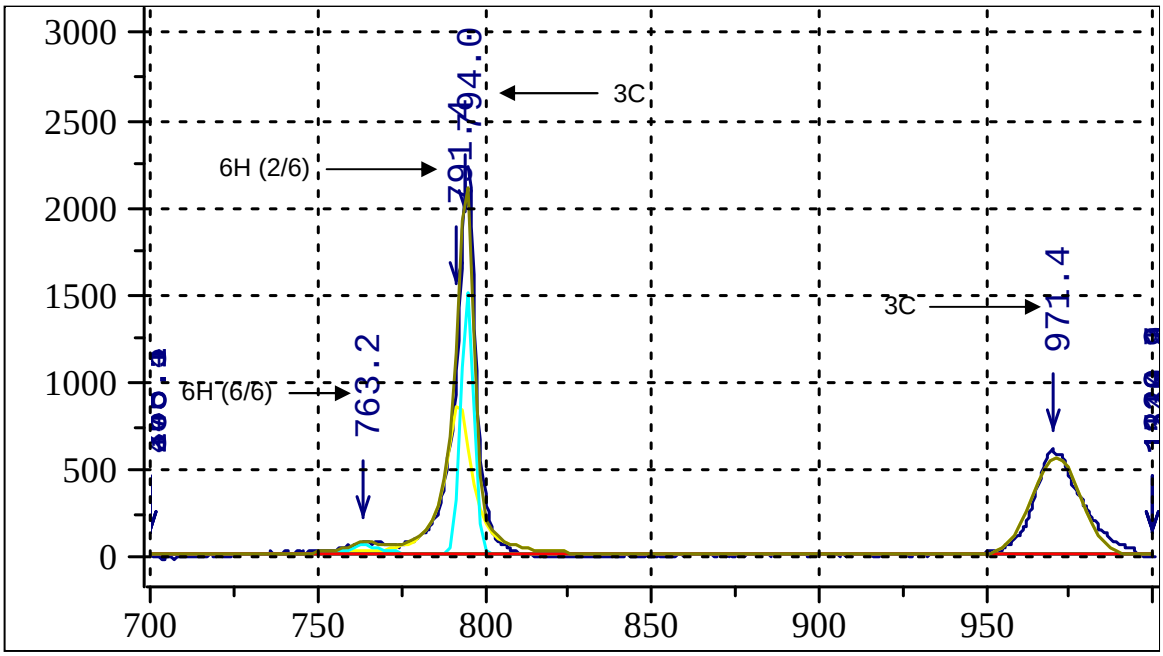

Raman spectra of the TO SiC peaks after deconvolution for analysis 5A (polished). It was assumed that there were two components making up the main peak. The peaks indicate the presence of the 3C and 6H polytypes.

Sample PO6

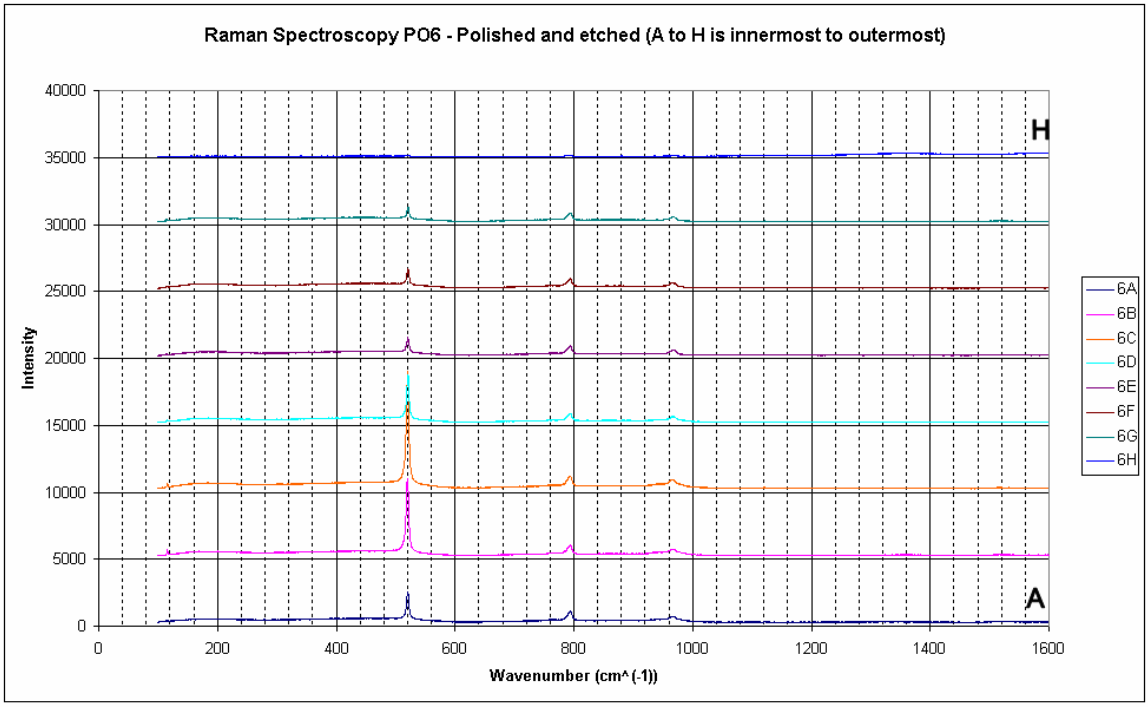

Raman spectra of the SiC coating of PO6 etched and polished coated particle. A is the innermost and H is the outermost spot along the SiC cross-section. The crystalline silicon progressively increases from analysis A to C before declining again. The silicon to SiC ratio of peaks is particularly high relative to that of other samples. Consequently, there is very little that can be said about the SiC peaks. There is a hint of graphite detected from the slight change of slope from analysis B.

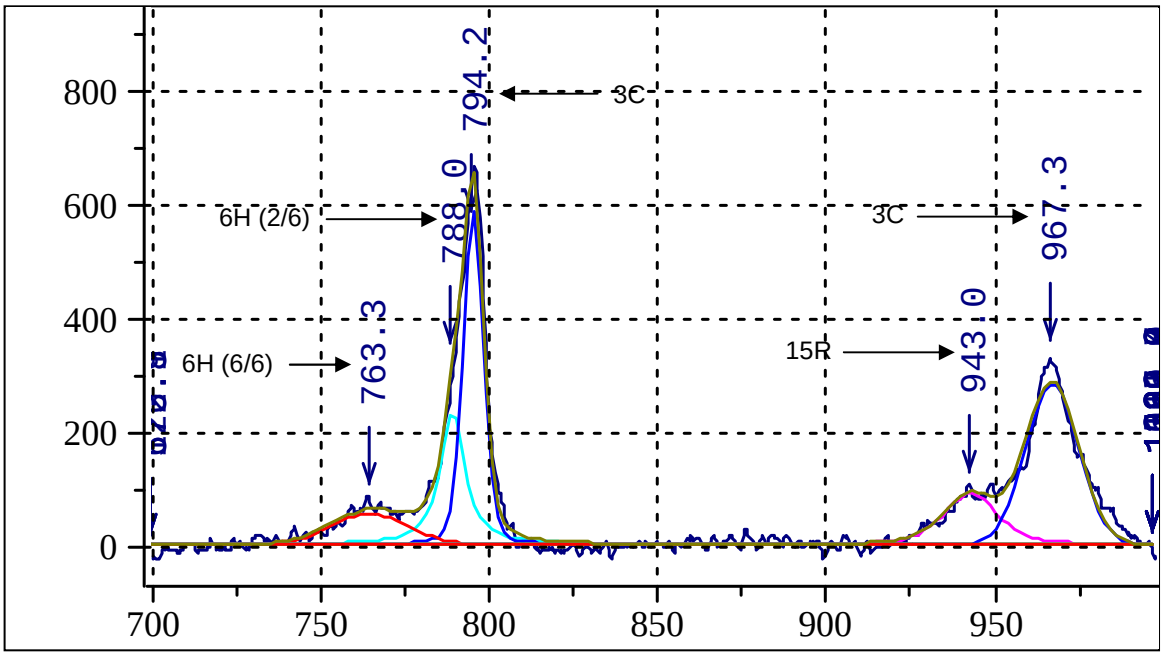

Raman spectra of the TO SiC peaks after deconvolution for analysis 6A (etched). It was assumed that there were two components making up the main peak. The peaks indicate the presence of the 3C and 6H polytypes.

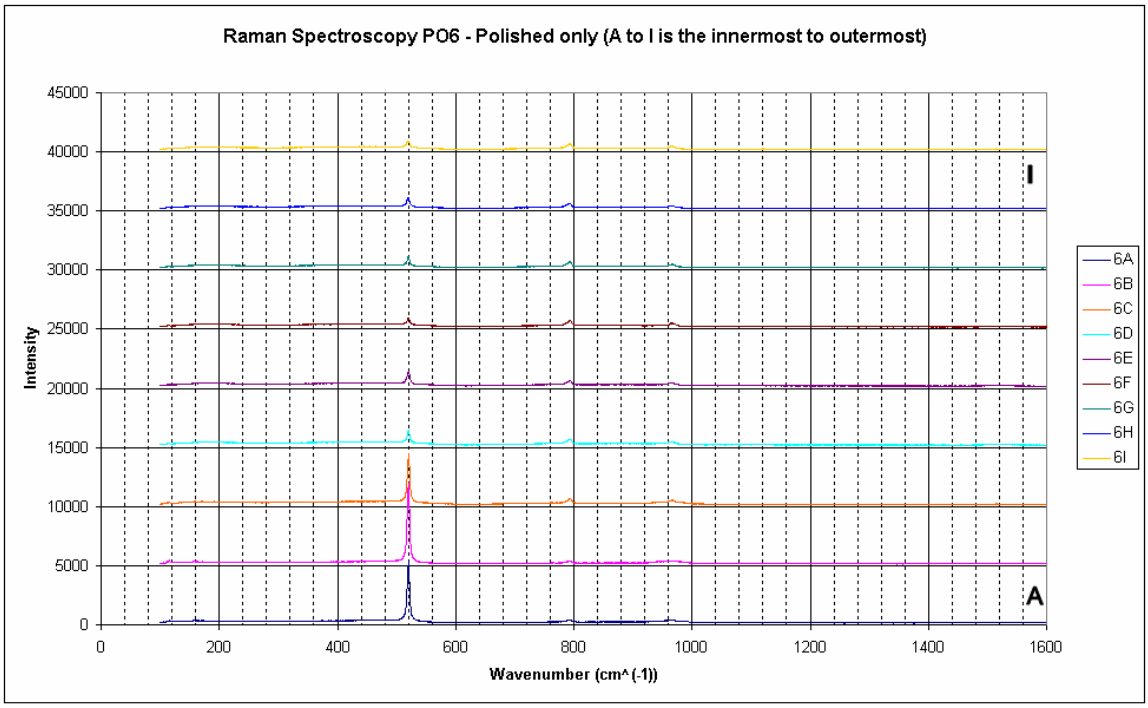

Raman spectra of the SiC coating of PO6 polished coated particle. A is the innermost and I is the outermost spot along the SiC cross-section. The crystalline silicon increases from analysis A to B before progressively declining up to analysis I. The silicon to SiC ratio of some peaks is particularly high relative to that of other samples. There is no evidence of graphite.

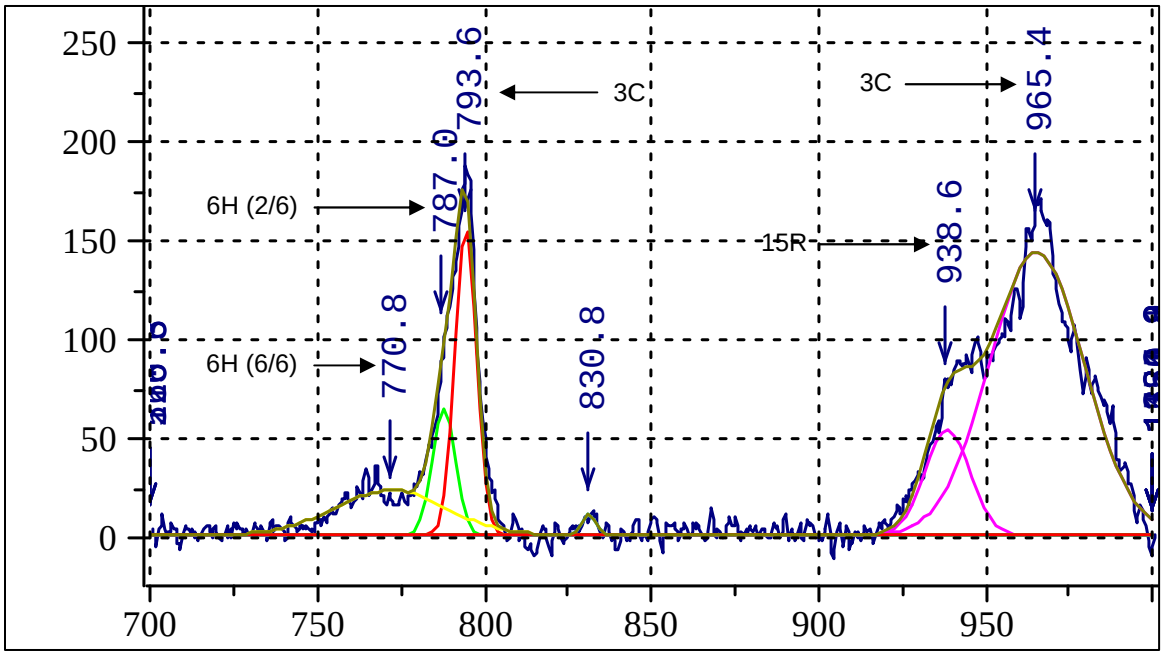

Raman spectra of the TO SiC peaks after deconvolution for analysis 6A (polished). It was assumed that there were two components making up the main peak. The peaks indicate the presence of the 3C and 6H polytypes.

Sample PO8

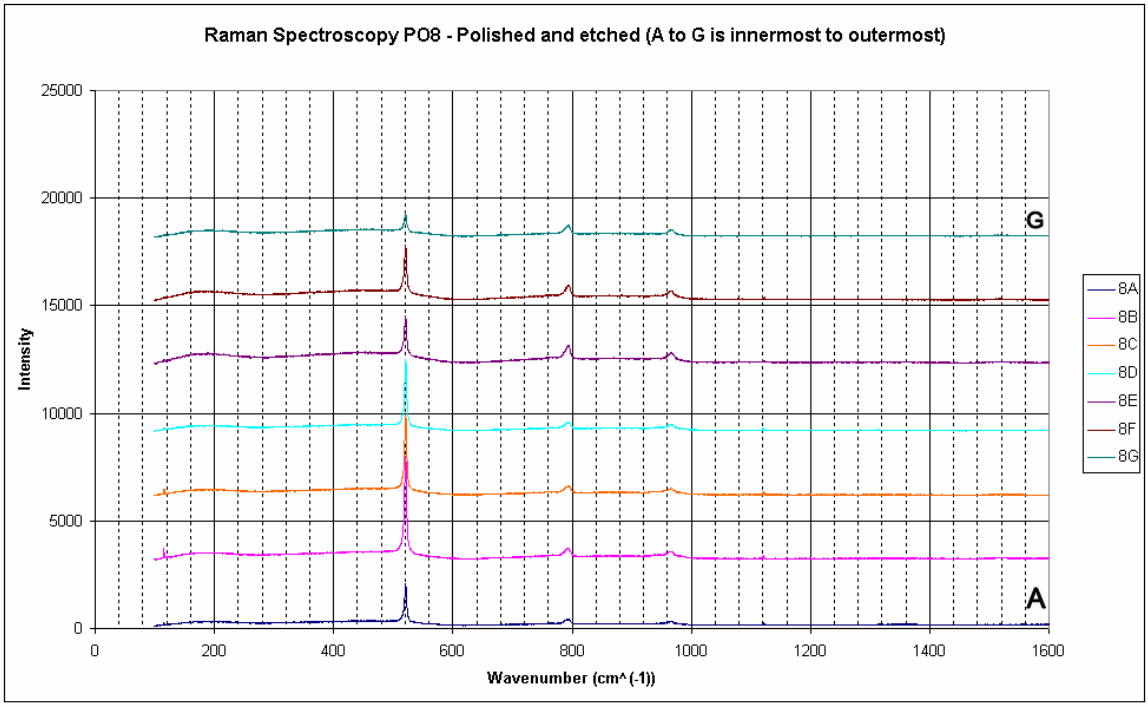

Raman spectra of the SiC coating of PO8 etched and polished coated particle. A is the innermost and G is the outermost spot along the SiC cross-section. The crystalline silicon increases from analysis A to C before progressively declining up to analysis G. The silicon to SiC ratio of peaks is particularly high relative to that of other samples, with the exception of sample PO6. There is little detail that can be extracted from the SiC peaks. There is no evidence of graphite being present.

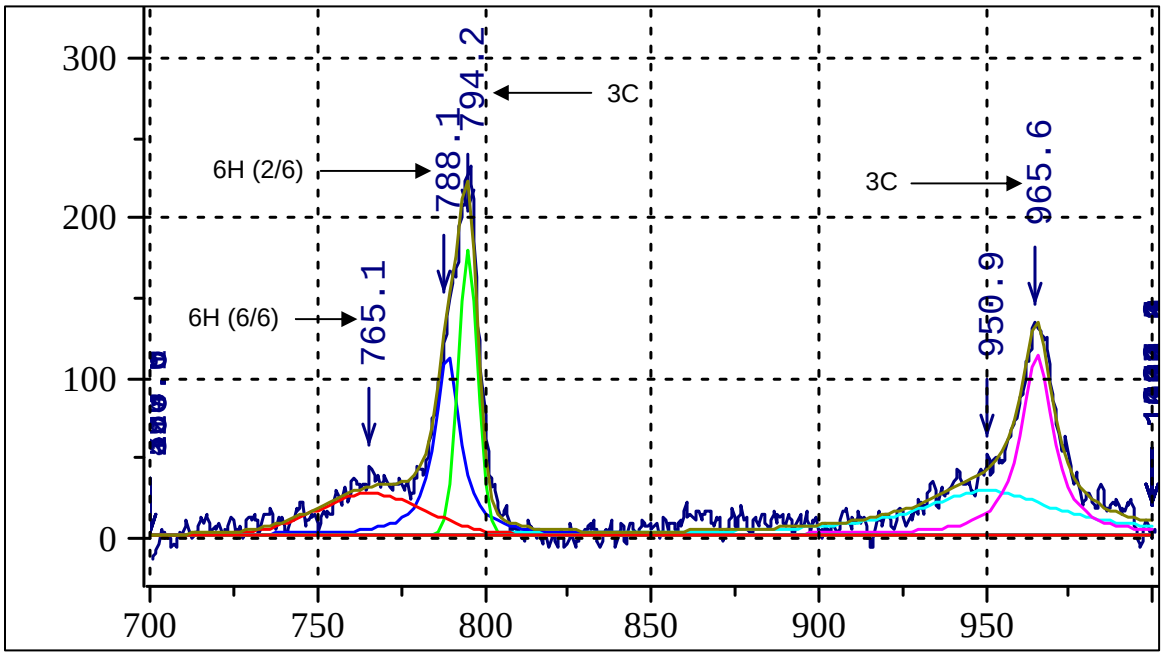

Raman spectra of the TO SiC peaks after deconvolution for analysis 8A (etched). It was assumed that there were two components making up the main peak. The peaks indicate the presence of the 3C and 6H polytypes.

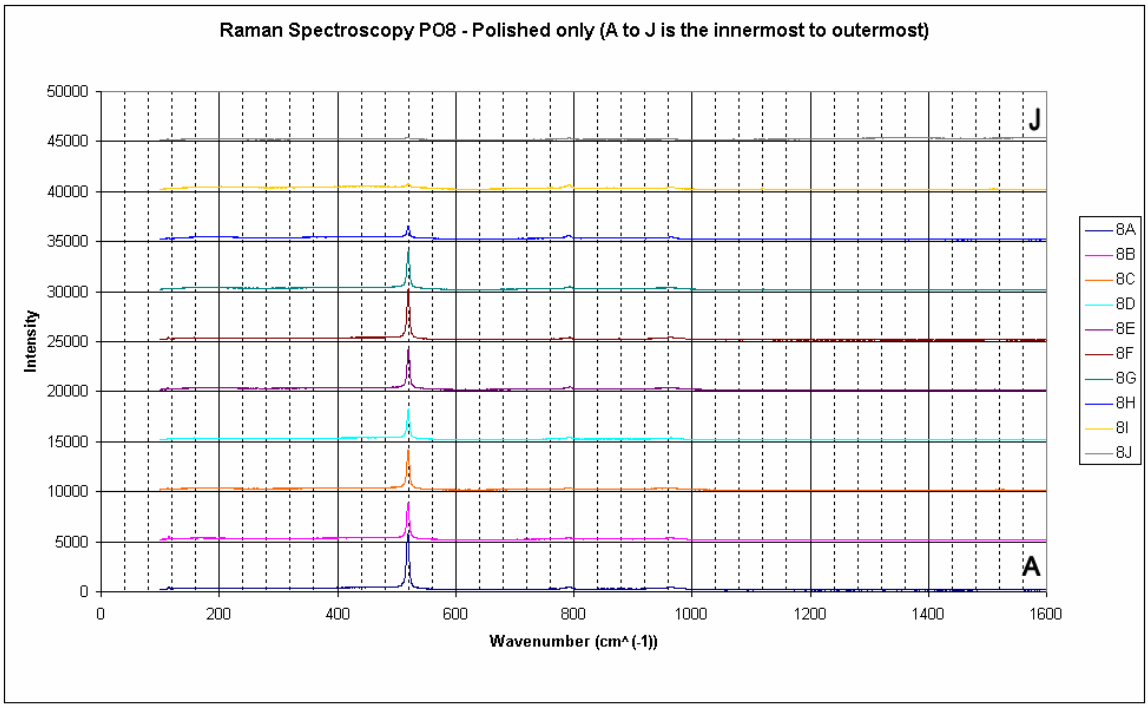

Raman spectra of the SiC coating of PO8 polished coated particle. A is the innermost and J is the outermost spot along the SiC cross-section. The crystalline silicon progressively increases from analysis A to G, before declining up to analysis J. As with the etched sample, the silicon to SiC ratio of peaks is particularly high relative to that of other samples, with the exception of sample PO6. There is little that can be concluded regarding the SiC peaks. There is no evidence of graphite being present.

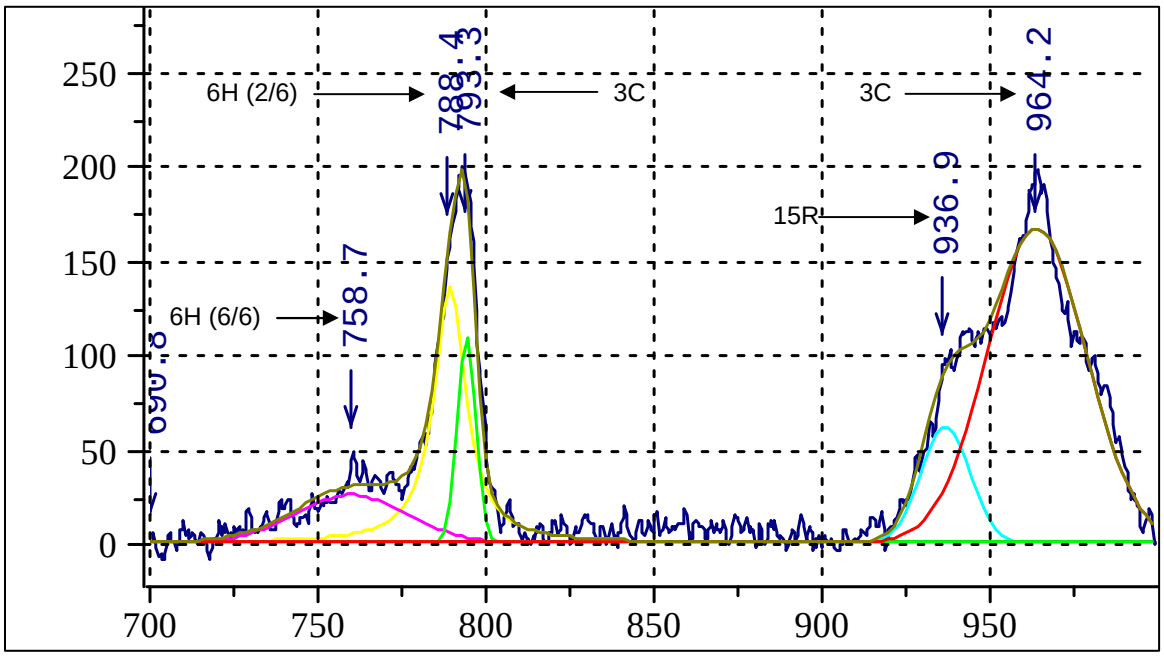

Raman spectra of the TO SiC peaks after deconvolution for analysis 8A (polished). It was assumed that there were two components making up the main peak. The peaks indicate the presence of the 3C and 6H polytypes.

Sample PO9

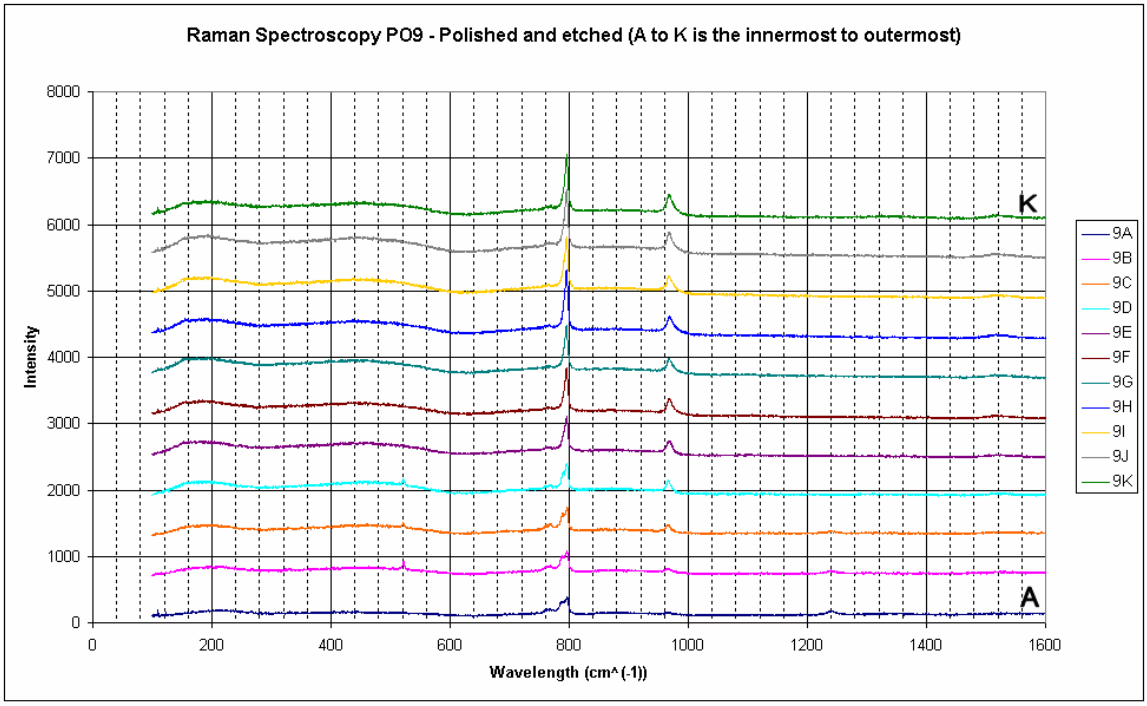

Raman spectra of the SiC coating of PO9 etched and polished coated particle. A is the innermost and K is the outermost spot along the SiC cross-section. Amorphous silicon is generally found throughout the analyses. Small peaks of crystalline silicon are also found along the inner parts of the SiC layer. Peak splitting is clearly more evident along the inner parts of the SiC layer. The SiC peak intensity also increases outwards reaching the maximum at analysis K. This is thought to be as a result of crystallinity and absorption. There is no evidence of graphite.

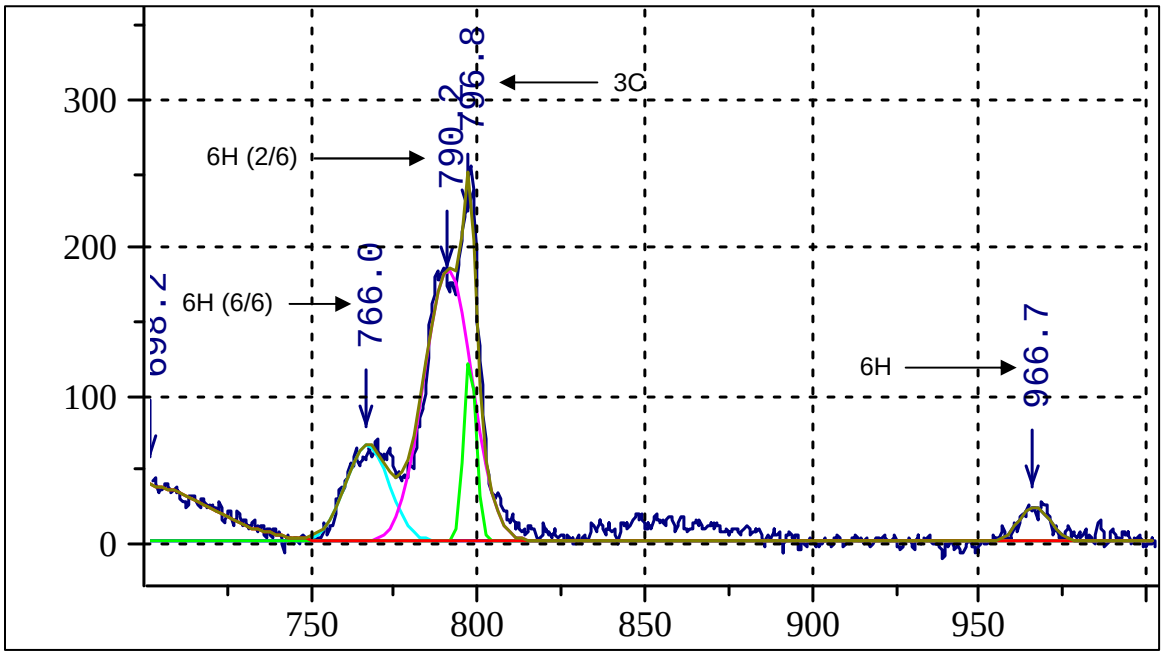

Raman spectra of the TO SiC peaks after deconvolution for analysis 9A (etched). It was assumed that there were two components making up the main peak. The peaks indicate the presence of the 3C and 6H polytypes.

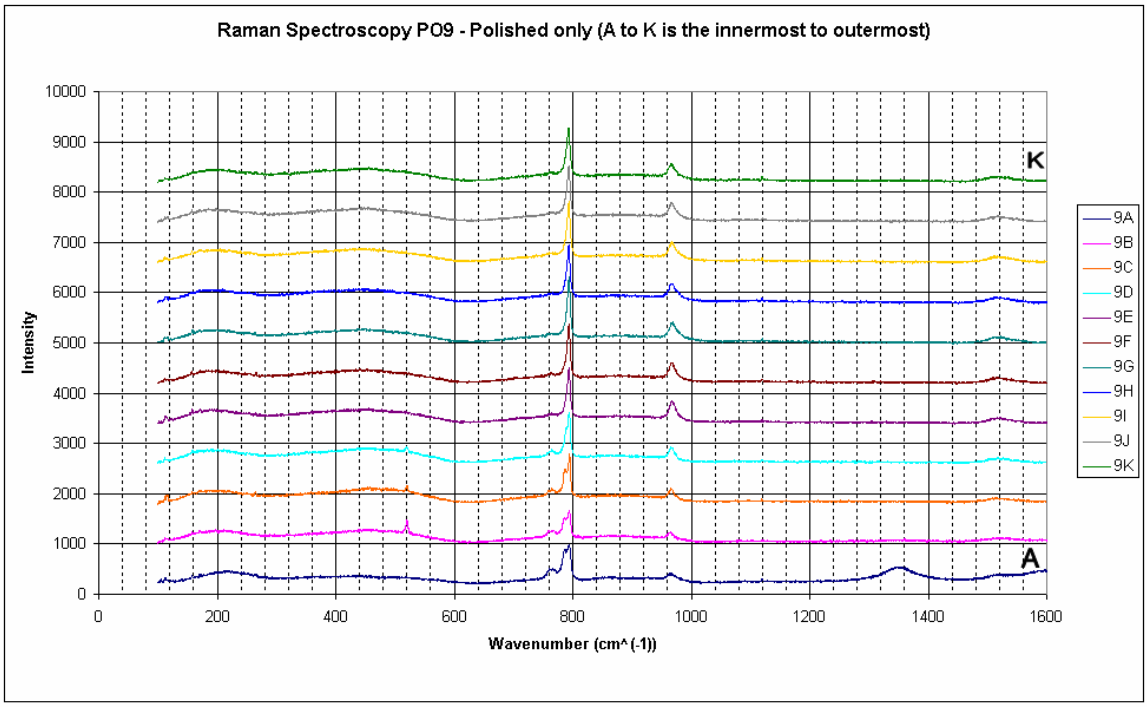

Raman spectra of the SiC coating of PO9 polished coated particle. A is the innermost and K is the outermost spot along the SiC cross-section. Amorphous silicon is generally found throughout the analyses. Small peaks of crystalline silicon are also found along the inner parts of the SiC layer. As with the etched sample, peak splitting is more evident along the inner parts of the SiC layer. Unlike with the etched sample, the SiC peak intensity remains rather consistent throughout the analyses. Graphite is only seen from analysis A.

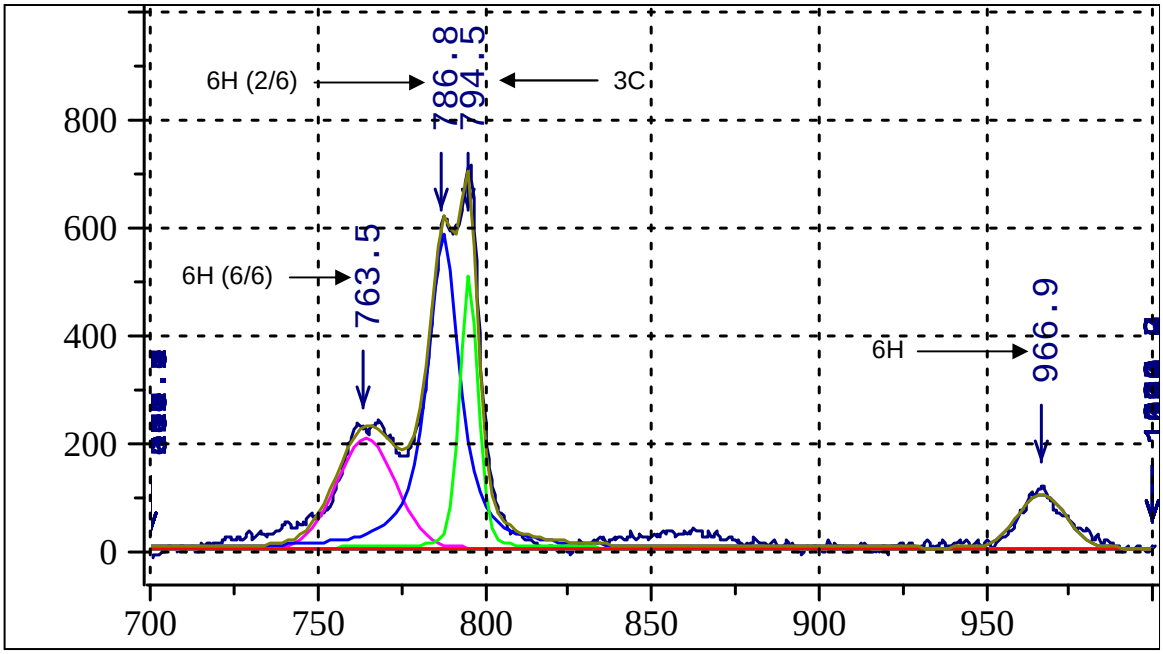

Raman spectra of the TO SiC peaks after deconvolution for analysis 9A (polished). It was assumed that there were two components making up the main peak. The peaks indicate the presence of the 3C and 6H polytypes.

Sample PO10

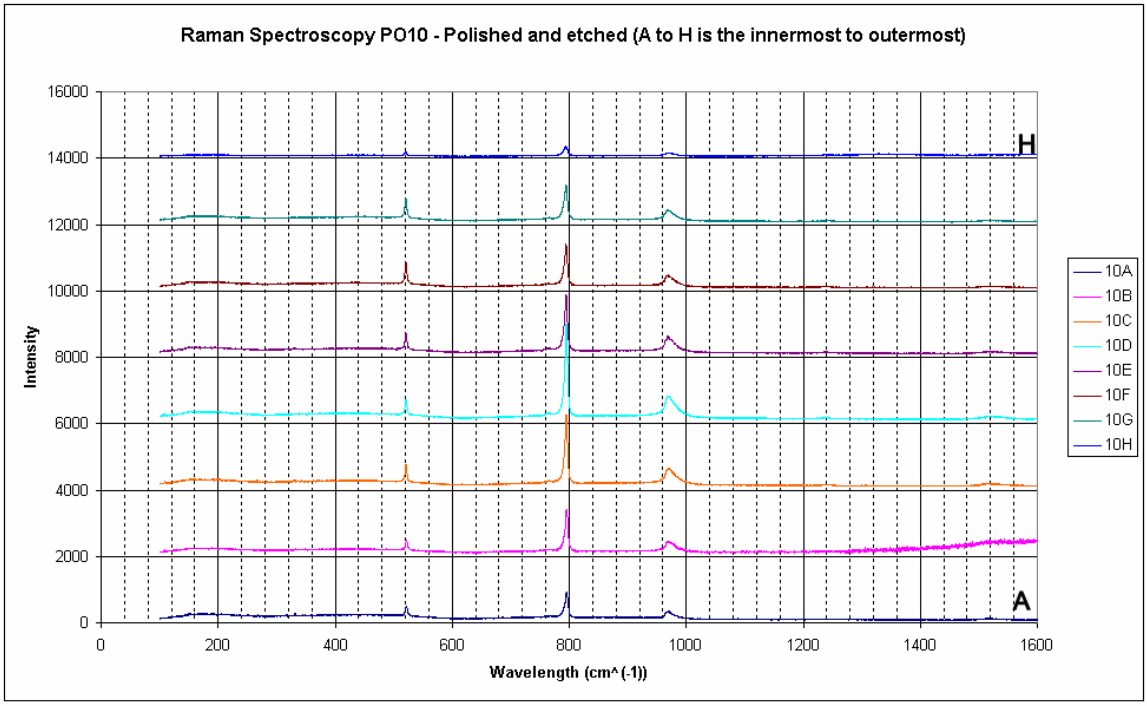

Raman spectra of the SiC coating of PO10 etched and polished coated particle. A is the innermost and H is the outermost spot along the SiC cross-section. Crystalline silicon peaks are evident throughout the analyses. Peak splitting is not evident but is confirmed by the deconvolution. The middle of the SiC layer has the most intense SiC peak as a result of improved crystallinity and absorption. There is no evidence of graphite.

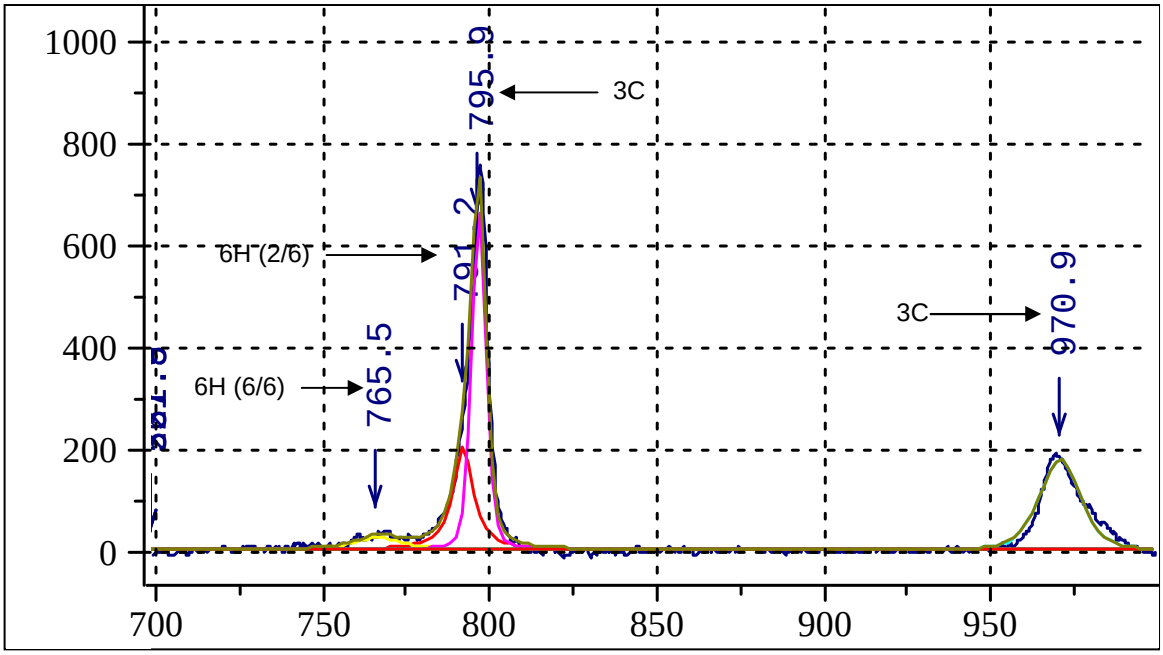

Raman spectra of the TO SiC peaks after deconvolution for analysis 10A (etched). It was assumed that there were two components making up the main peak. The peaks indicate the presence of the 3C and 6H polytypes.

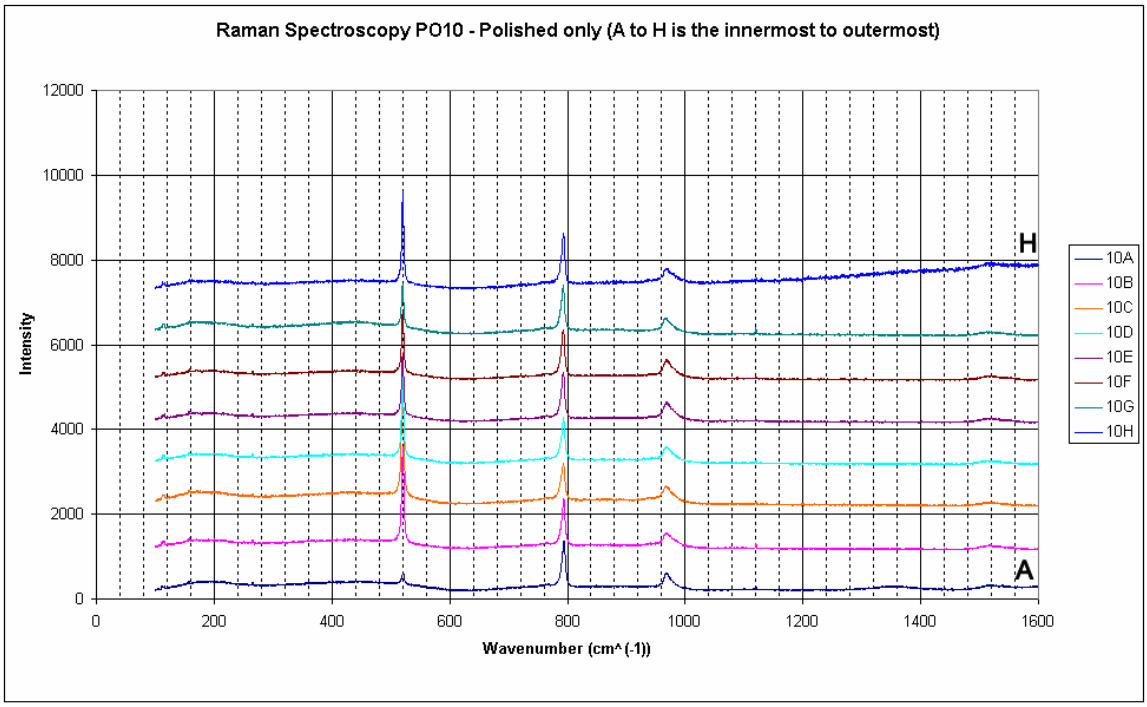

Raman spectra of the SiC coating of PO10 polished coated particle. A is the innermost and H is the outermost spot along the SiC cross-section. Crystalline silicon peaks are evident throughout the analyses. Unlike with the etched sample the silicon peaks vary significantly, with a maximum at analysis B. Peak splitting is not evident but is confirmed by the deconvolution. Also in contrast to the etched sample, the SiC intensities remain fairly consistent. There is no evidence of graphite.

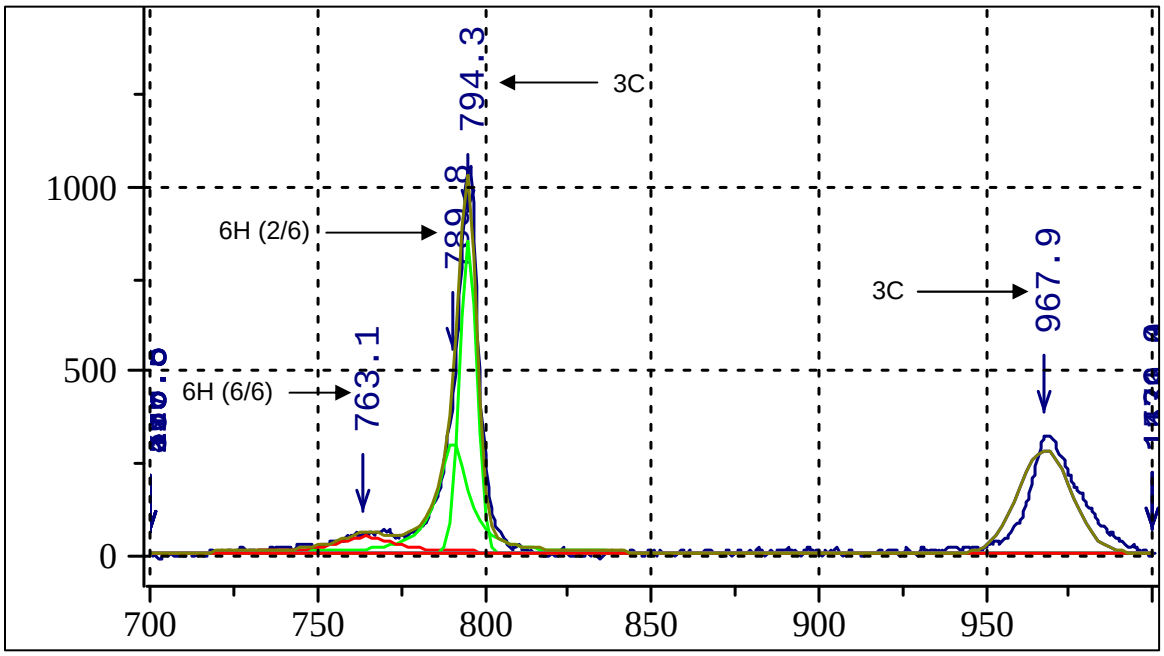

Raman spectra of the TO SiC peaks after deconvolution for analysis 10A (polished). It was assumed that there were two components making up the main peak. The peaks indicate the presence of the 3C and 6H polytypes.

APPENDIX B
XRD 3C NECSA sample & high temperature data

3C NECSA sample

- XRD quantitative analysis in AUTOQUAN

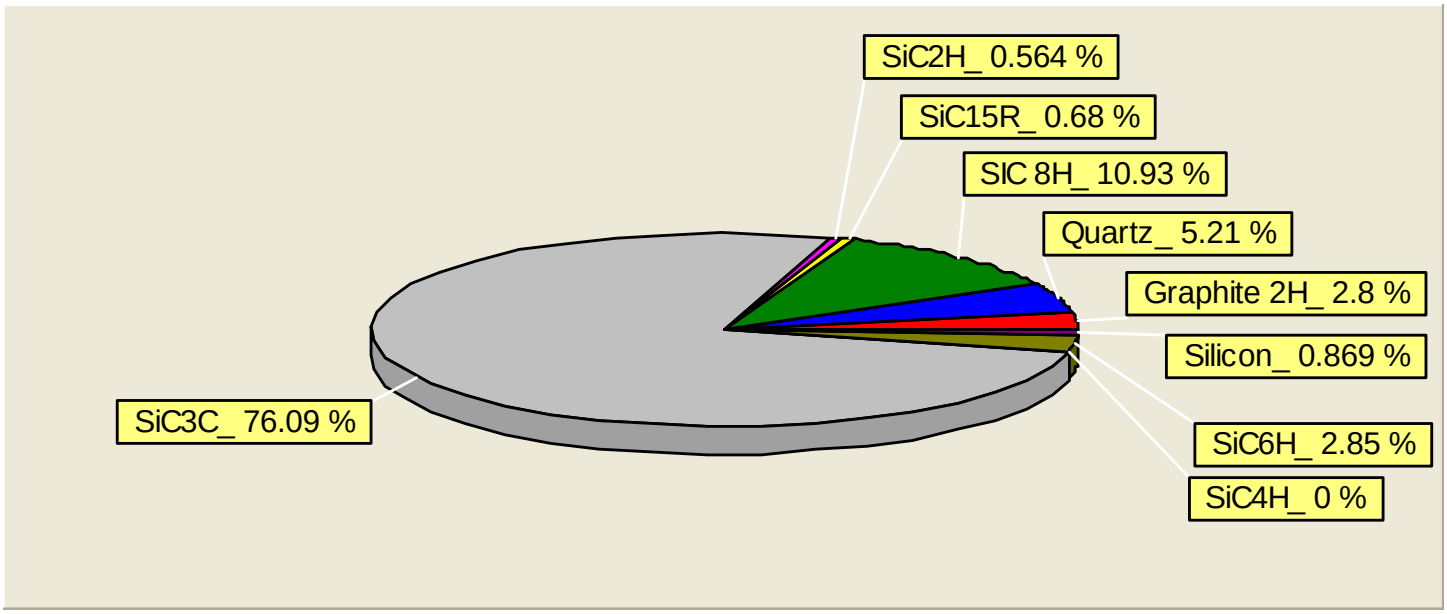

High temperature data

- G102
  - Lattice parameters (units in Å)

EXPERIMENTAL VALUES				
Temp	a - 3C-SiC	a - Al_2O_3	c - Al_2O_3	c - graphite
25	4.361	4.76456	12.99708	7.01469
100	4.36178	4.76635	13.00309	7.02852
200	4.36348	4.76969	13.01653	7.04916
300	4.36505	4.77258	13.02489	7.06377
400	4.36695	4.77593	13.03497	7.0744
500	4.36889	4.77918	13.05006	7.08981
600	4.37059	4.78293	13.06044	7.1058
700	4.37241	4.78657	13.07039	7.11968
800	4.37448	4.78987	13.08358	7.13734
900	4.37612	4.79342	13.0951	7.15452
1000	4.37801	4.79631	13.10834	7.1728
1100	4.3796	4.79984	13.11777	7.18882
1125	4.38005	4.80082	13.12004	7.19605
1150	4.38054	4.80143	13.12284	7.19713
1175	4.38123	4.80195	13.12613	7.20159
1200	4.38165	4.80285	13.12948	7.18689
1225	4.38206	4.804	13.12936	7.20292
1250	4.3826	4.80502	13.13498	7.19772
1275	4.38338	4.80659	13.13886	7.19527
1300	4.38363	4.80623	13.14206	7.21384
1325	4.38439	4.80691	13.1445	7.21233
1350	4.38461	4.80741	13.14245	7.21976
1375	4.38533	4.80837	13.14965	7.22768
1400	4.38569	4.81056	13.15212	7.2051
1400	4.38569	4.81056	13.15212	7.2051
1350	4.38515	4.80845	13.15067	7.16657
1300	4.38392	4.80744	13.14543	7.17392
1250	4.38308	4.80602	13.13871	7.15682
1200	4.38213	4.80438	13.1334	7.14617
1150	4.381	4.80233	13.12732	7.13675
1100	4.38007	4.80044	13.121	7.14869
26	4.36032	4.76259	13.00579	6.95403

High temperature data

- PO4
  - Lattice parameters (units in Å)

EXPERIMENTAL VALUES				
T	a - Al_2O_3	c - Al_2O_3	a-SiC	c-graphite
25	4.76112	12.991	4.35961	6.90744
100	4.76367	13.00066	4.36174	6.9206
200	4.76639	13.00855	4.36243	6.93873
300	4.76998	13.01769	4.36444	6.96462
400	4.77309	13.02669	4.3661	6.98457
500	4.77574	13.03619	4.36763	6.99705
600	4.77874	13.04637	4.36929	7.01692
700	4.78245	13.05822	4.37153	7.0401
800	4.78576	13.06687	4.37335	7.05911
900	4.78873	13.07505	4.37494	7.07995
1000	4.79196	13.08348	4.37637	7.095
1100	4.79474	13.09292	4.37808	7.11209
1125	4.79589	13.09663	4.3786	7.11849
1150	4.79643	13.09642	4.37853	7.12101
1175	4.79729	13.09927	4.37895	7.125
1200	4.79838	13.10301	4.37977	7.12981
1225	4.79914	13.10683	4.38014	7.13532
1250	4.79975	13.10927	4.38056	7.13836
1275	4.80077	13.11273	4.38072	7.14048
1300	4.80125	13.11557	4.38122	7.14847
1325	4.80226	13.11711	4.3815	7.15292
1350	4.80324	13.12162	4.38198	7.15384
1375	4.80443	13.12518	4.38286	7.1618
1400	4.80577	13.12877	4.38362	7.16708
1400	4.80577	13.12877	4.38362	7.16708
1350	4.80471	13.12379	4.38293	7.1608
1300	4.80318	13.11856	4.38199	7.14987
1250	4.80125	13.11328	4.38111	7.14228
1200	4.79971	13.10852	4.38046	7.13038
1150	4.79836	13.10514	4.377	7.1226
1100	4.79701	13.1003	4.37936	7.11683
26	4.76213	12.99382	4.36063	6.91399

APPENDIX C
TEM images and diffraction patterns

PO 5 Image 1

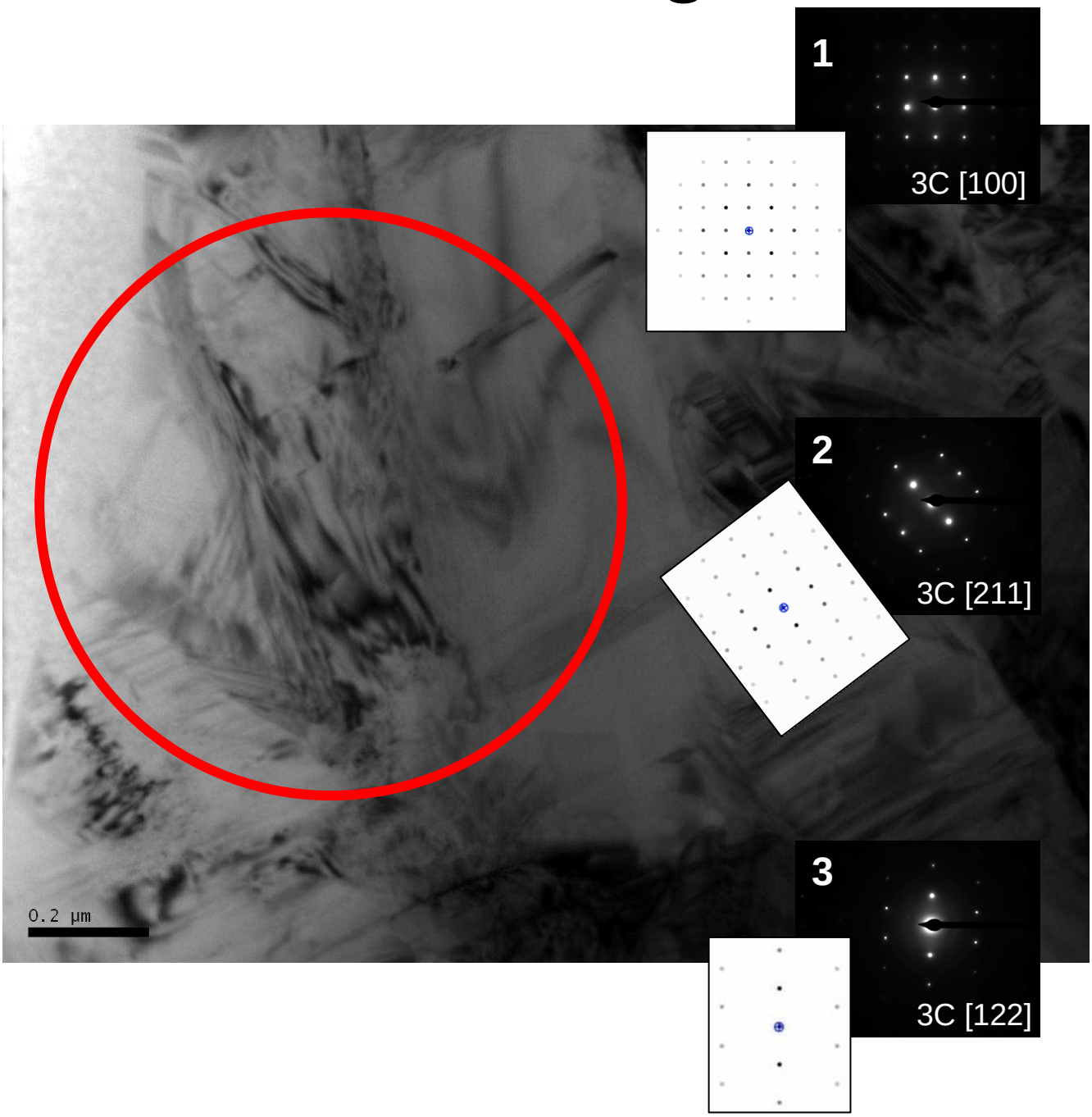

UNIVERSITEIT VAN PRETORIA
UNIVERSITY OF PRETORIA
YUNIBESITHI YA PRETORIA

PO 5 image 2

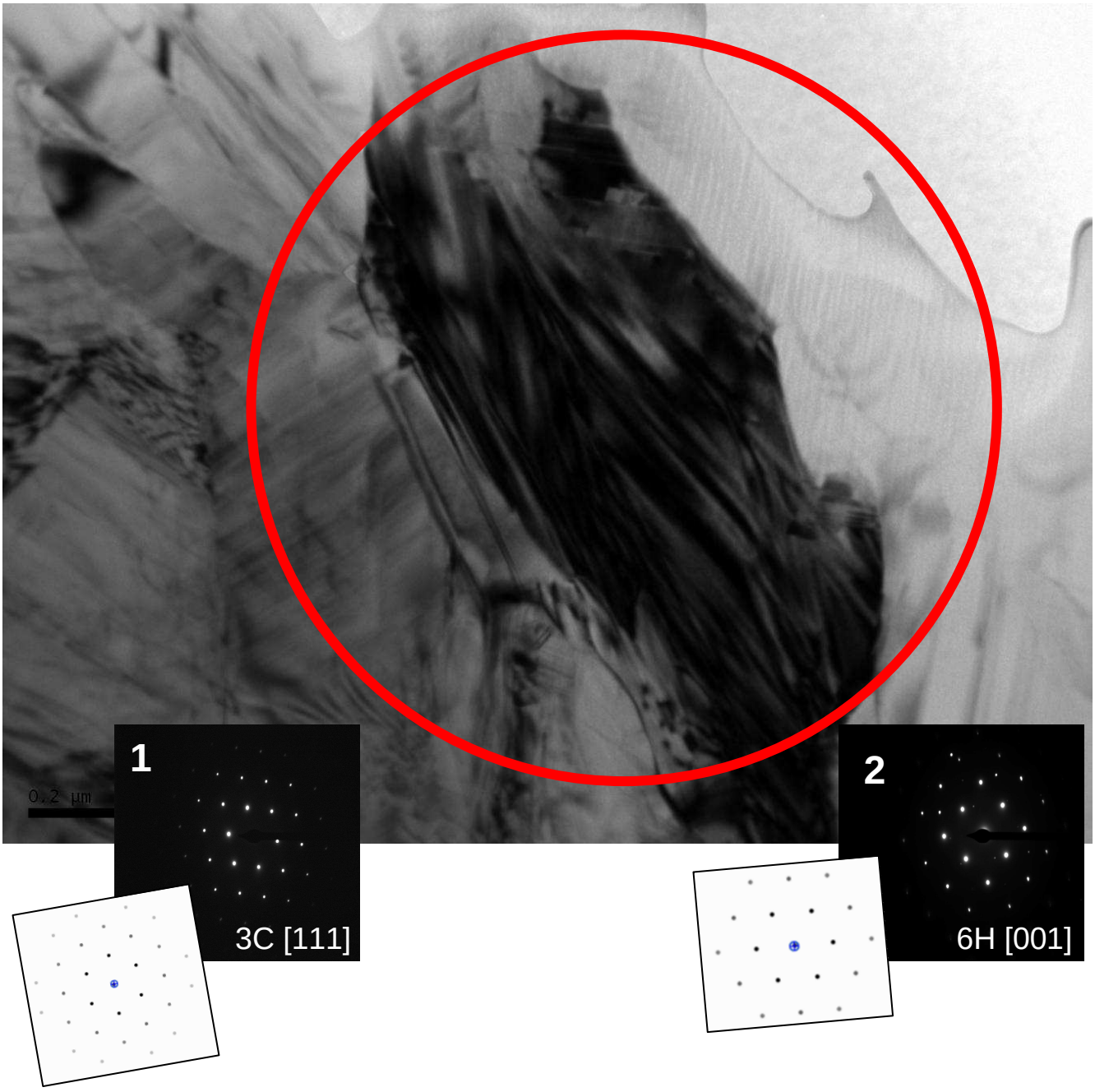

PO5 image 3

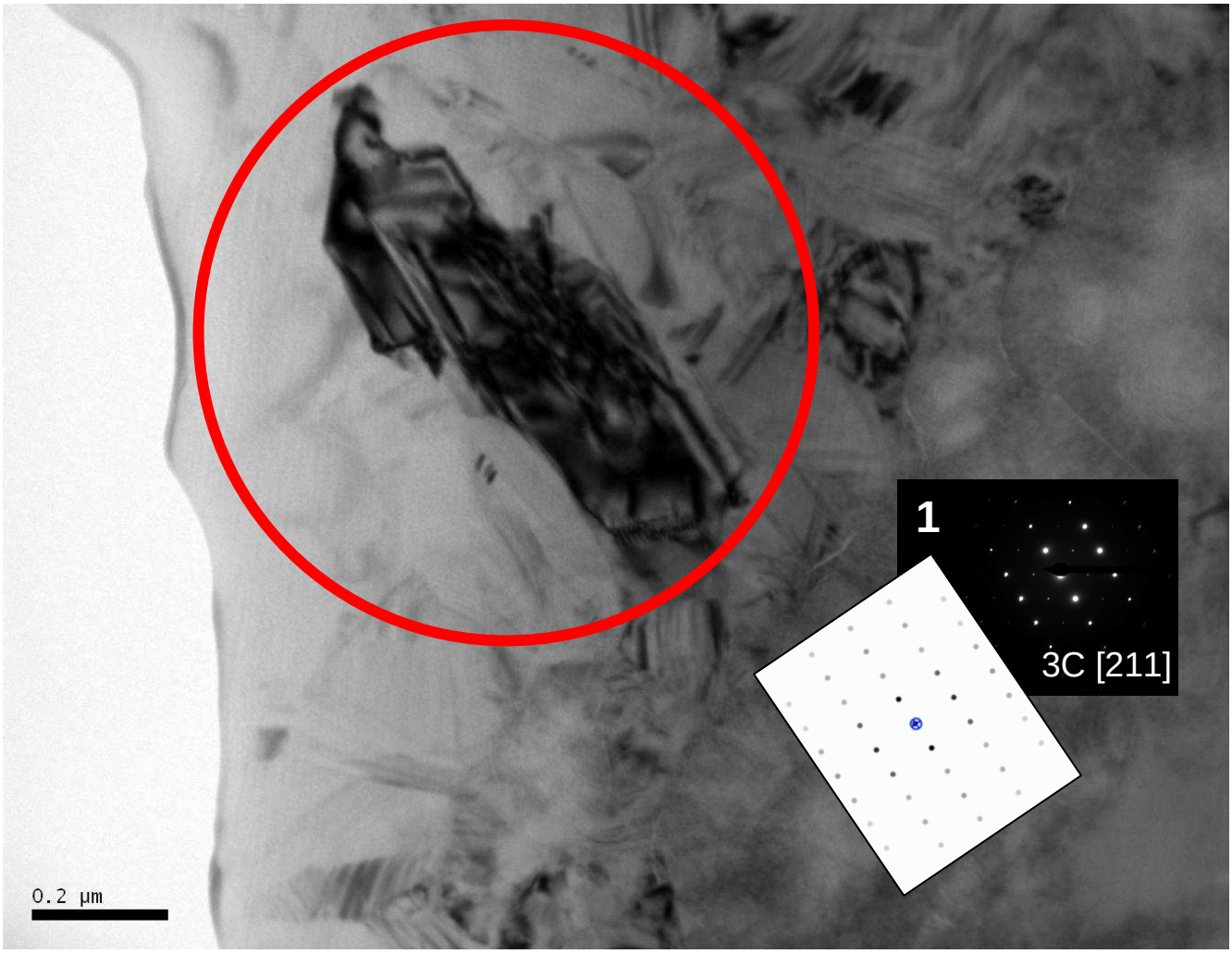

PO5 Image 4

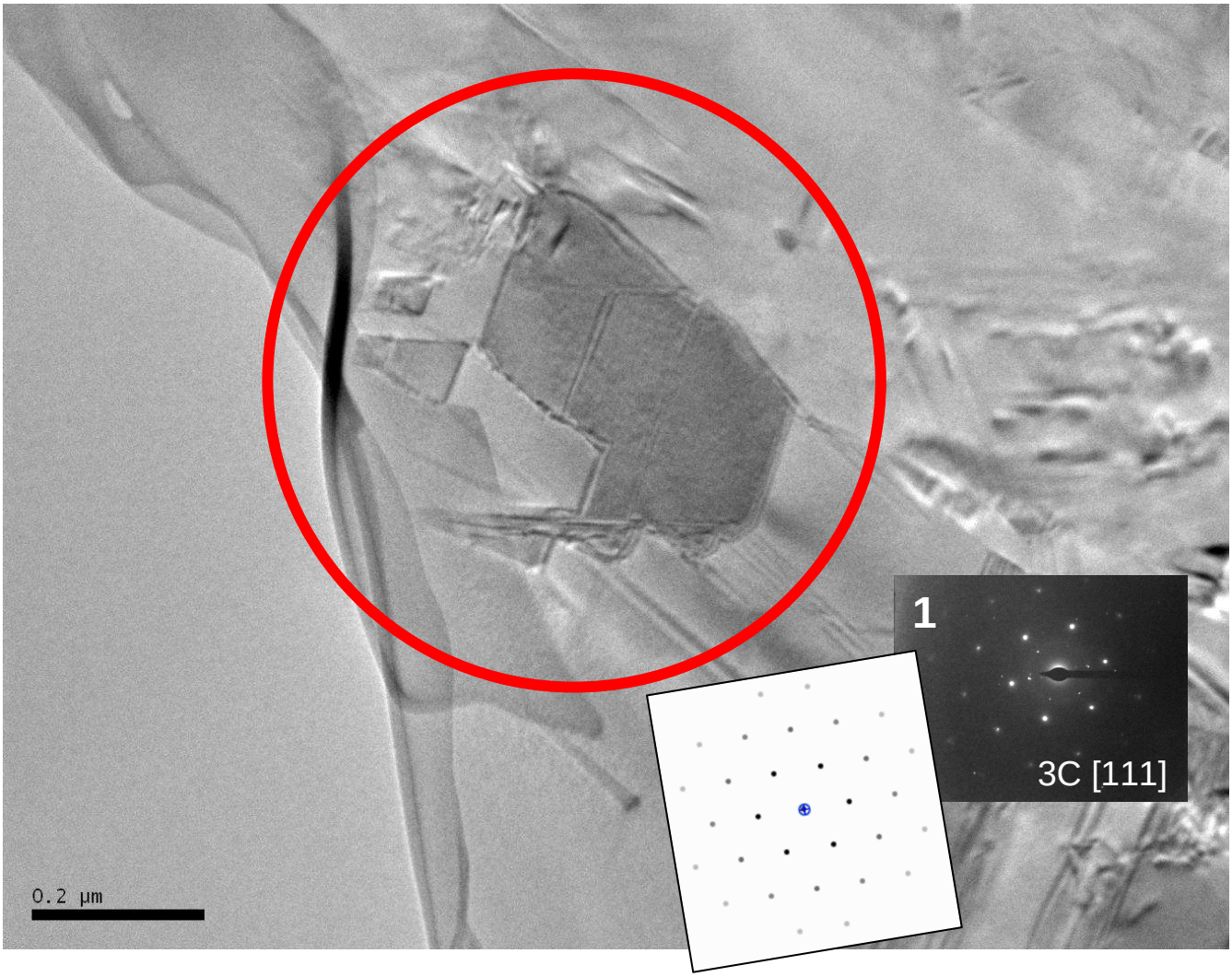

UNIVERSITEIT VAN PRETORIA
UNIVERSITY OF PRETORIA
YUNIBESITHI YA PRETORIA

PO5 Image 5

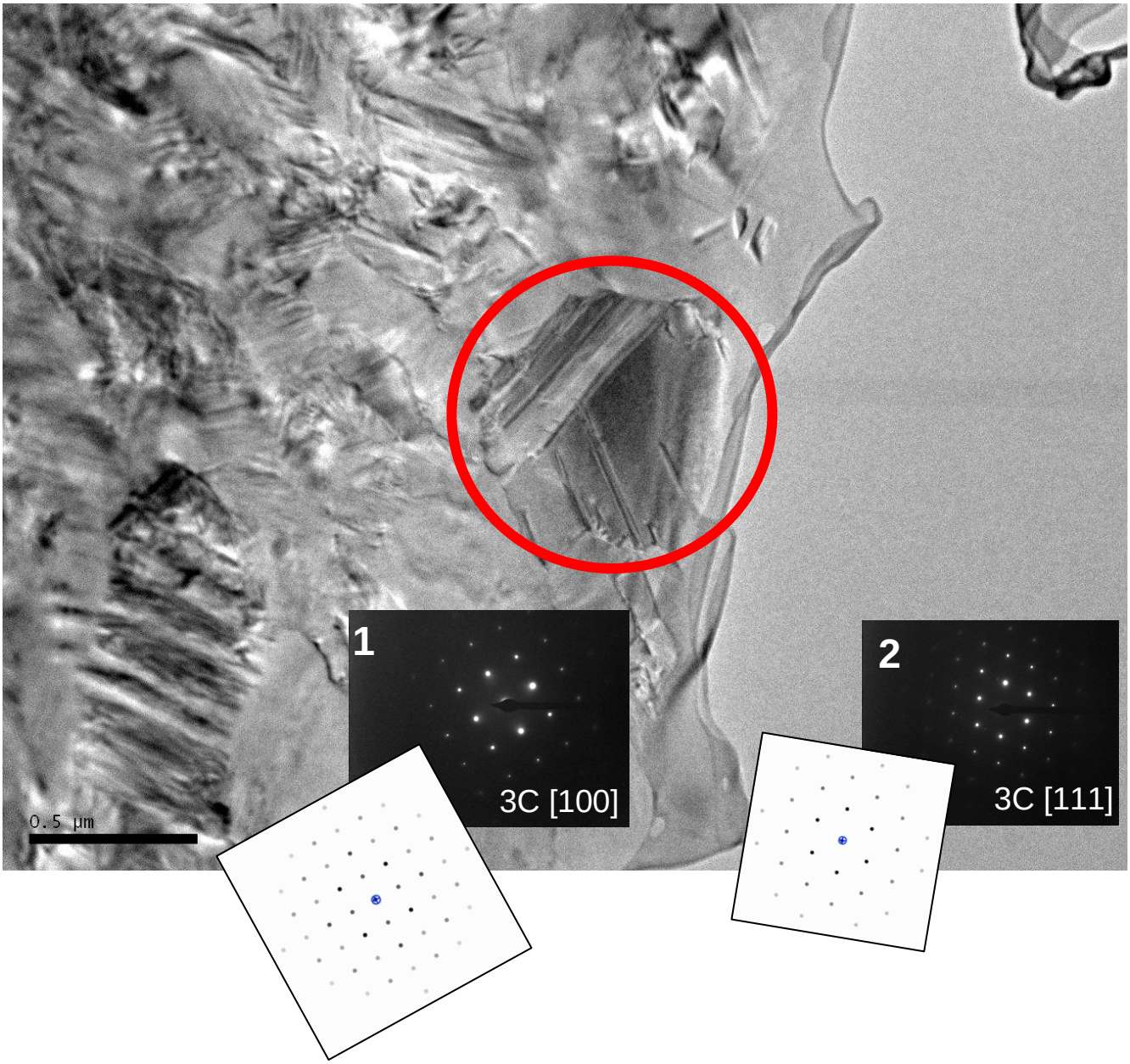

PO5 Image 6

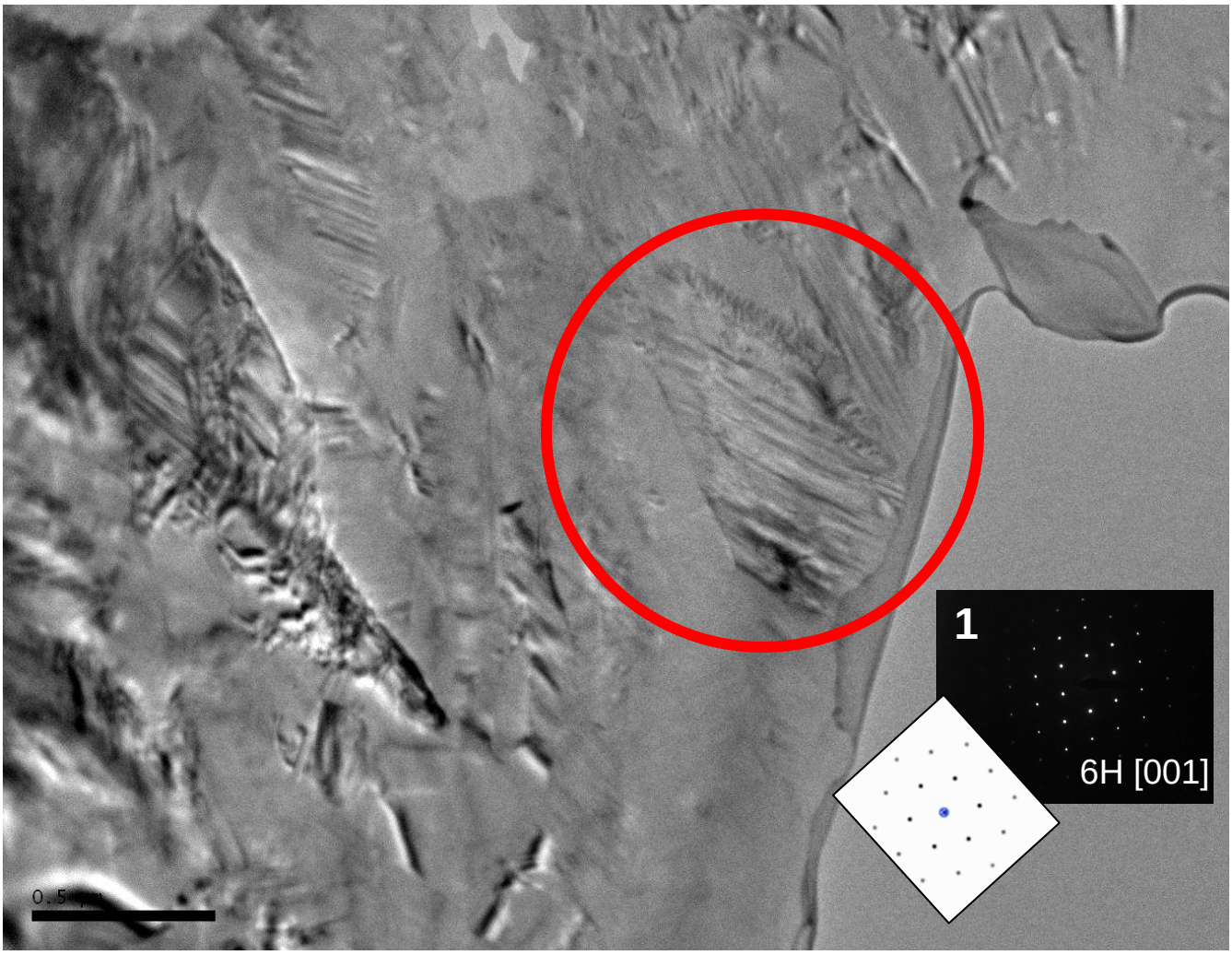

UNIVERSITEIT VAN PRETORIA
UNIVERSITY OF PRETORIA
YUNIBESITHI YA PRETORIA

PO5 Image 7

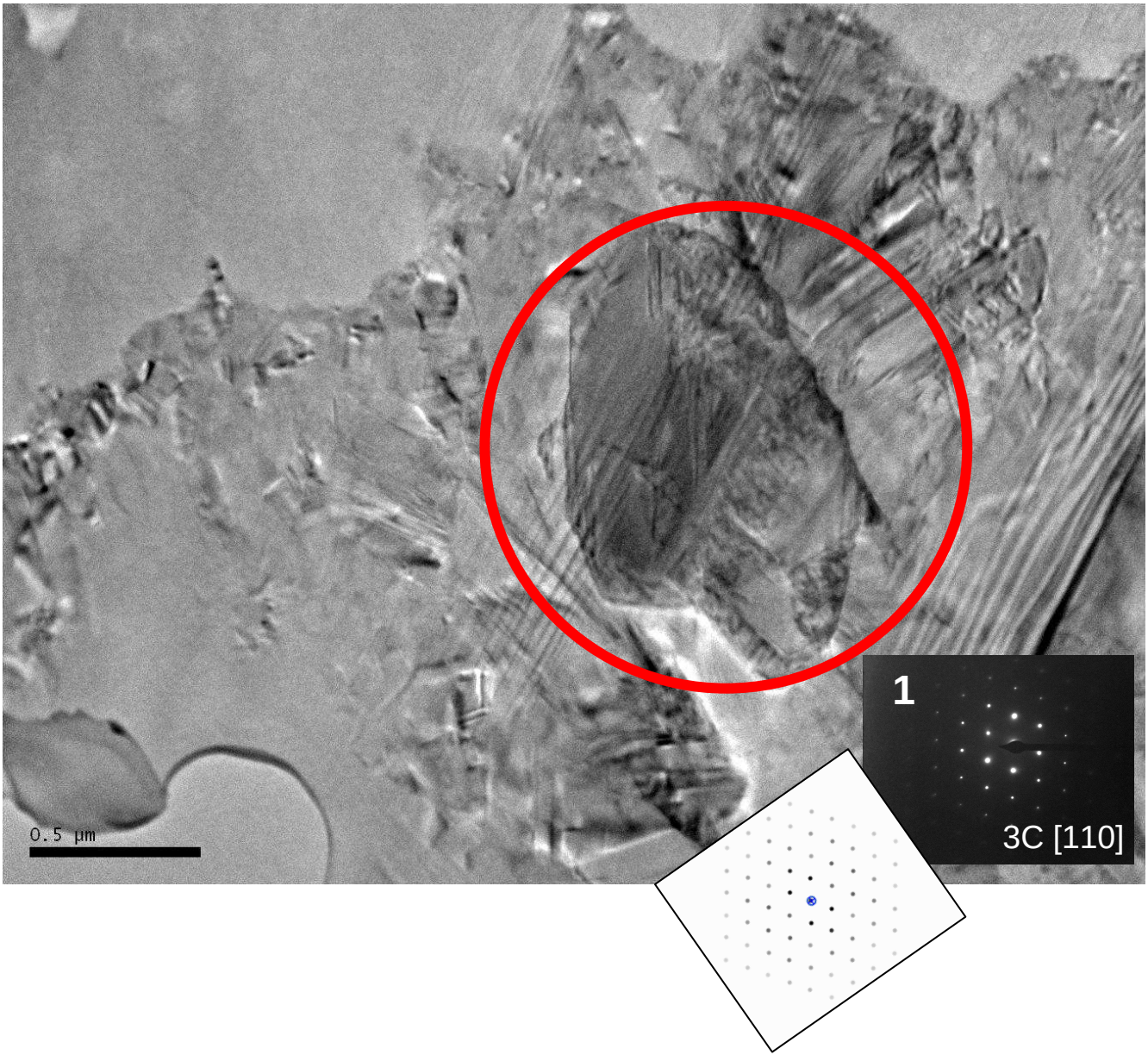

UNIVERSITEIT VAN PRETORIA
UNIVERSITY OF PRETORIA
YUNIBESITHI YA PRETORIA

PO5 Image 8

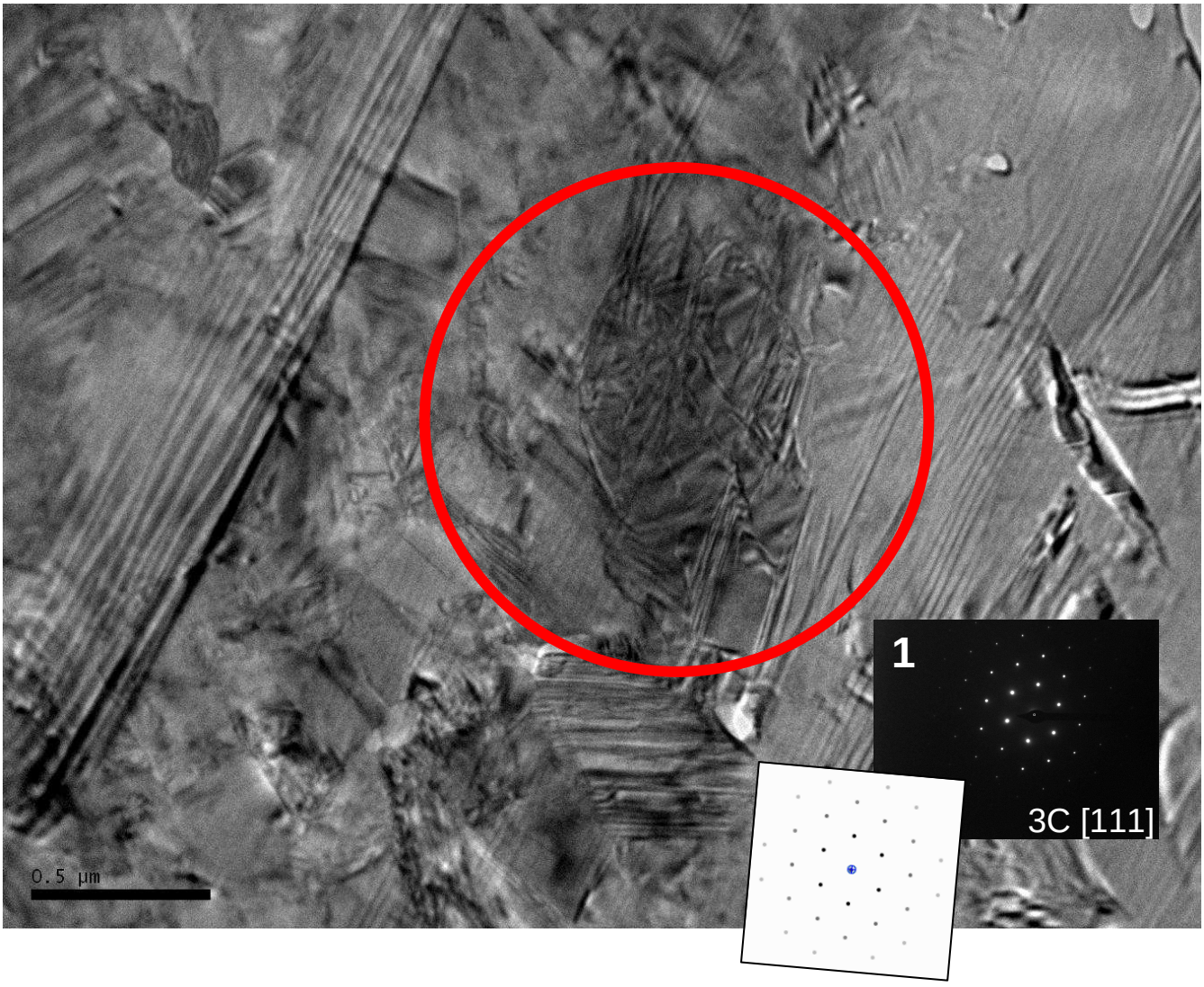

UNIVERSITEIT VAN PRETORIA
UNIVERSITY OF PRETORIA
YUNIBESITHI YA PRETORIA

PO6 Image 1

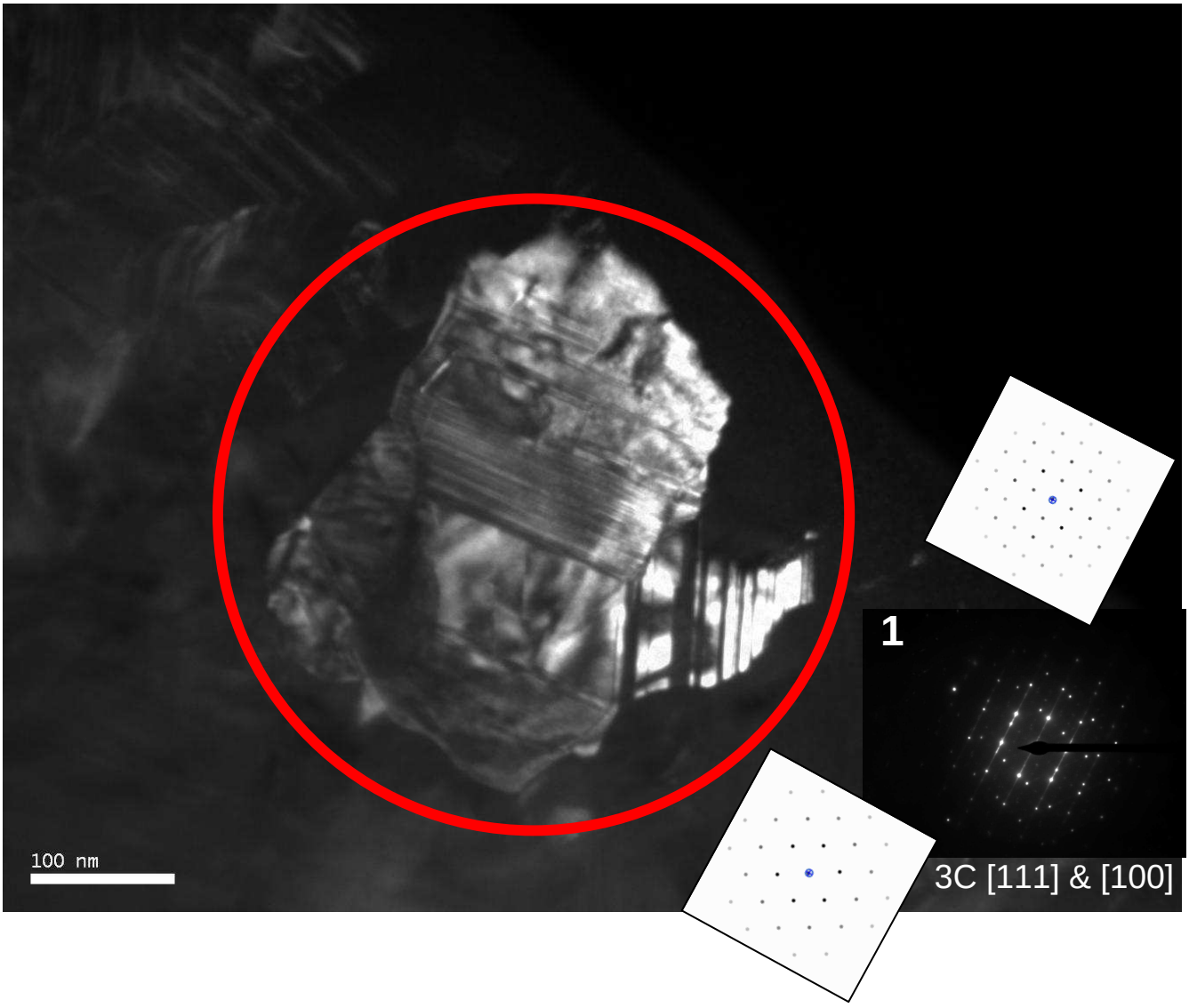

PO6 Image 2

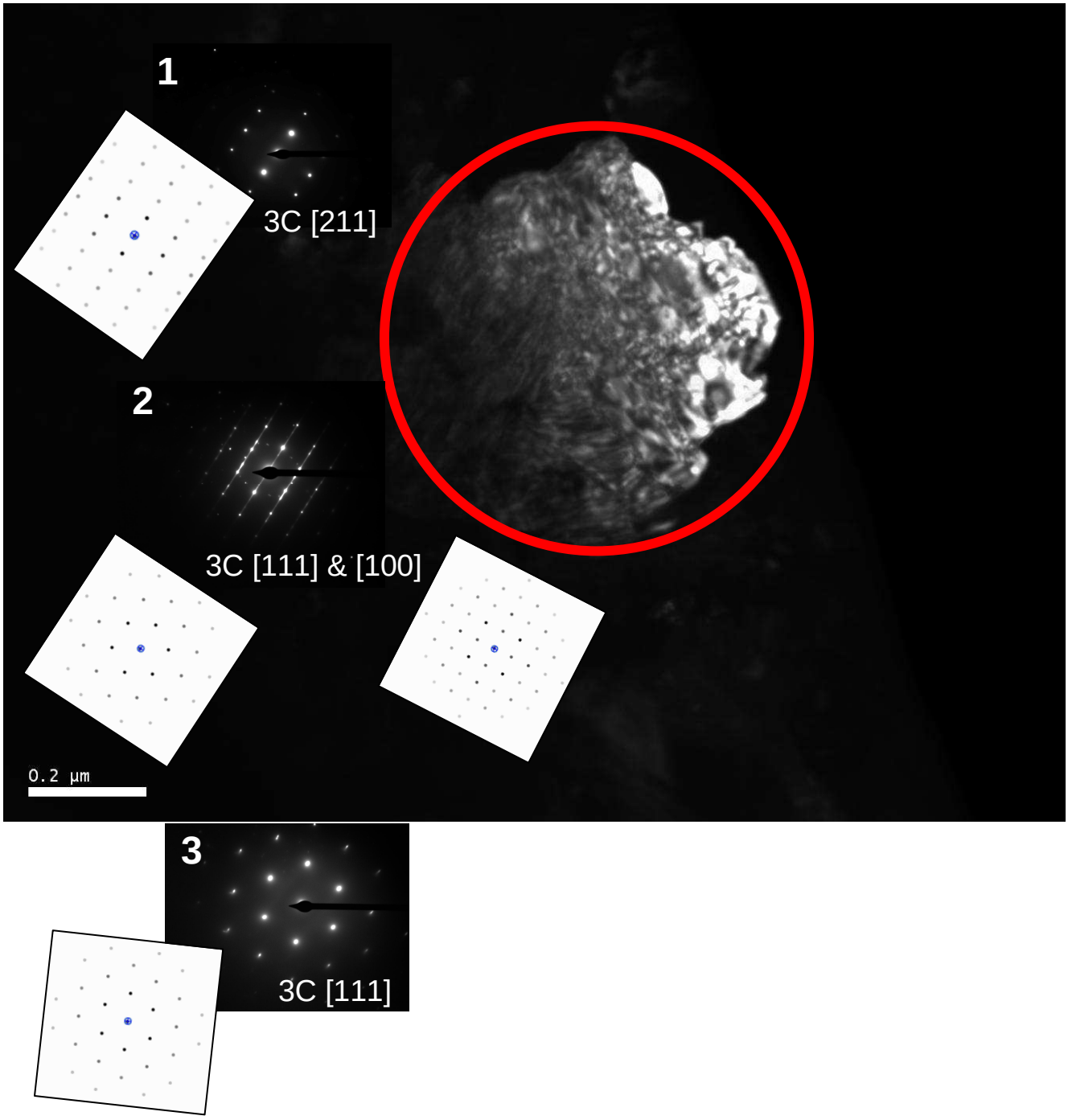

PO6 Image 3

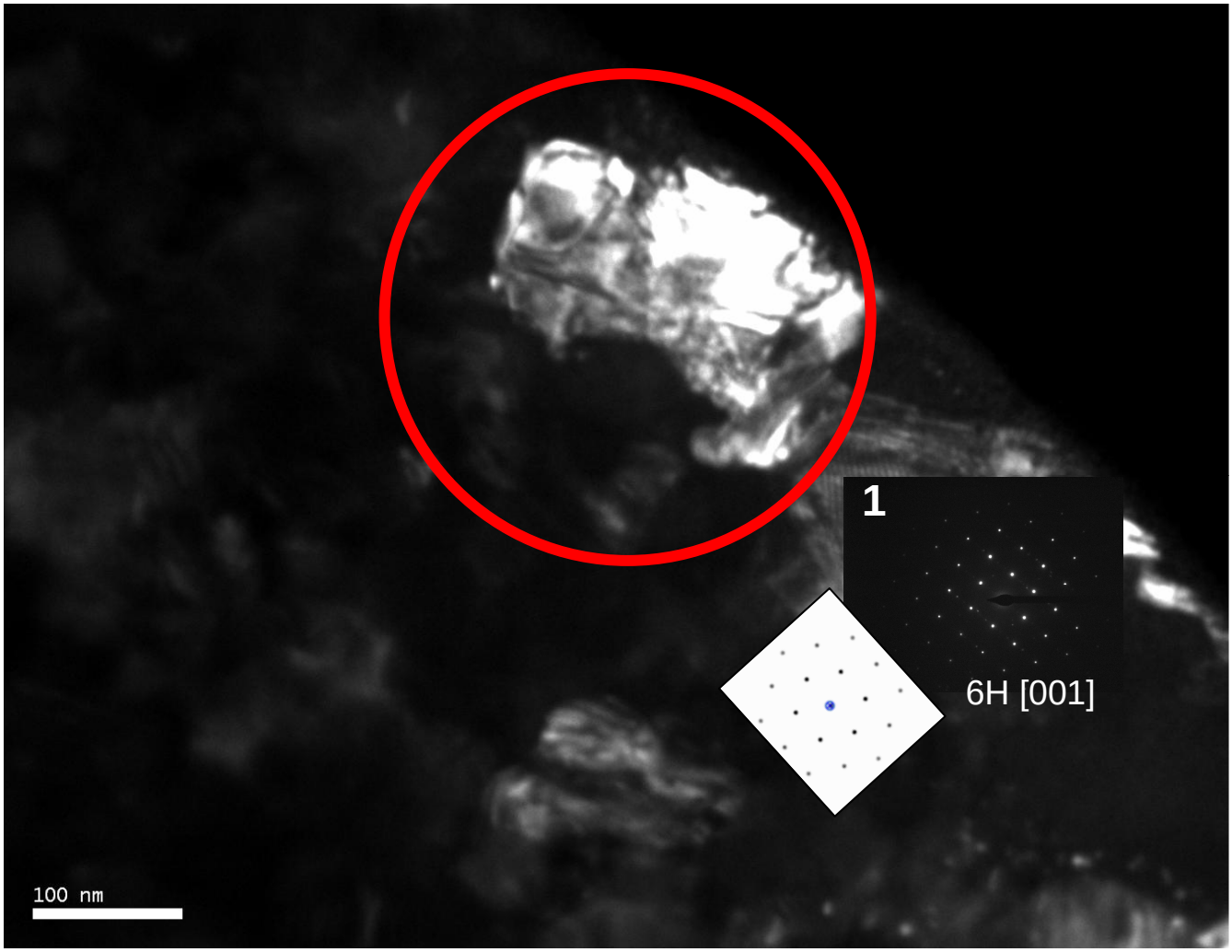

UNIVERSITEIT VAN PRETORIA
UNIVERSITY OF PRETORIA
YUNIBESITHI YA PRETORIA

PO6 Image 4

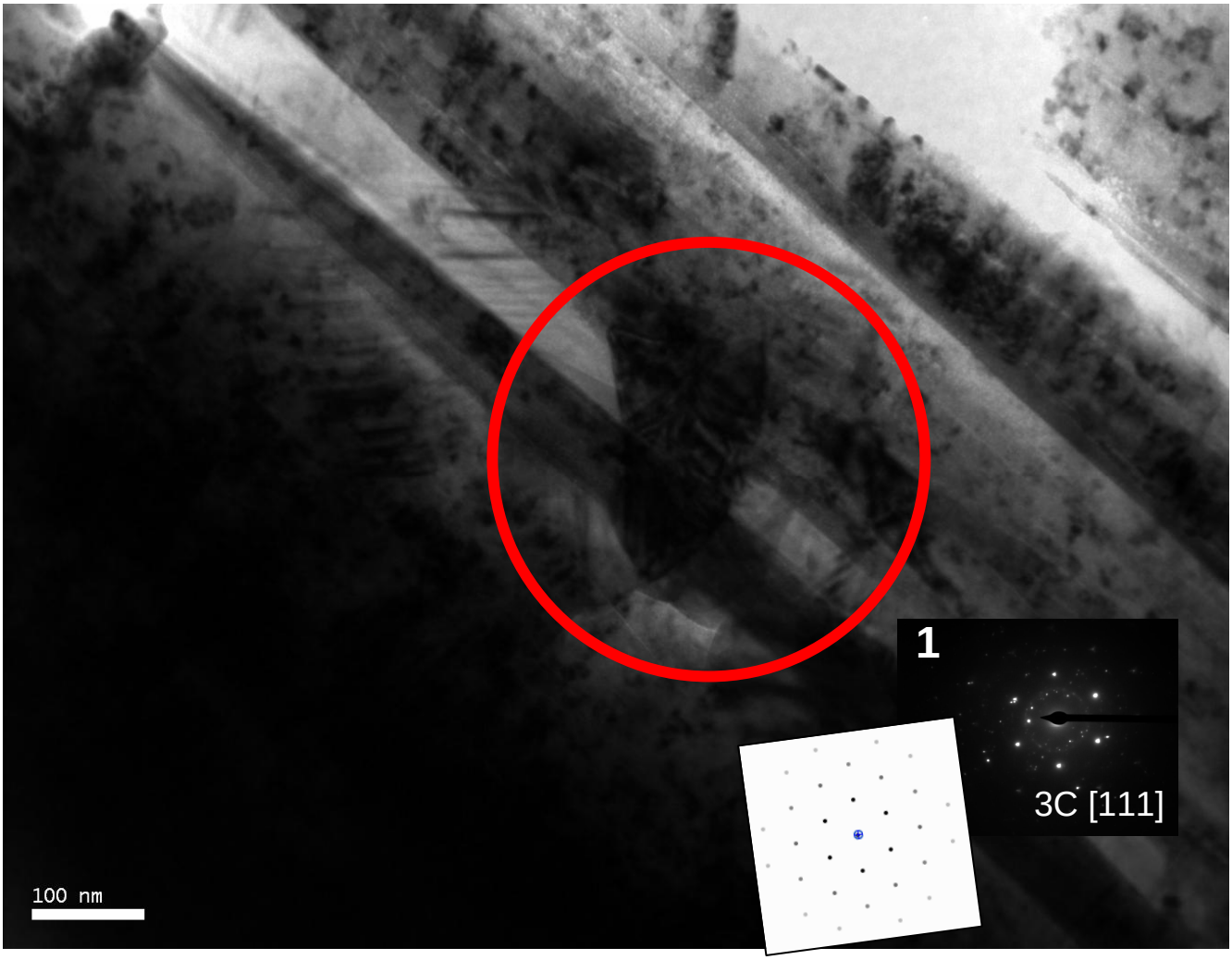

PO6 Image 5

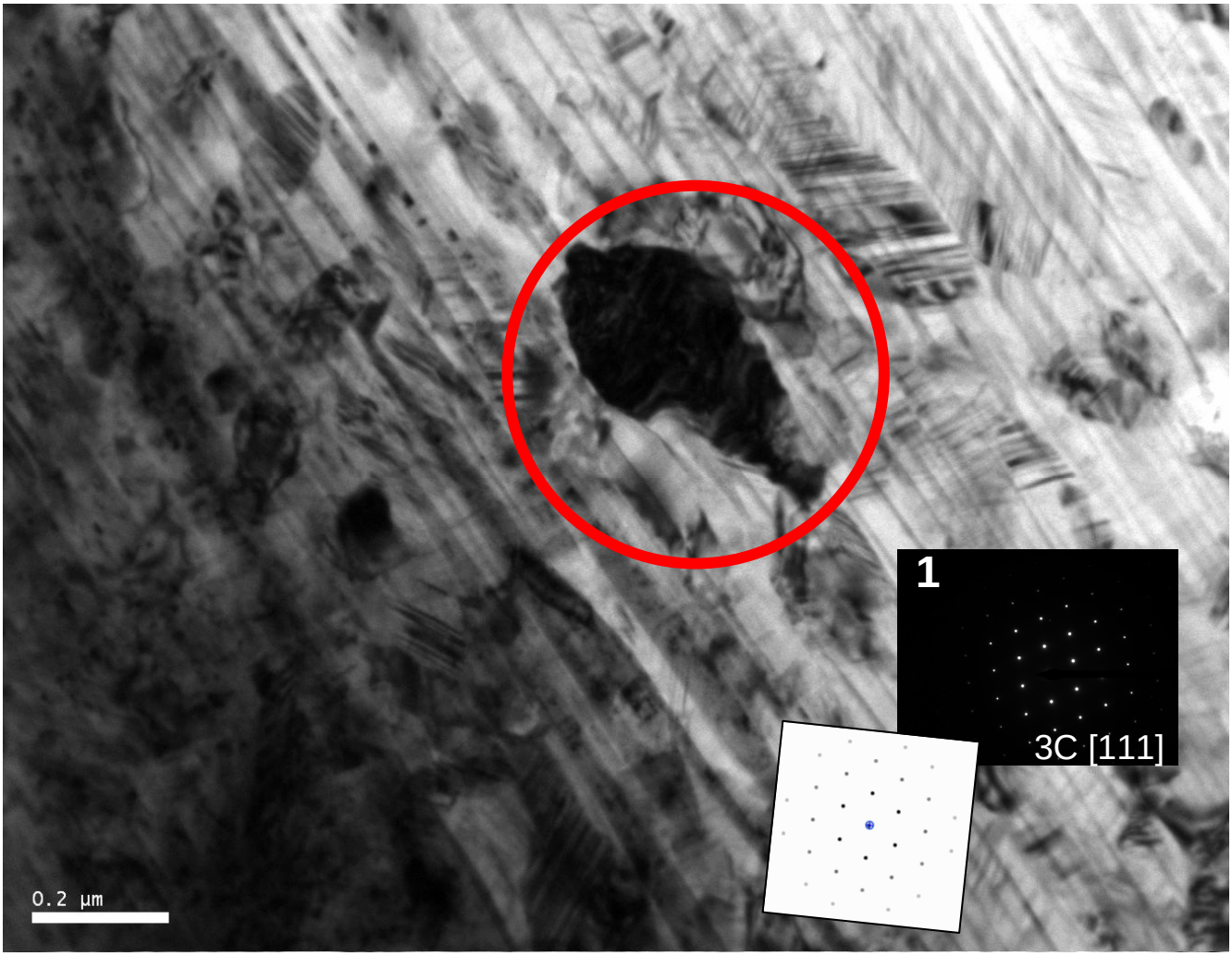

UNIVERSITEIT VAN PRETORIA
UNIVERSITY OF PRETORIA
YUNIBESITHI YA PRETORIA

PO6 Image 6

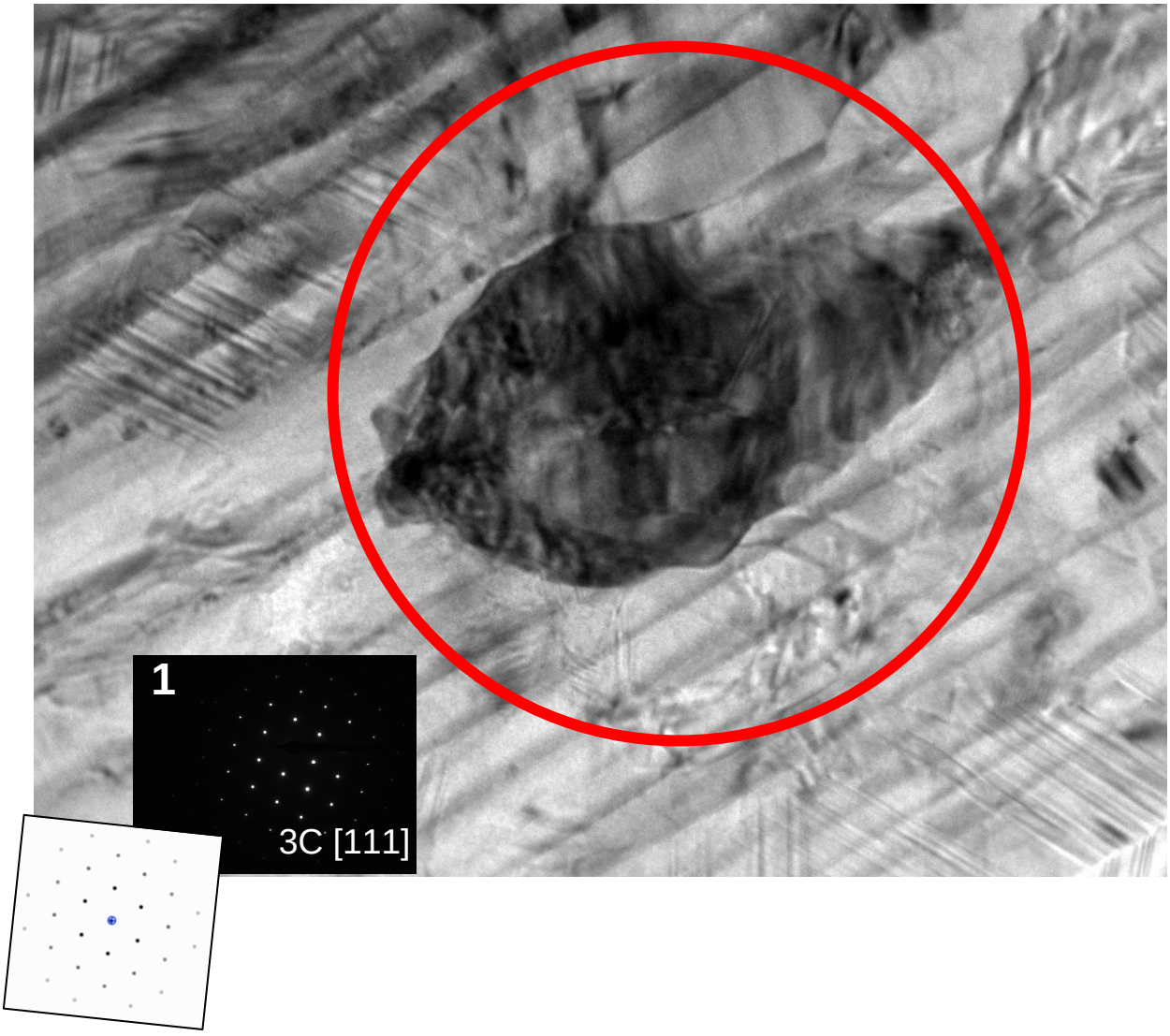

PO6 Image 7

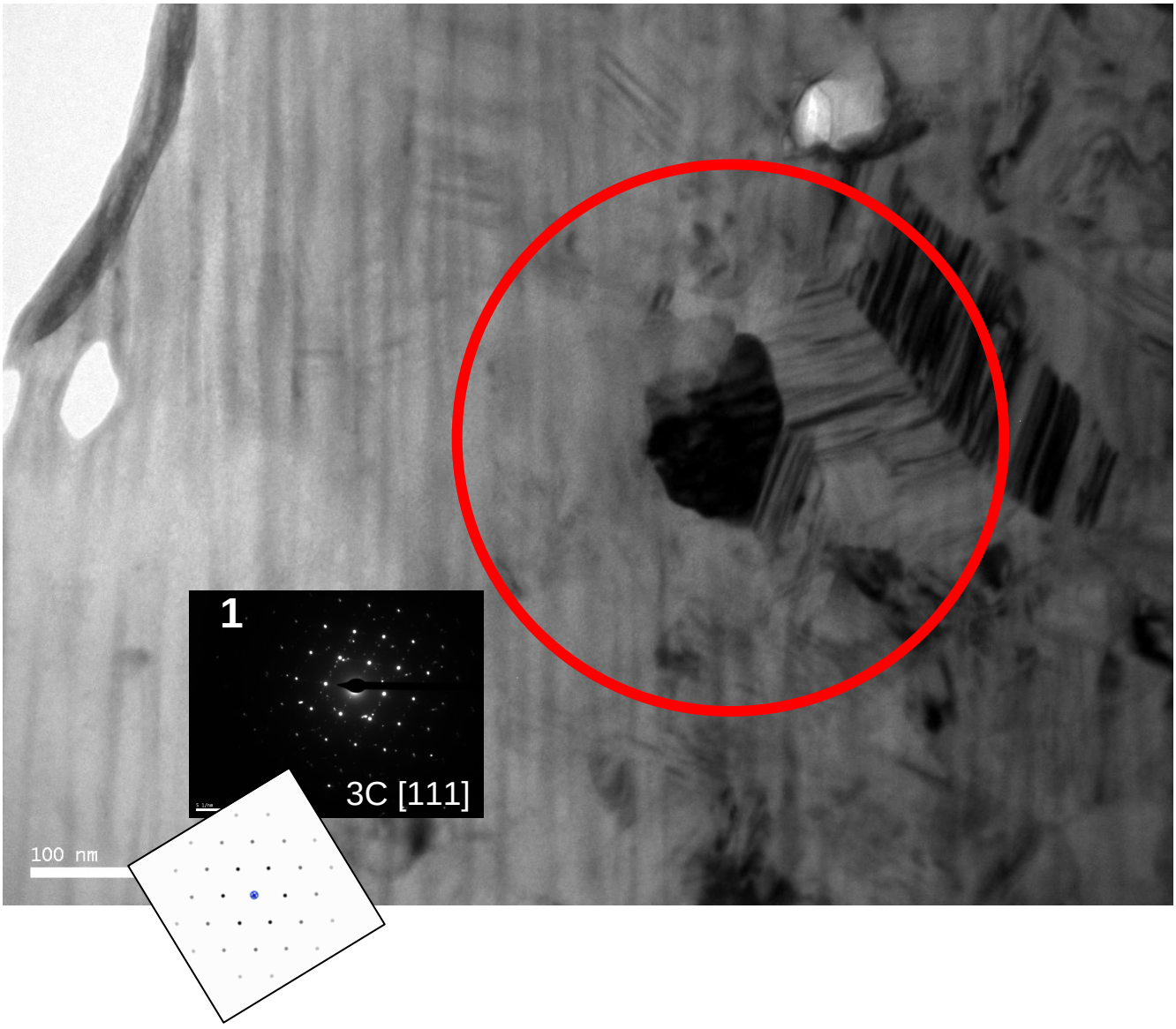

UNIVERSITEIT VAN PRETORIA
UNIVERSITY OF PRETORIA
YUNIBESITHI YA PRETORIA

PO6 Image 8

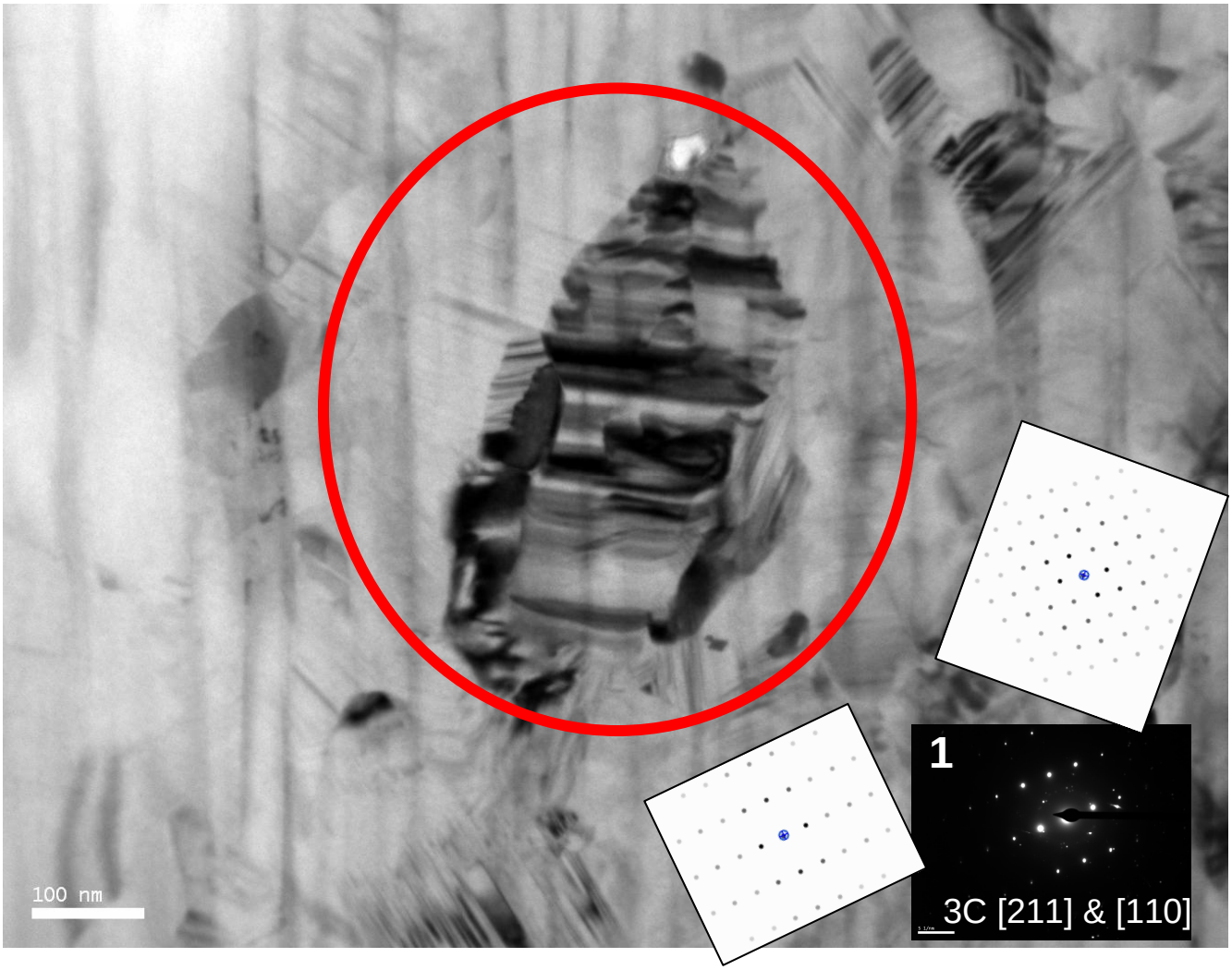

UNIVERSITEIT VAN PRETORIA
UNIVERSITY OF PRETORIA
YUNIBESITHI YA PRETORIA

PO9 Image 1

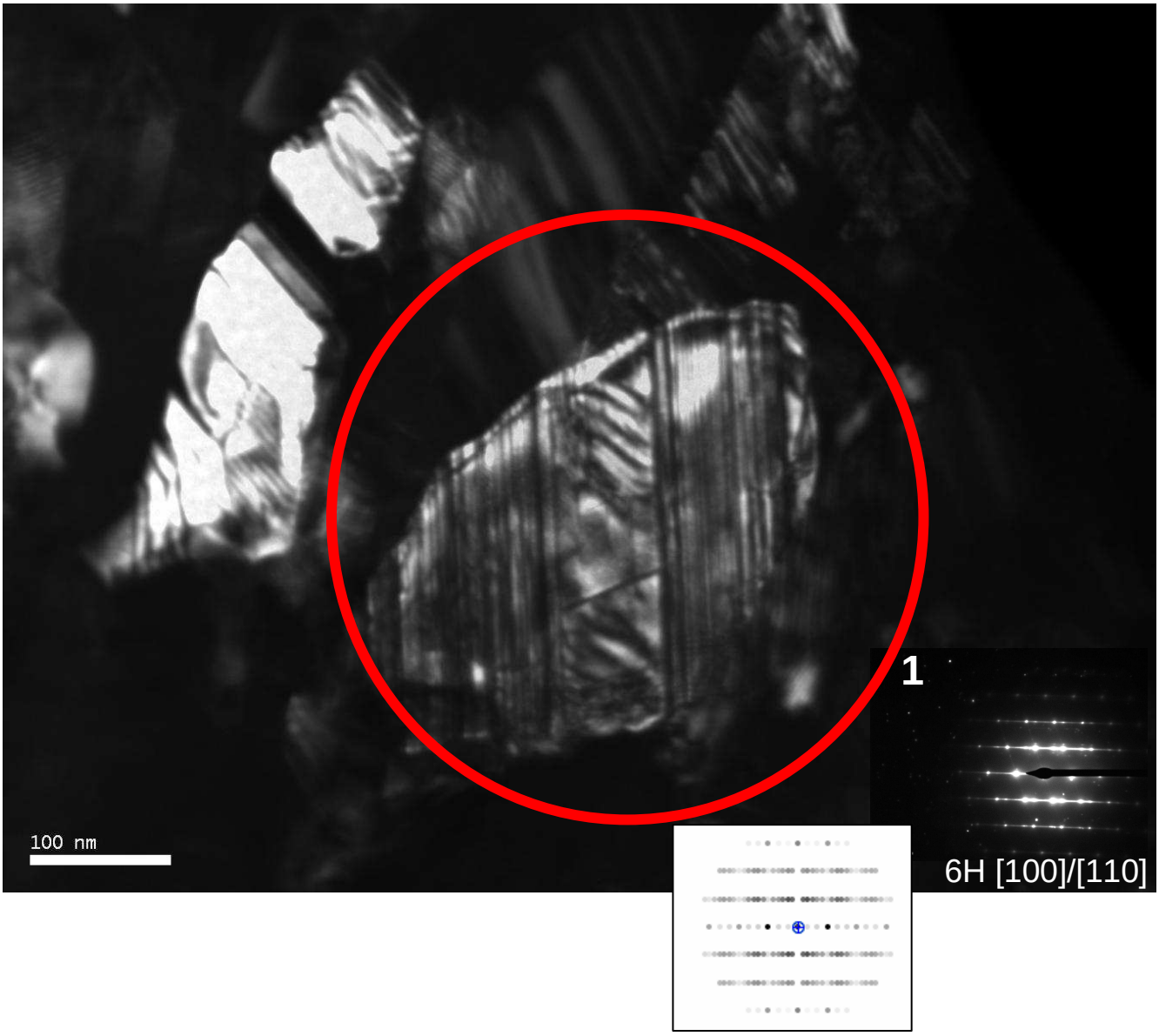

PO9 Image 2

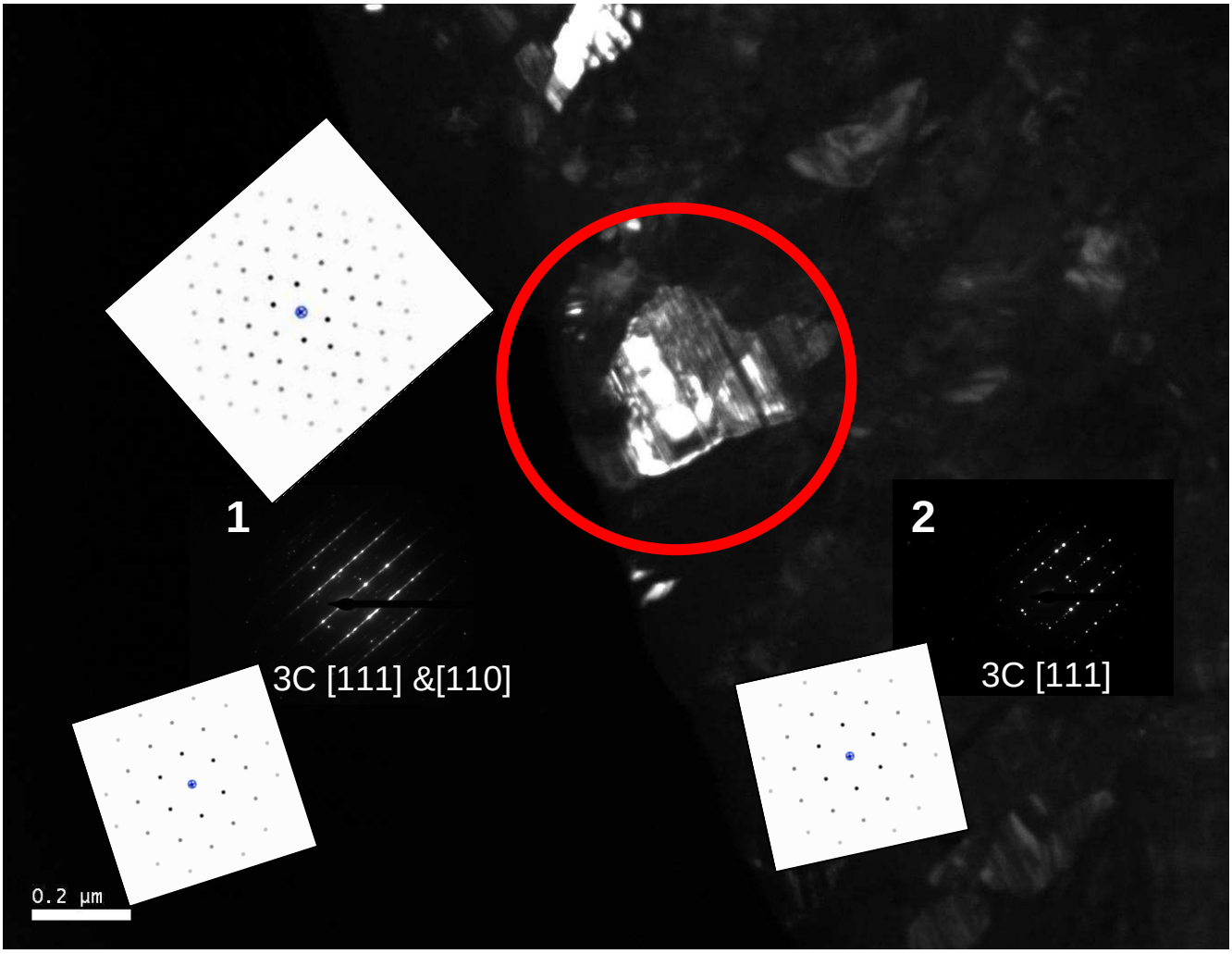

PO9 Image 3

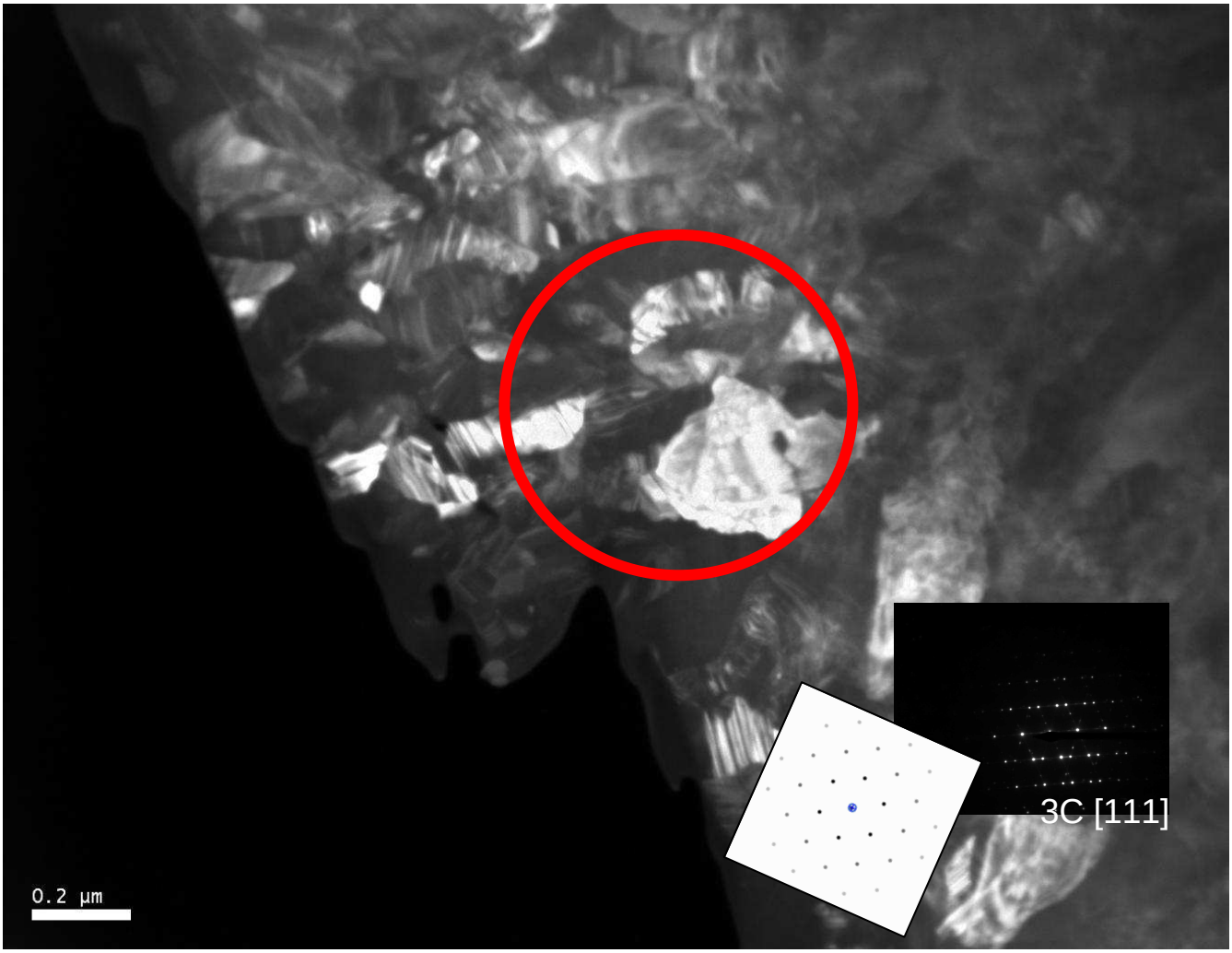

PO9 Image 4

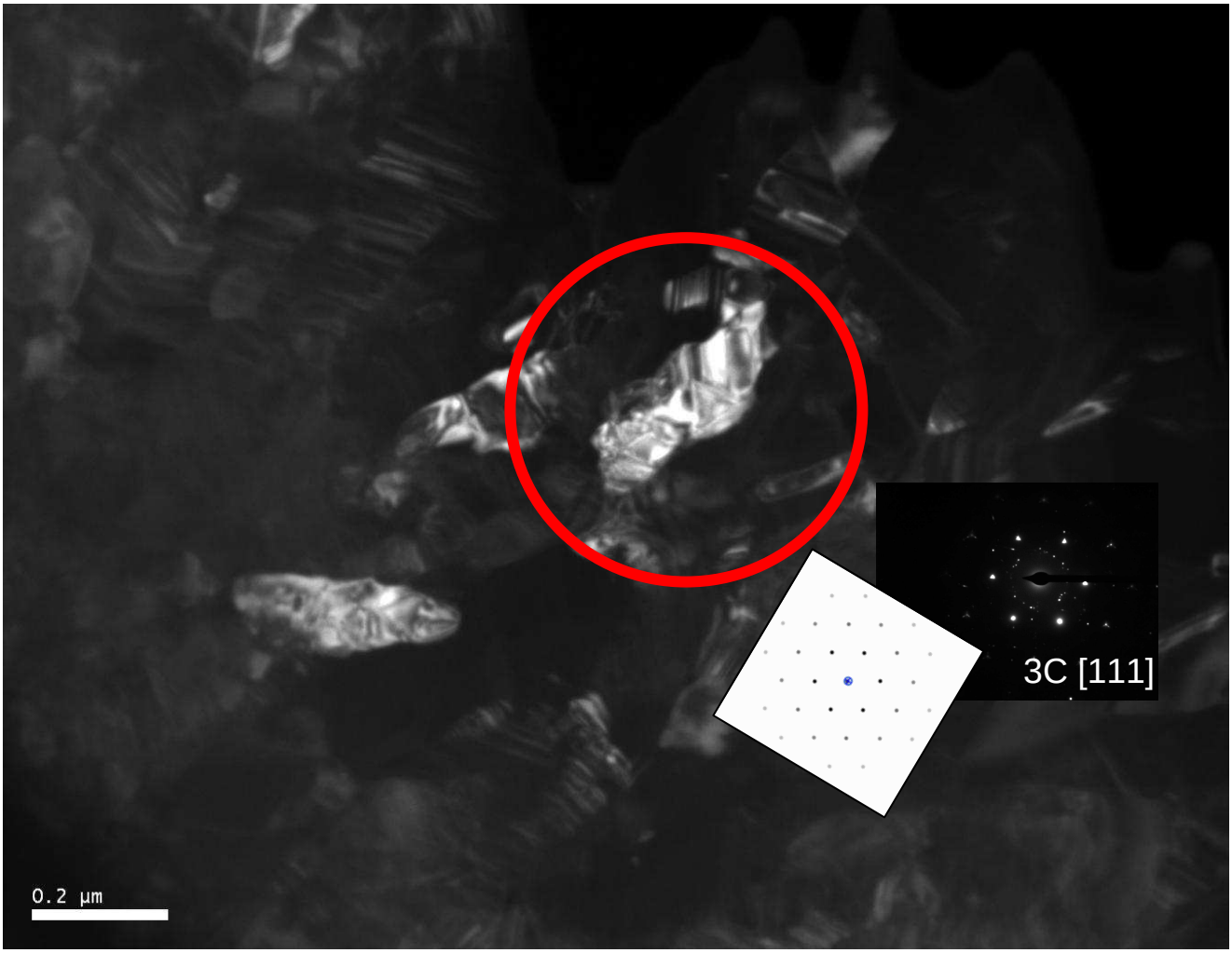

UNIVERSITEIT VAN PRETORIA
UNIVERSITY OF PRETORIA
YUNIBESITHI YA PRETORIA

PO Image 5

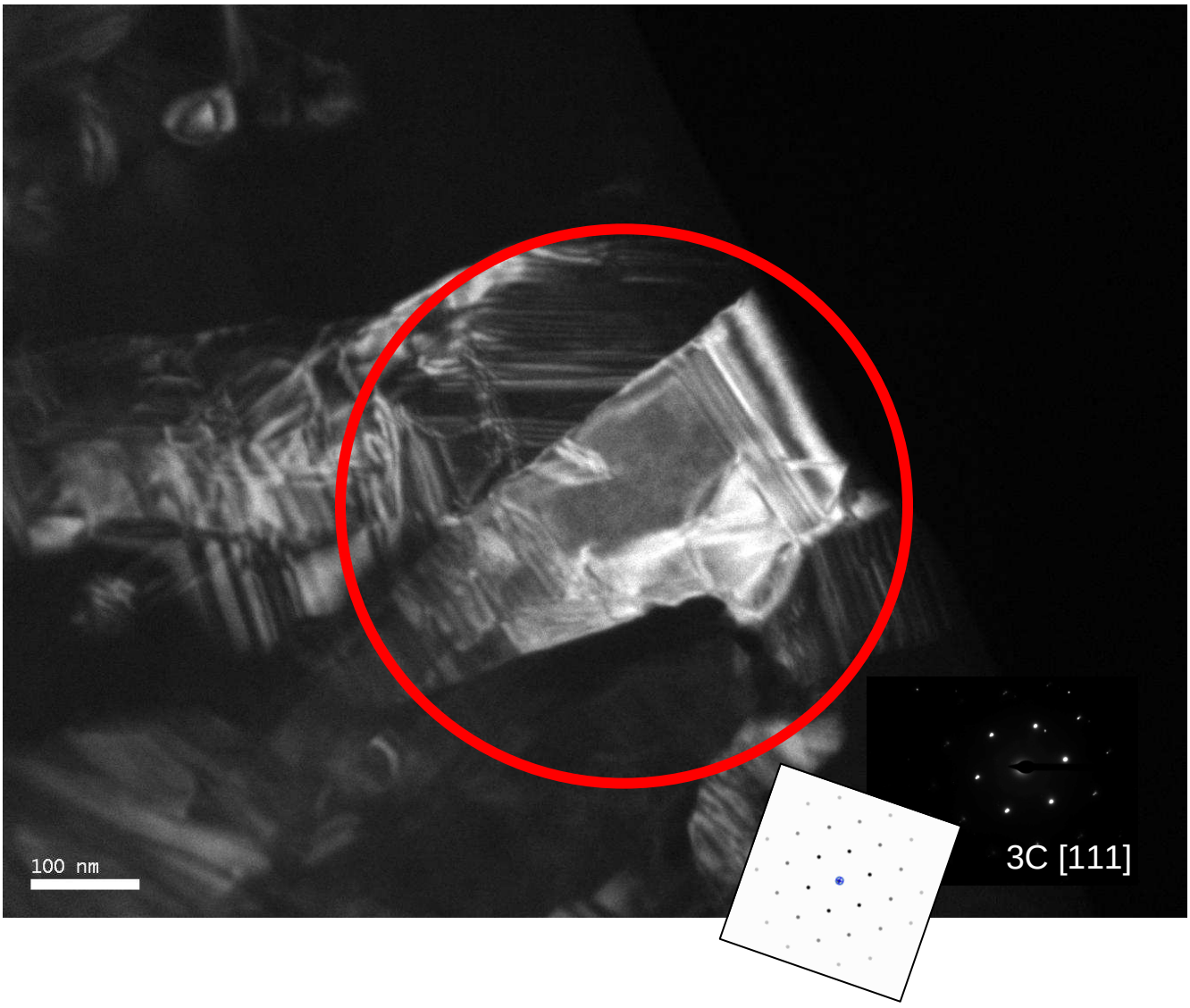

PO9 Image 6

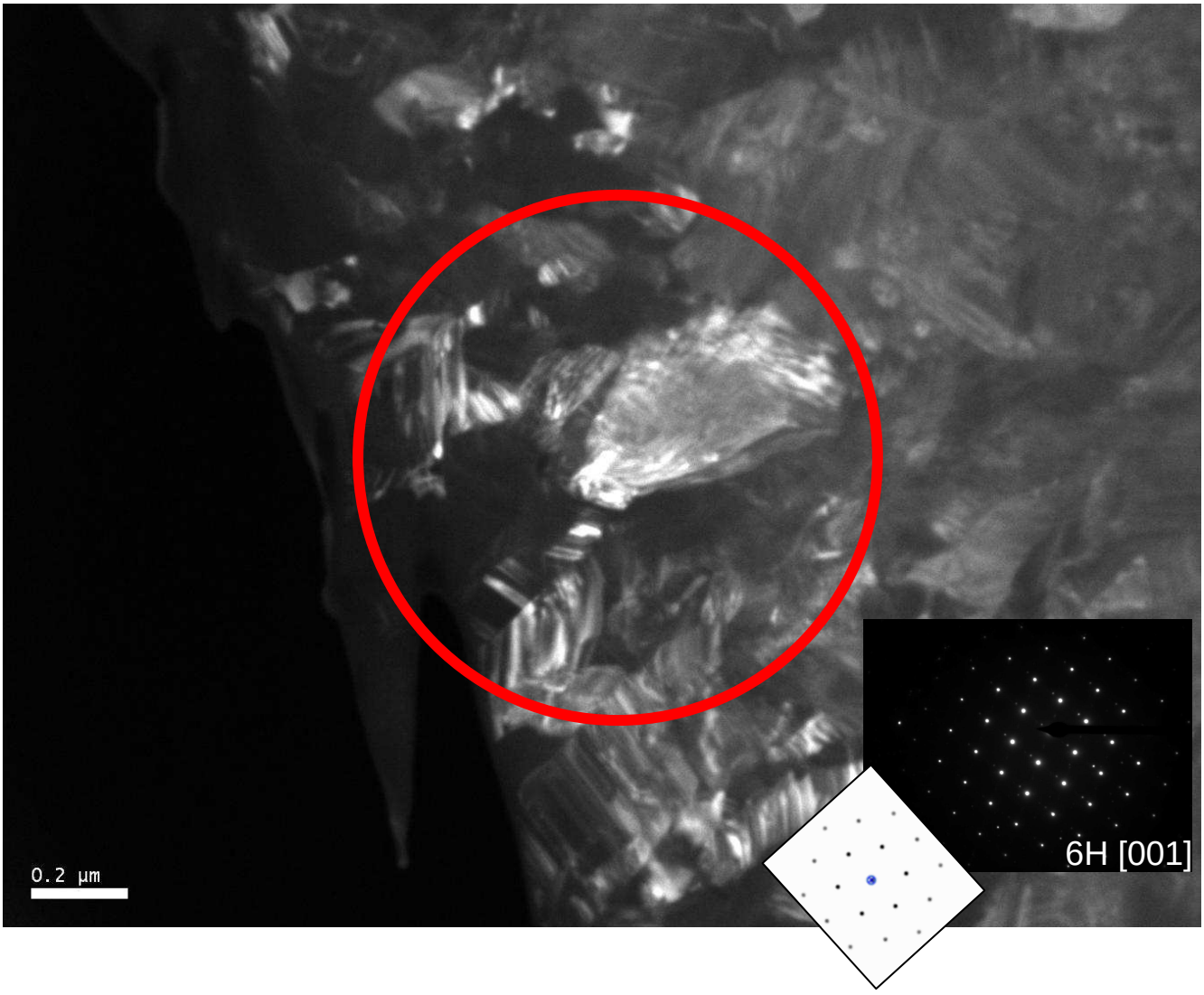

PO9 Image 7

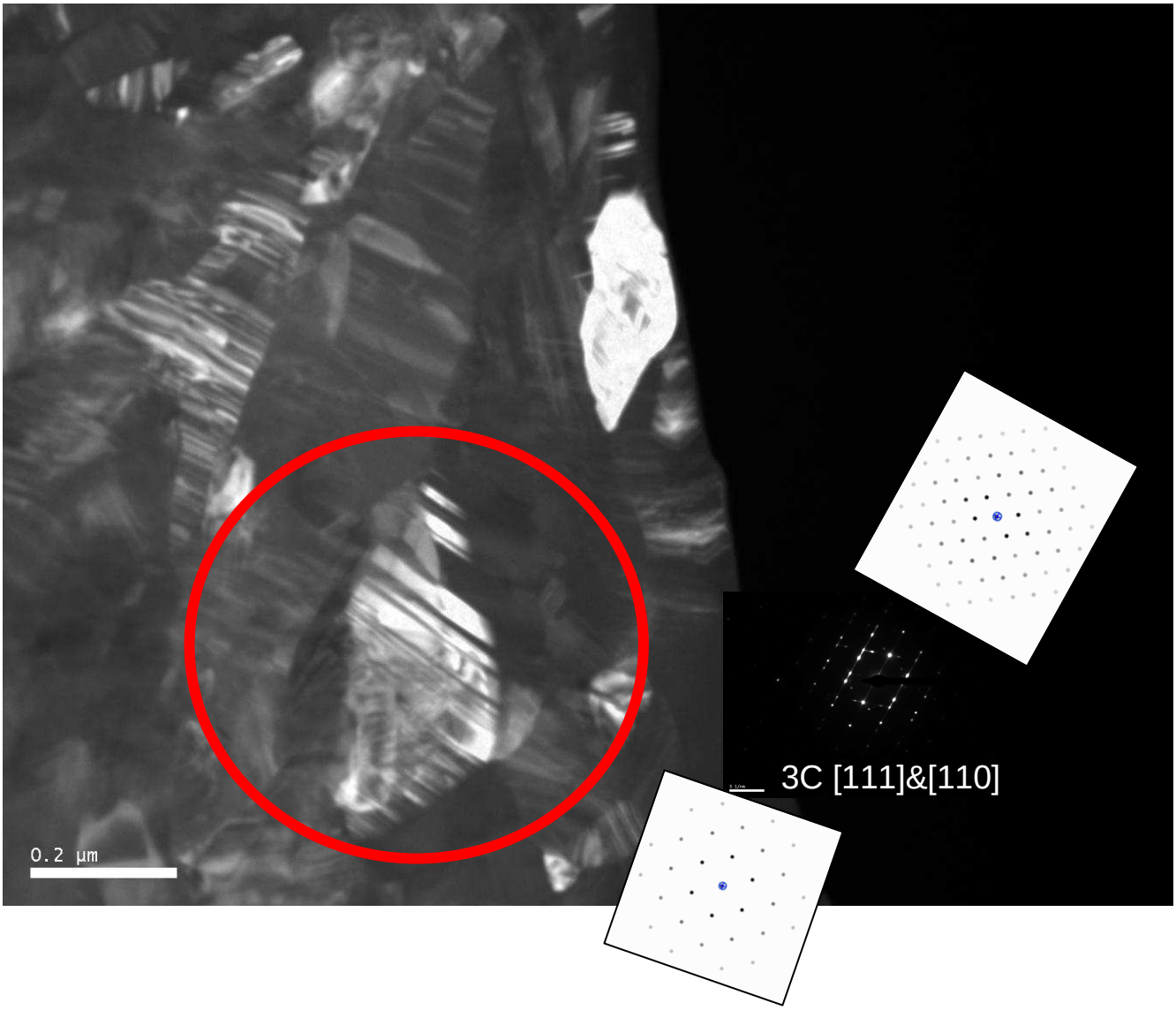

PO9 Image 8

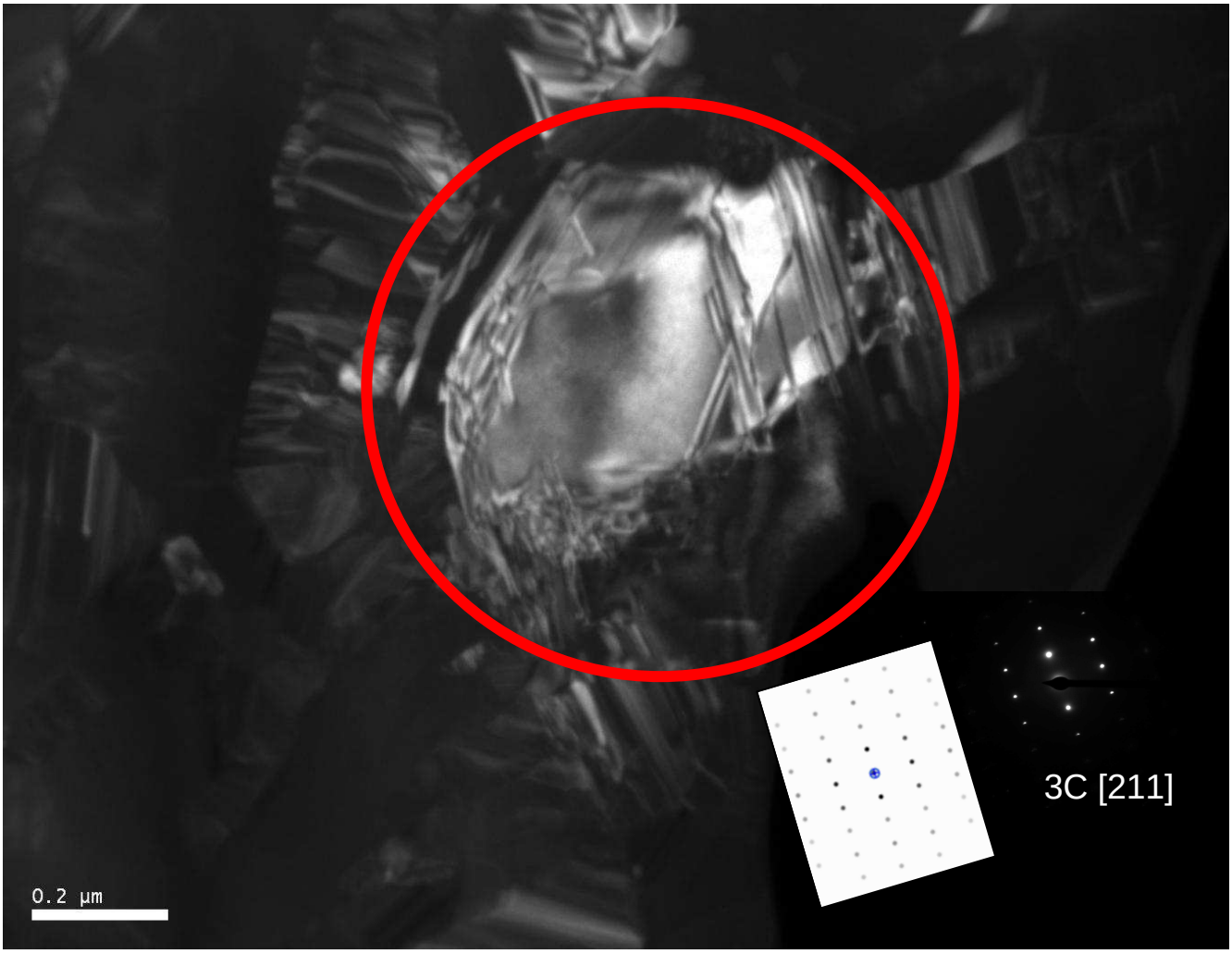

PO9 Image 9

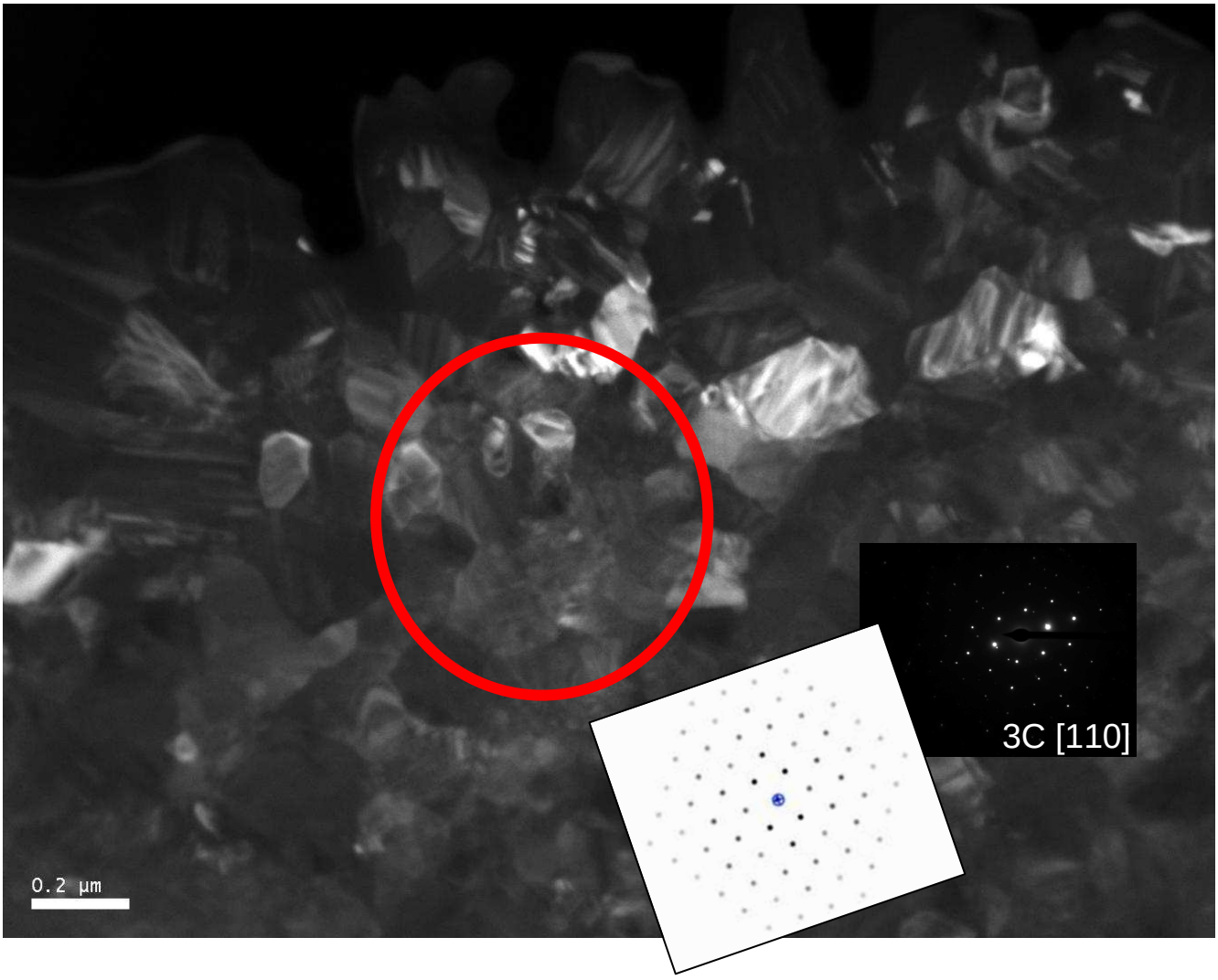

PO9 Image 10

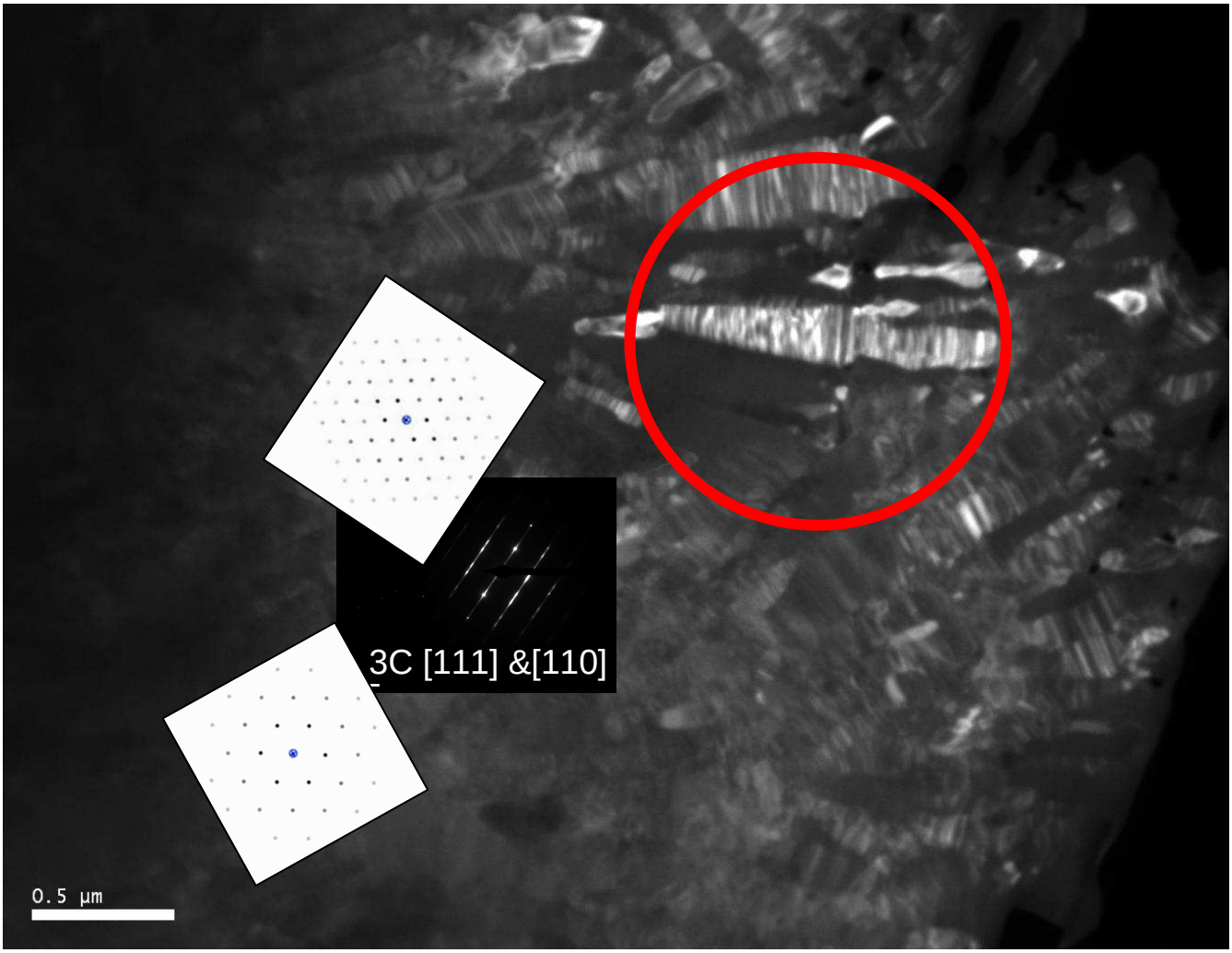

UNIVERSITEIT VAN PRETORIA
UNIVERSITY OF PRETORIA
YUNIBESITHI YA PRETORIA

PO9 Image 11

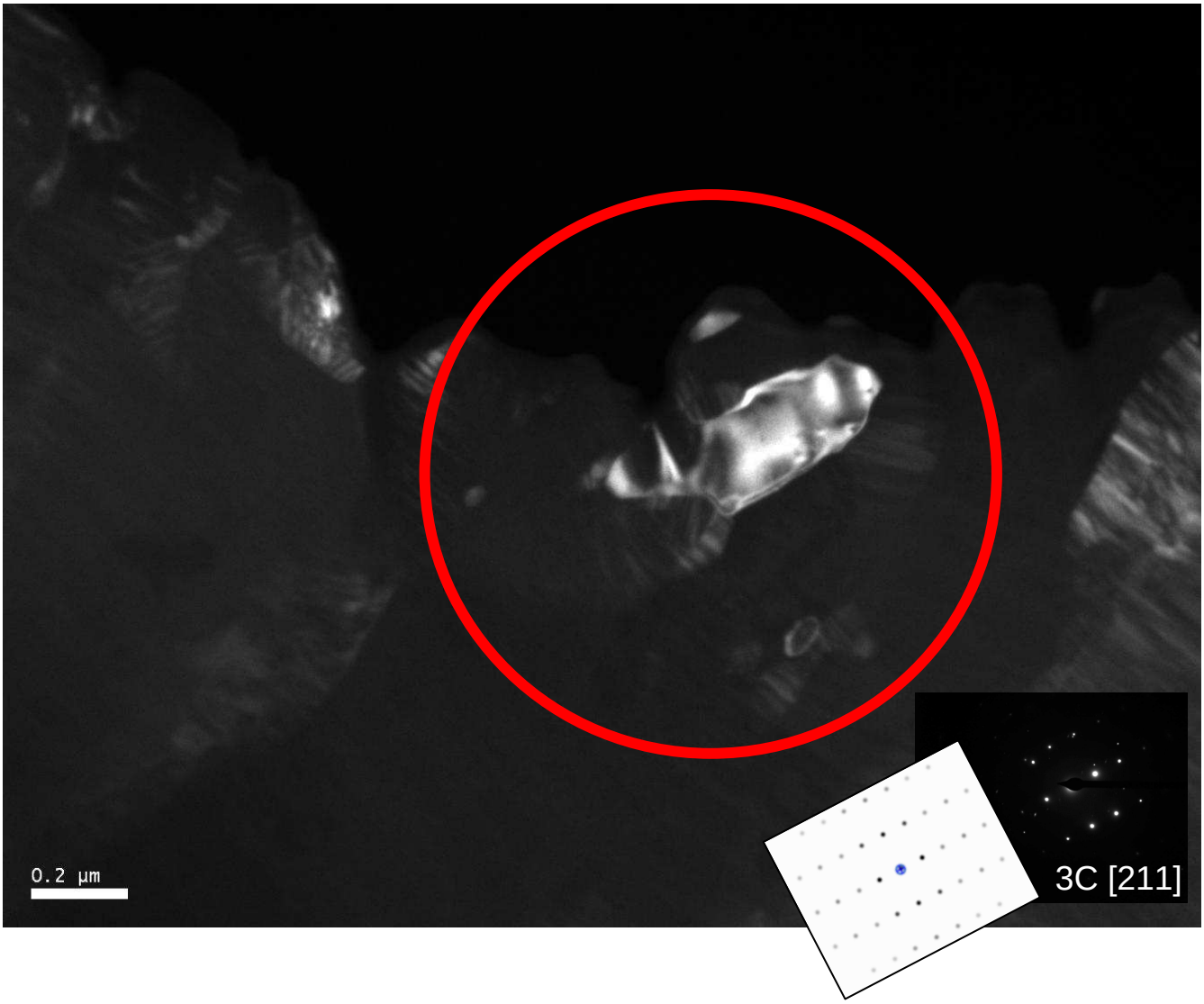

PO9 Image 12

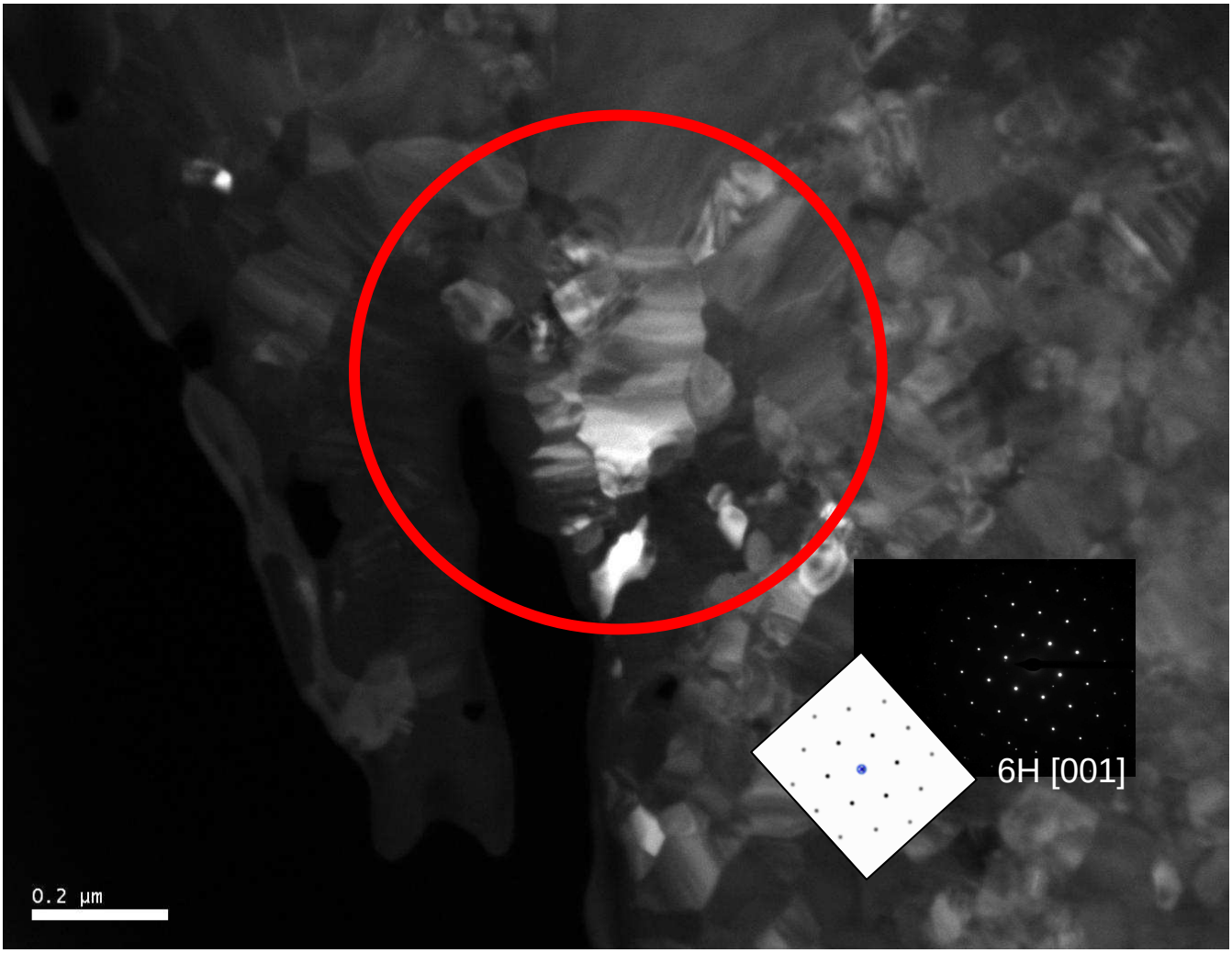

UNIVERSITEIT VAN PRETORIA
UNIVERSITY OF PRETORIA
YUNIBESITHI YA PRETORIA

PO9 Image 13

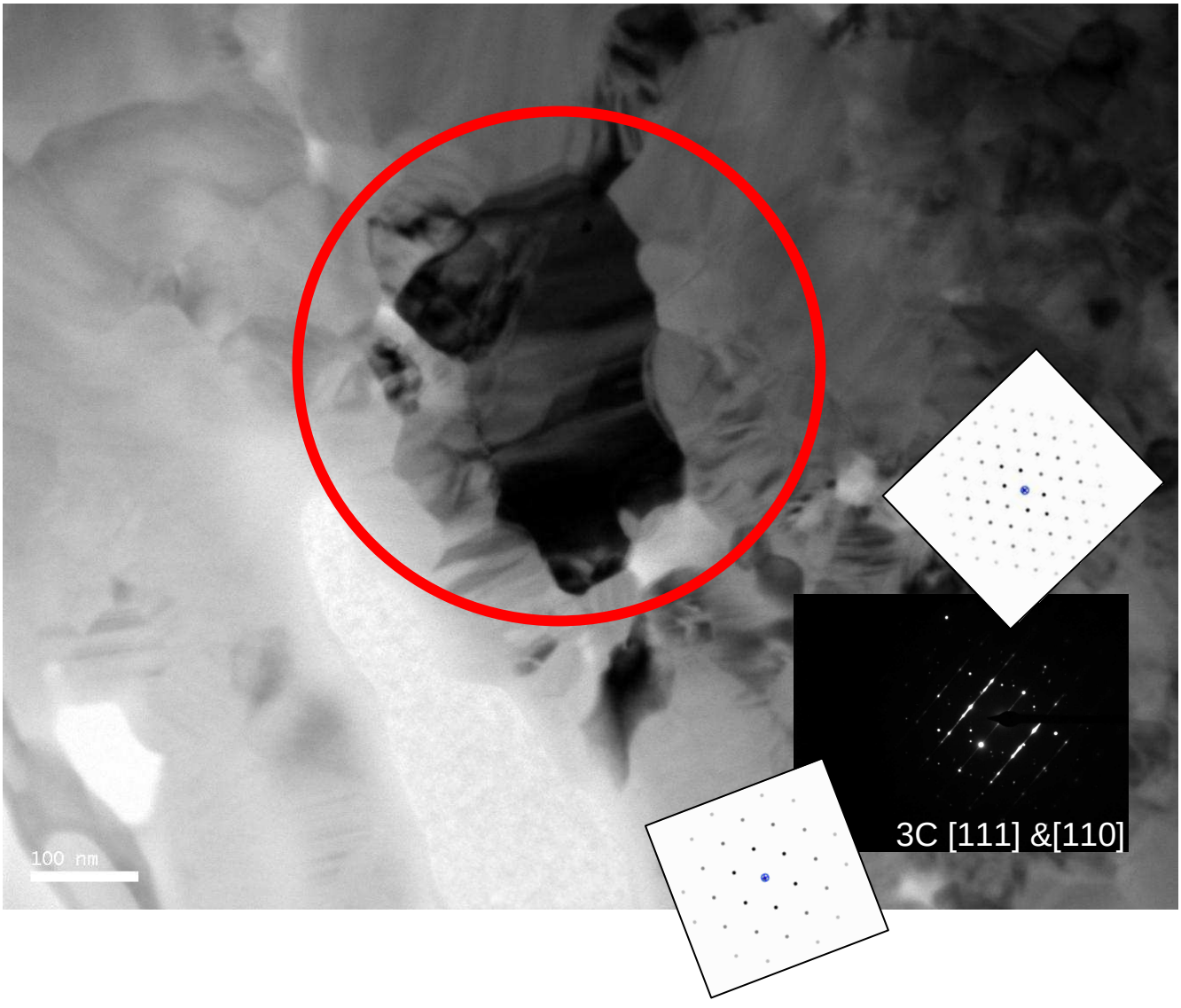

UNIVERSITEIT VAN PRETORIA
UNIVERSITY OF PRETORIA
YUNIBESITHI YA PRETORIA

PO9 Image 14

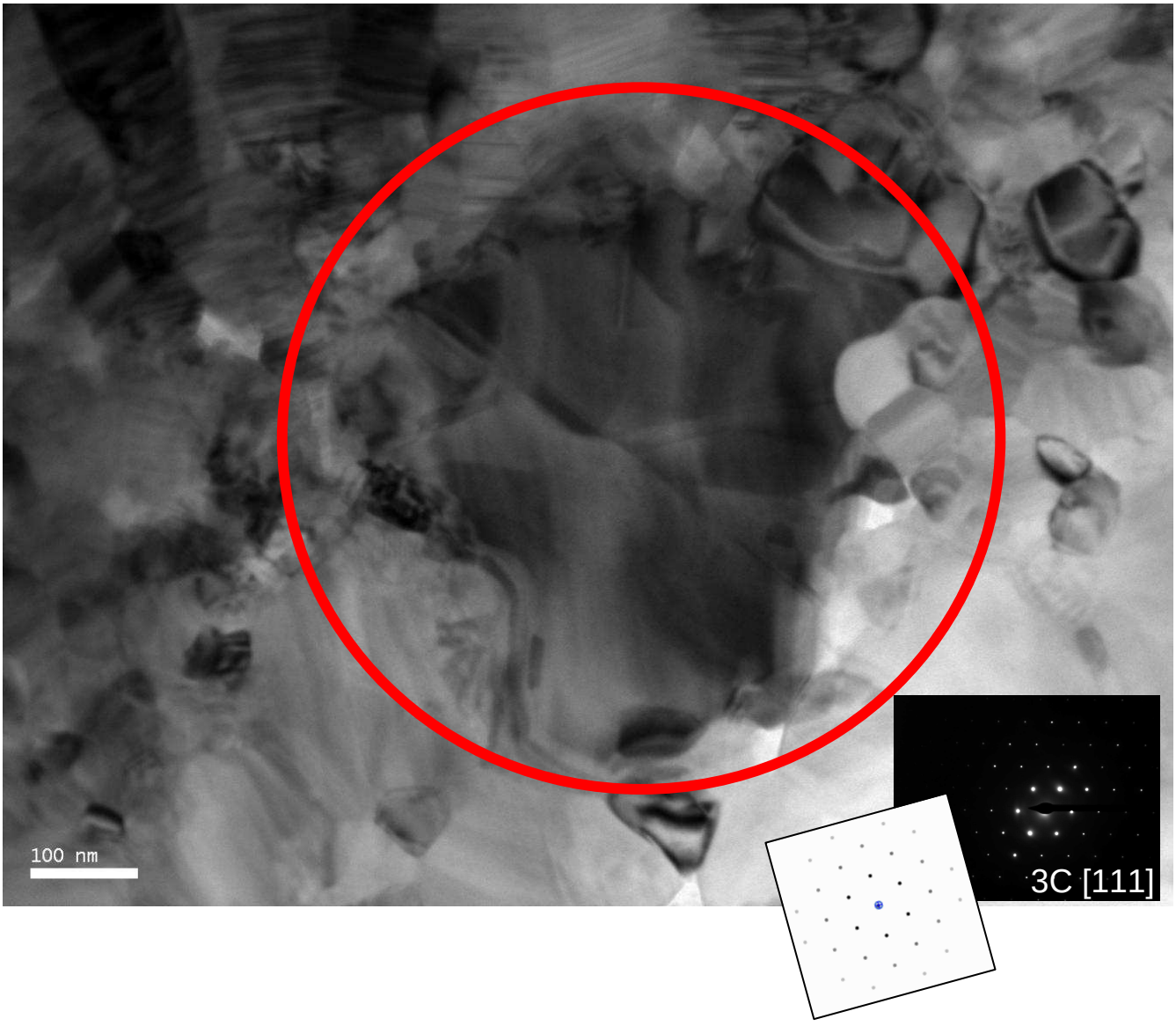

UNIVERSITEIT VAN PRETORIA
UNIVERSITY OF PRETORIA
YUNIBESITHI YA PRETORIA

PO9 Image 15

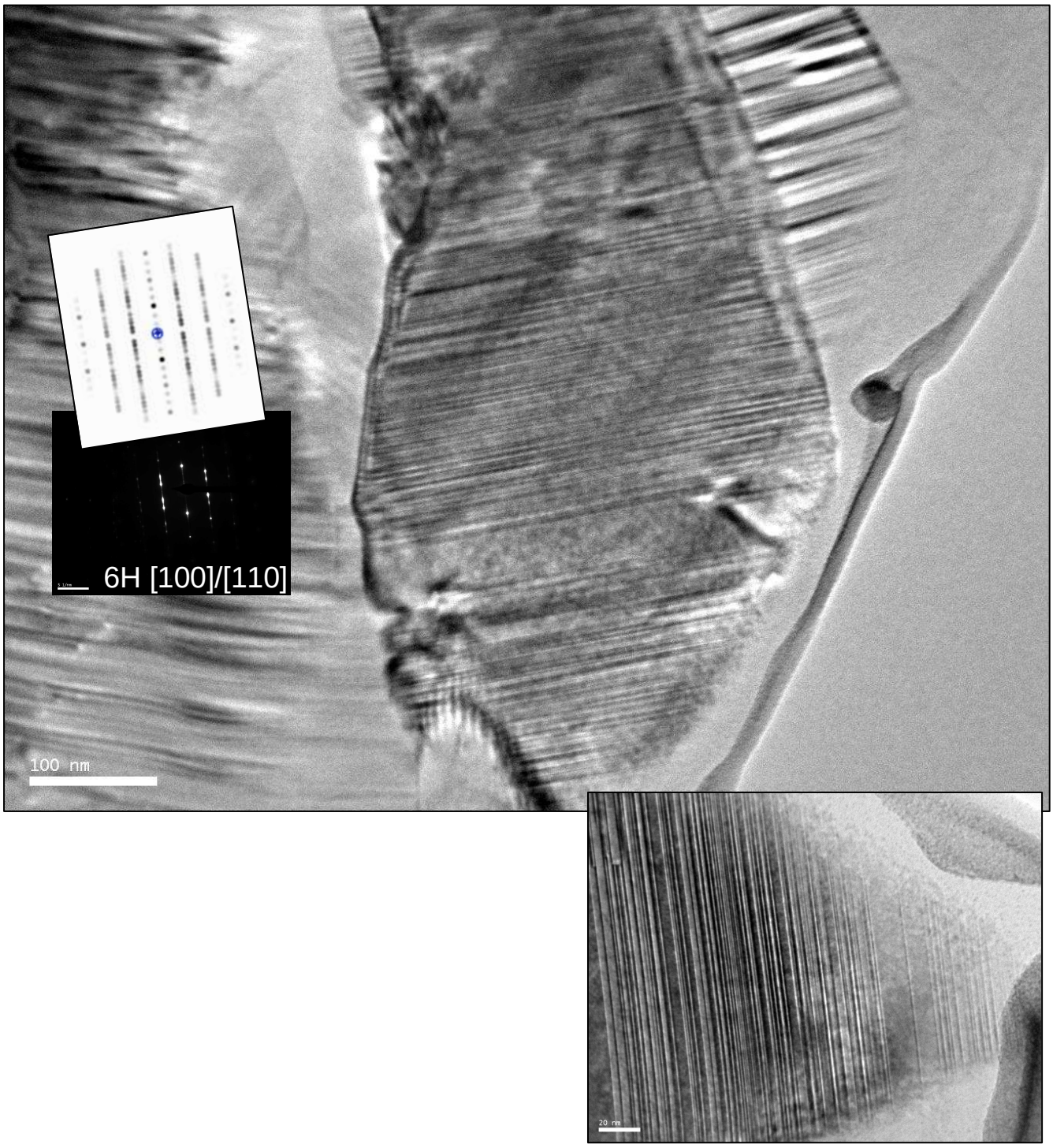

PO9 Image 16

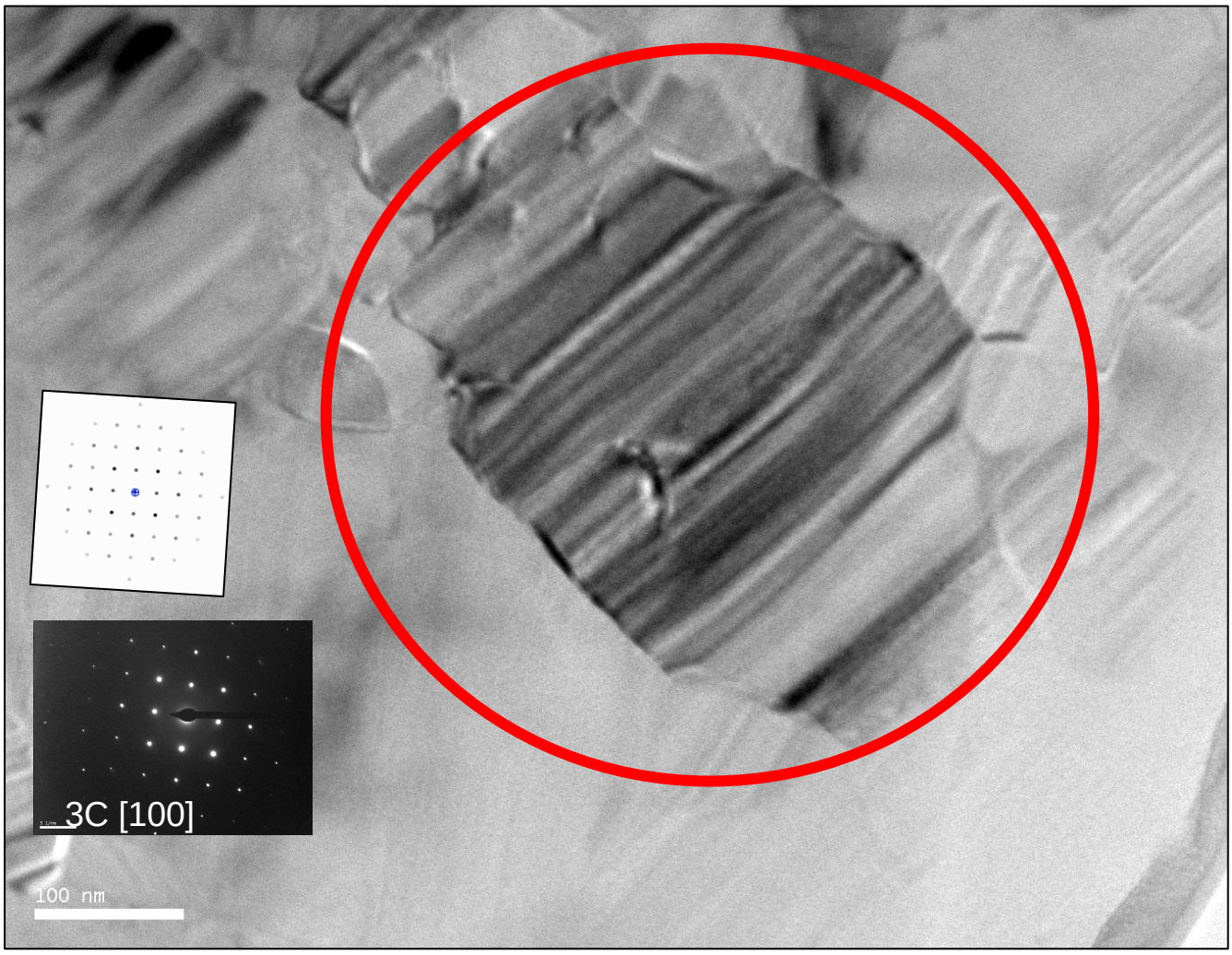

High temperature data

- PO9
  - Lattice parameters (units in Å)

EXPERIMENTAL VALUES				
T	a - Al_2O_3	c - Al_2O_3	c-graphite	a-SiC
25	4.76182	12.99269	6.95261	4.35972
100	4.76399	12.99832	6.96335	4.36038
200	4.76692	13.00881	6.98064	4.36192
300	4.77019	13.02118	7.0149	4.36421
400	4.77309	13.03091	7.02579	4.36526
500	4.77657	13.0417	7.04581	4.36726
600	4.77966	13.05079	7.05891	4.36894
700	4.78277	13.06108	7.077	4.37064
800	4.78542	13.07075	7.08706	4.37223
900	4.7882	13.07963	7.1011	4.37363
1000	4.79099	13.08833	7.11972	4.37491
1100	4.79435	13.09828	7.13628	4.37706
1125	4.79477	13.10019	7.13666	4.37706
1150	4.79531	13.10262	7.14042	4.37755
1175	4.7962	13.10427	7.14197	4.37794
1200	4.79714	13.10536	7.14978	4.37804
1225	4.79779	13.10757	7.15186	4.37843
1250	4.79824	13.11146	7.15506	4.37917
1275	4.79949	13.11442	7.16239	4.37974
1300	4.80077	13.11851	7.16351	4.38054
1325	4.80114	13.1201	7.16618	4.38048
1350	4.80272	13.12333	7.16964	4.38106
1375	4.80361	13.12732	7.17442	4.38174
1400	4.80394	13.12673	7.19272	4.38132
1400	4.80394	13.12673	7.19272	4.38132
1350	4.80256	13.12303	7.16977	4.38083
1300	4.80099	13.11813	7.16192	4.37993
1250	4.79963	13.11412	7.16058	4.37949
1200	4.79808	13.10907	7.14562	4.37843
1150	4.79658	13.10388	7.14152	4.37782
1100	4.79532	13.09964	7.13344	4.37689
26	4.76203	12.99573	6.9647	4.35966